

Data Collection and Baseline Coastal Conditions Report

Jumby Bay & Maiden Island:
Historical and Existing Conditions

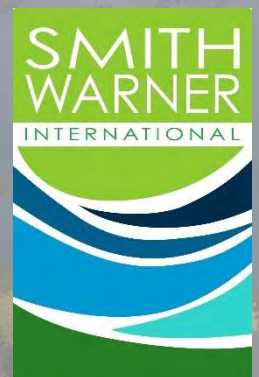
Prepared for:

Jumby Bay Island Company Ltd
Jumby Bay, Antigua

Submitted by:

Smith Warner International Limited
Unit 13, Seymour Park, 2 Seymour Avenue
Kingston 10, JAMAICA

26 May 2023





Contents

| | | |
|-----|---|----|
| 1 | Background..... | 1 |
| 1.1 | Location and Description of Study Area..... | 1 |
| 1.2 | Study Objectives..... | 2 |
| 2 | Data Collection..... | 3 |
| 2.1 | Bathymetry and Topography..... | 3 |
| 2.2 | Seafloor Classification..... | 10 |
| 2.3 | Beach Sediment | 16 |
| 2.4 | Land Use Changes..... | 20 |
| 2.5 | Rainfall Patterns..... | 21 |
| 2.6 | Stakeholder Identification | 23 |
| 2.7 | Coastal Structures Inventory | 24 |
| 3 | Evolution of Coastal Areas..... | 26 |
| 3.1 | Shoreline Changes | 26 |
| 3.2 | Bathymetry Changes | 42 |
| 3.3 | Seafloor Classification Changes | 46 |
| 4 | Hazard Exposure | 50 |
| 4.1 | Scenario Selection for Planning Development | 50 |
| 5 | Wave Climate Analysis | 56 |
| 5.1 | Operational Wave Climate..... | 56 |
| 5.2 | Hurricane Wave Climate | 64 |
| 6 | Currents and Tides..... | 79 |
| 6.1 | Global Tide Model..... | 80 |
| 6.2 | Nearshore Tidal Currents..... | 81 |
| 7 | Floodplain Modelling | 88 |
| 7.1 | Flooding Depth | 88 |
| 7.2 | Overland Flow Speeds..... | 90 |
| 8 | Shoreline Stability and Sediment Transport Potential..... | 92 |
| 8.1 | Sediment Transport Potential Zones | 92 |





| | | |
|-----|--|-----|
| 8.2 | Shoreline Retreat | 94 |
| 8.3 | Sediment Stability Zones..... | 96 |
| 9 | Key Results Summary and Recommendations..... | 105 |
| 9.1 | Summary of Bathymetric Changes | 105 |
| 9.2 | Summary of Seafloor Classification Changes..... | 105 |
| 9.3 | Summary of Operational Wave Conditions | 105 |
| 9.4 | Summary of Hurricane Conditions..... | 107 |
| 9.5 | Summary of Currents and Tides | 107 |
| 9.6 | Summary of Beach Stability | 108 |
| | Appendix A – Numerical Modelling..... | 109 |
| A.1 | MIKE 21 Description and Additional Data..... | 109 |
| A.2 | HURWave Description | 112 |
| A.3 | XBEACH Plots | 114 |
| | Appendix B – Additional Data Collection Reporting..... | 122 |
| | Appendix C – Coastal Structures Inventory | 126 |



1 Background

1.1 Location and Description of Study Area

Long Island, a private island locally known as Jumby Bay, and Maiden Island, sometimes referred to as "Maid Island" or "Maiden Islet," are both owned by Jumby Bay Company and situated offshore of Antigua in the eastern Caribbean Sea. With a land area of approximately 300 acres (121 hectares) and a 6km (3.7-mile) coastline, Jumby Bay is primarily composed of limestone and features a relatively flat topography with a maximum elevation of only 12m (39 feet) above mean sea level. Conversely, Maiden Island, formed from dredged material originating from the nearby channel, has an average elevation of 2 to 4m above mean sea level and is known for its natural beauty and ten moorings, making it a popular tourist destination.

Both islands, located to Antigua's northeast, are accessible primarily by ferry from the Antiguan mainland to Jumby Bay. Their low-lying topography makes them highly vulnerable to sea level rise, coastal flooding, and erosion. The Intergovernmental Panel on Climate Change (IPCC) 2021 report projects that under a high greenhouse gas emissions scenario, sea levels could rise by up to 1.3m (4.3 feet) by the end of the century, significantly impacting the infrastructure and communities on these islands. As such, the future development of these islands must rely on comprehensive data collection and baseline investigations to mitigate potential risks and adverse effects.

Satellite imagery in Figure 1.1 displays the geography of both Jumby Bay and Maiden Island.

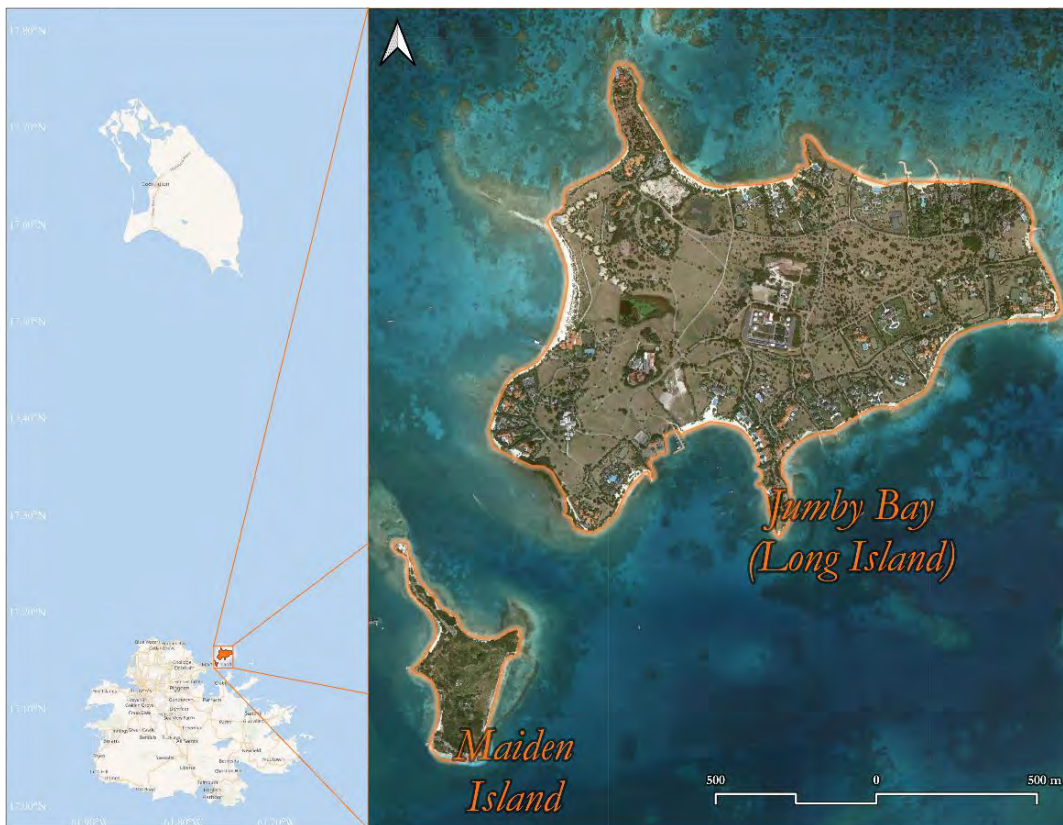


Figure 1.1 Location of project sites.



1.2 Study Objectives

The study objectives of the Jumby Bay Baseline Coastal Study are to develop and document a holistic understanding of the island's coastline morphology, predominant trends, and exposure to natural hazards. This information will enable the integration of development or conservation goals with the natural attributes of the coastal environment in order to achieve sustainability and optimize operational or capital investments. The study aims to establish the historical and current predominant conditions of the various elements that shape the coastal environment and answer critical questions related to the current state of the coastal zone, present approaches to protect and enhance the island's shoreline and sandy beaches, identify vulnerabilities to hurricanes and surges, assess potential impact of planned developments around the island, and recommend sediment sizes for sand for beach enhancement. The report can serve as a baseline for all future coastal projects and streamline potential coastal projects on the island, inform planning decisions and facilitate more consistent environmental permitting.

2 Data Collection

This section of the report describes the data collection exercises that were conducted and highlights their key outcomes.

2.1 Bathymetry and Topography

The elevations of the seafloor (bathymetry) and on land (topography) are useful when describing a coastal environment. The seafloor contours will determine how and where waves break. The land contours are useful when determining the possibility of overland flooding in the area. A few sources were used to determine these elevations, described in further detail below.

2.1.1 Satellite-Derived Bathymetry and LiDAR Data

Bathymetric data was obtained through a sophisticated satellite imaging processing routine implemented by EOMAP®, a leading company in this field. The method employs a physics-based analysis of the different colour and multi-spectral bands of satellite imagery to accurately determine water depths. As the data is derived from satellite imagery, the calculated depths encompass a considerably larger area than traditional boat-based bathymetry. The satellite-derived bathymetric (SDB) data collected at a density of 2m spacing and spans 4.6km. Additionally, the SDB dataset excels at identifying unexpected features, such as the boat channel near Maiden Island and the reef line 2km away from Jumby Bay. Further, the data is presented in a gridded format, effectively capturing small and steep features like reef heads.

However, there are certain limitations associated with this remotely sourced data. It is crucial to verify the data against physical measurements, as was done in this case using additional beach profile measurements for shallow water elevations. This routine's capabilities are restricted to extracting water depths between 0.5m and 16m below mean sea level (MSL) and are not able to be used in deeper areas.

Topographic data was acquired using a DJI Matrice 300 drone, equipped with a Zenmuse L1 sensor (illustrated in Figure 2.1). This state-of-the-art combination produces high-resolution Light Detection and Ranging (LiDAR) data. Under typical wind conditions, the LiDAR drone can effectively cover an area of 0.5km² in a single drone flight, as demonstrated during the Maiden Island survey. LiDAR datasets are incredibly dense, capturing any feature capable of reflecting its signal. The raw LiDAR data yielded approximately 20 points per square meter across both Jumby Bay and Maiden Island, resulting in 41 million data points. This data required extensive processing for subsequent modelling and client deliverables. Figure 2.2 showcases both the satellite derived bathymetry and LiDAR dataset.



Figure 2.1 Apparatus used for the LiDAR survey and initial results for the islands surveyed.

The post-processing involved implementing a classification algorithm to identify ground points and eliminate underwater points. This algorithm analyzed the return signal detected by the sensor and assessed the elevation changes between neighboring points. When there is a significant elevation change, such as between the ground and a rooftop, the algorithm categorizes the higher point as noise.

After extracting the ground elevations, the data was interpolated to produce a high-resolution dataset with a 0.5m grid spacing. The post-processed dataset yielded a more refined terrain model consisting solely of ground elevations. A comparison between the datasets before and after the post-processing routine can be observed in Figure 2.3, which clearly highlights the improvements in terrain representation and data accuracy.

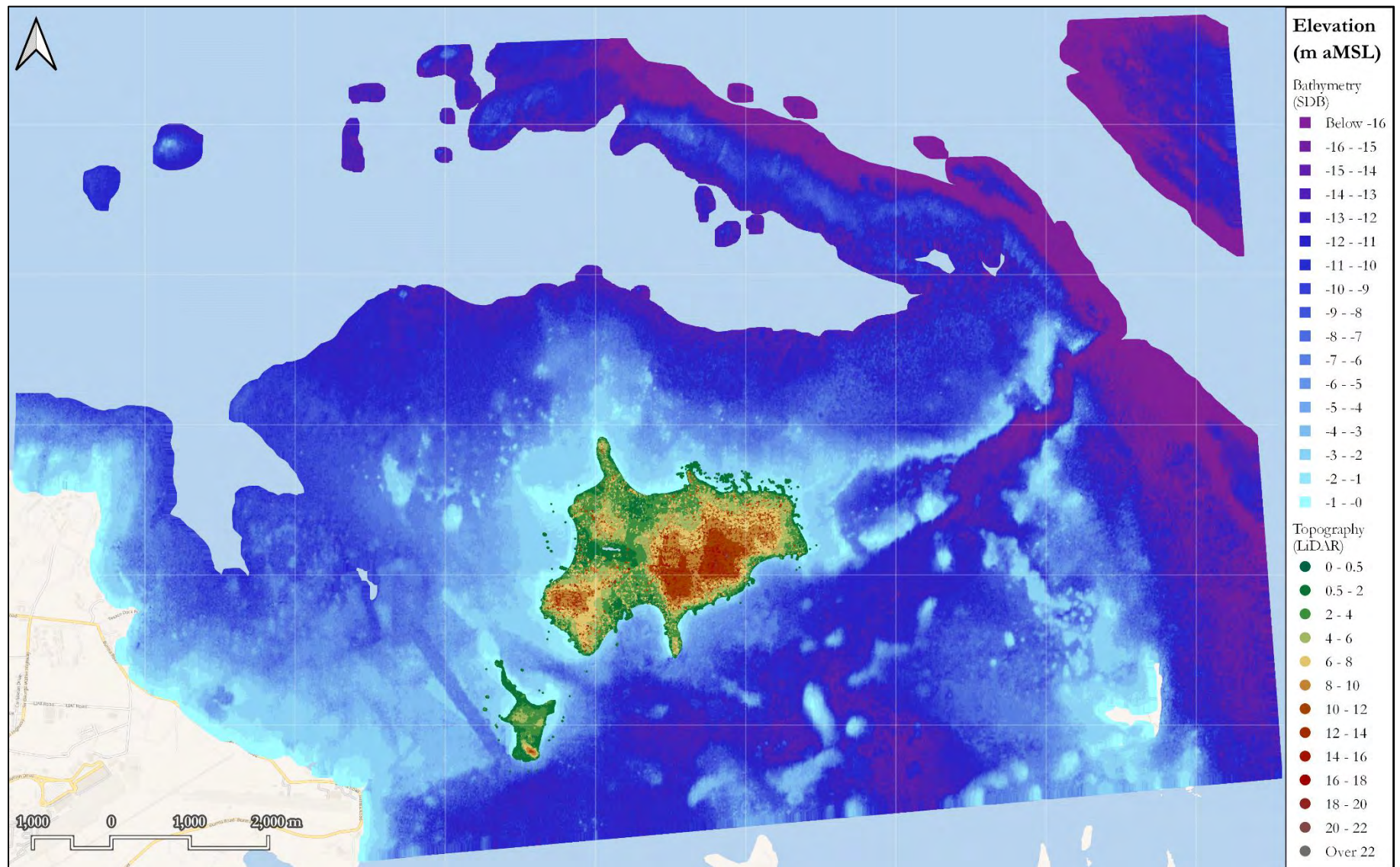


Figure 2.2 Satellite-derived bathymetry and raw LiDAR dataset for Jumby Bay and Maiden Island.

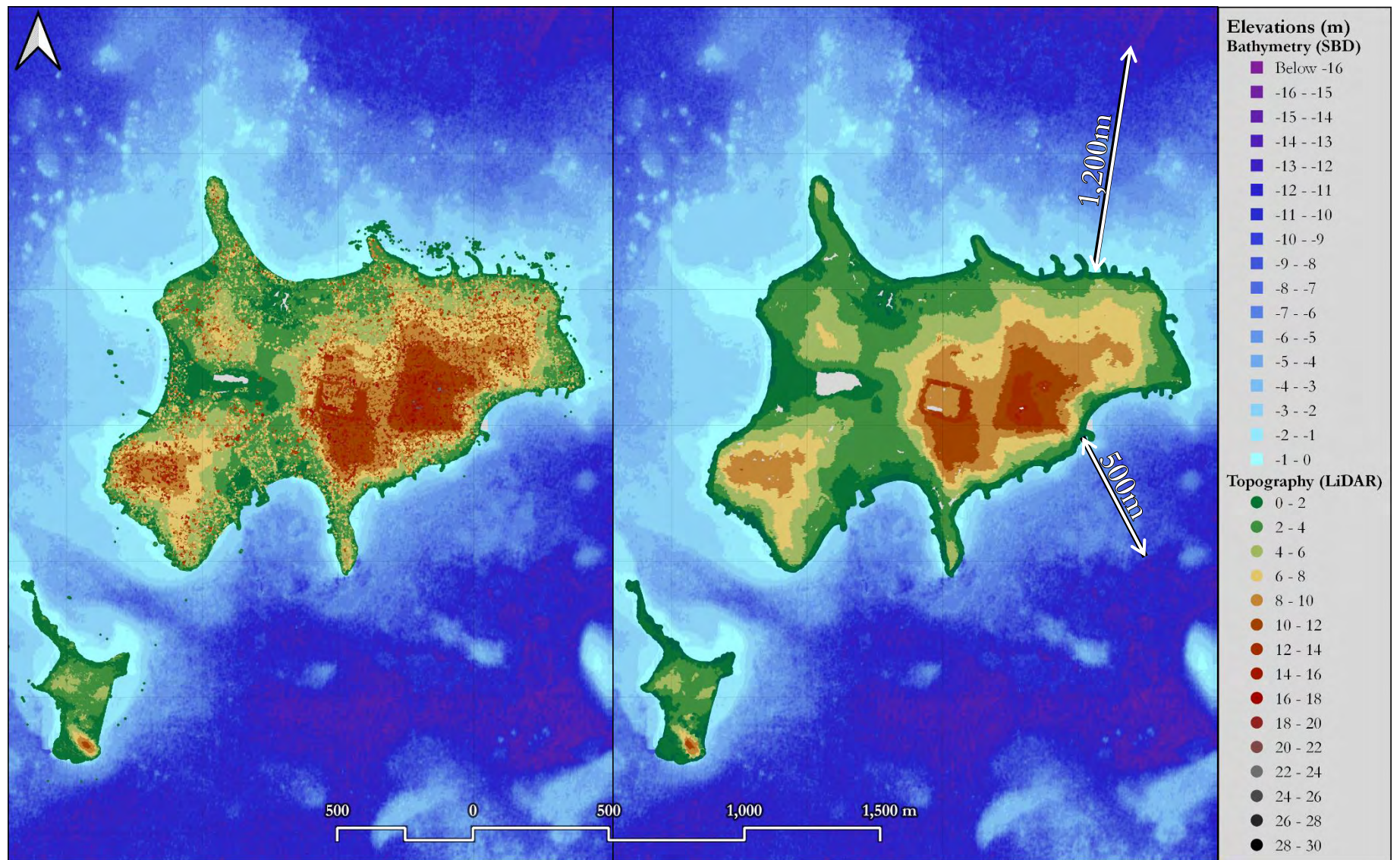


Figure 2.3 LiDAR dataset before (left) and after (right) the data classification algorithm was used to extract terrain levels.

The acquired data offers invaluable insights into the topography and bathymetry of the study sites. Figure 2.2 shows that the islands are connected to Antigua by an underwater shelf with an elevation of approximately 3m below mean sea level. This shelf is interrupted by a dredged boat channel located to the west of Maiden Island. The southern regions of both islands exhibit steeper bathymetry compared to the northern regions. In the south, depths of 16m can be found within just 500-750m from the shoreline, whereas in the north, the same depth is reached at around 1,200m from the shoreline (Figure 2.2). These findings corroborate field observations of shallower rock and pavement platforms in the north.

Another noteworthy feature is the shallow platform situated to the northeast of Jumby Bay. This platform has a minimum depth of 2m below MSL and extends approximately 300m in width. It has the potential to offer shelter during northerly swell events. Additionally, a gap in the offshore reef line aligns with the North Sound body of water. This gap spans roughly 100m in width and reaches a depth of 16m. The gap in the reef line and the deep section to the west could contribute to increased wave exposure along the eastern shoreline. During the site visit, no natural beaches were observed on the eastern shoreline, which may indicate that the wave climate is too dynamic for stable beach formation.

2.1.2 Beach Profiles

The gridded data from the satellite-derived bathymetry (SDB) and LiDAR topography required georeferencing in two aspects: horizontal and vertical. Horizontal georeferencing ensures that the elevations correspond with the existing feature locations, while vertical georeferencing aligns all elevations in relation to a vertical datum, such as mean sea level (MSL). For georeferencing the elevation data, physical beach profiles were measured using a Real-time Kinematic (RTK) Global Positioning System (GPS) instrument setup. The setup involved establishing a fixed base station that communicates with a mobile receiver. The mobile receiver was employed to measure perpendicular beach profiles, focusing primarily on the sandy areas of the islands. Mangrove-covered regions, such as the southwestern shoreline of Jumby Bay, were not surveyed on land.

In total, 95 beach profiles were collected around both islands. These profiles extended from the back of beach areas to a nearshore depth of approximately 1.5m below MSL. Figure 2.4 illustrates the measured beach profiles for both islands, indicating the maximum and minimum elevations of each profile. Points in the figure follow the colour scale of previous figures, with blue points representing areas below MSL. After measuring the profiles, data processing was conducted to vertically rectify the points to MSL and horizontally rectify the data to the Universal Transverse Mercator (UTM) Zone 20 coordinate system.

The length of the beach profiles can be used to describe the steepness of an area, as the vertical ranges are similar. Generally, profiles taken on the western shoreline of Jumby Bay exhibited a more gradual slope, while profiles measured within the northeast beach cells were steeper. Along the northern coast, the back-of-beach elevations ranged between 0.7m and 2m. The main beach on the western coast had a back-of-beach elevation of approximately 1m, and the land behind this area would likely be flooded during a hurricane.

Beach profiles taken on Maiden Island revealed various features. The northeast and east beach areas had gentler slopes than other shoreline sections, possibly due to the reef platforms surrounding the island. Along the eastern coast, the shoreline had been cut back to form a 2m high scarp and a shallow wading area with depths of around 0.8m. The southern shoreline exhibited the steepest beach profiles and reef structures close to the waterline. Seven profiles have been plotted on the same scales in Figure 2.5, with the location of each profile denoted by letters A through F in Figure 2.4.

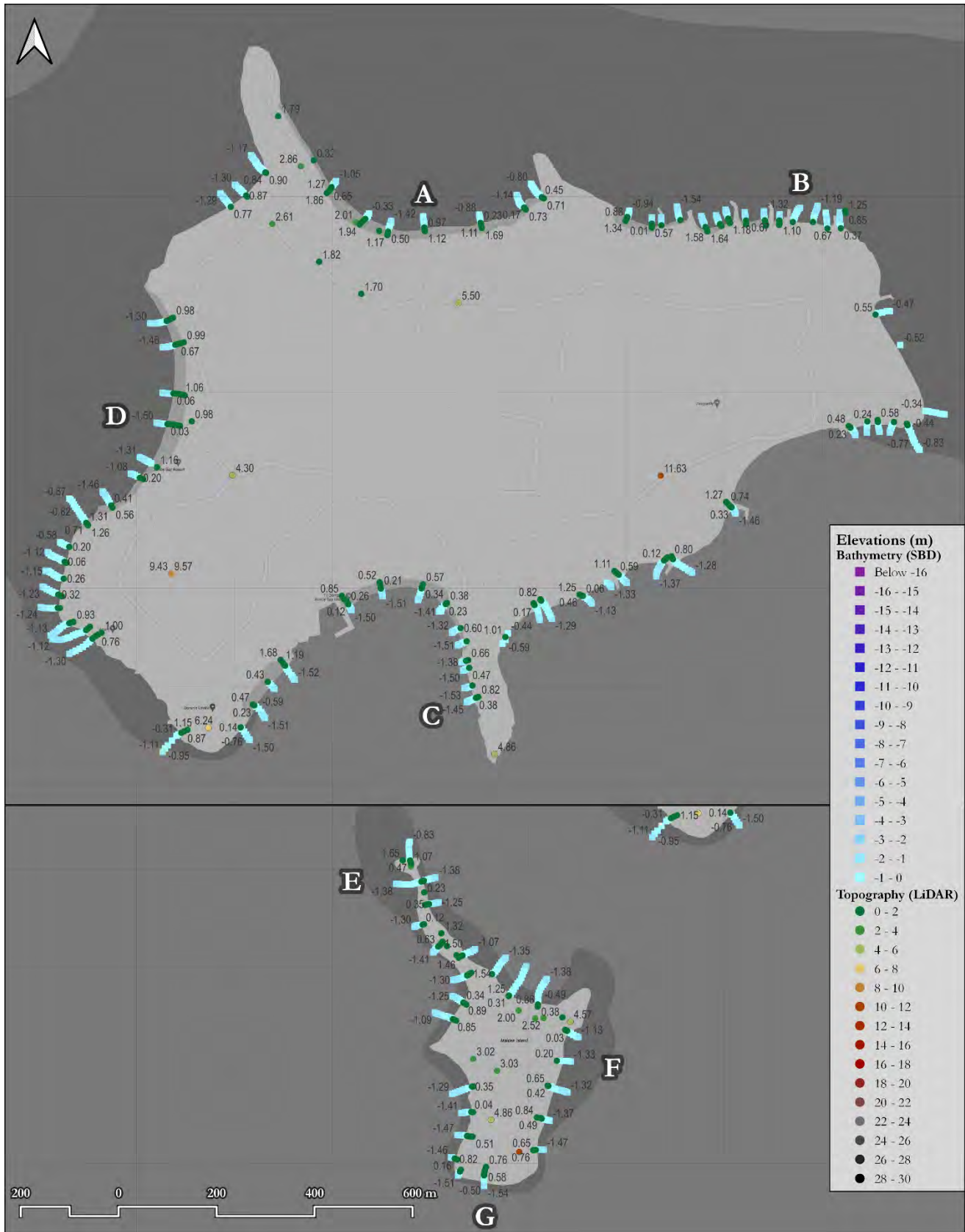


Figure 2.4 All beach profiles measured during the data collection exercise.

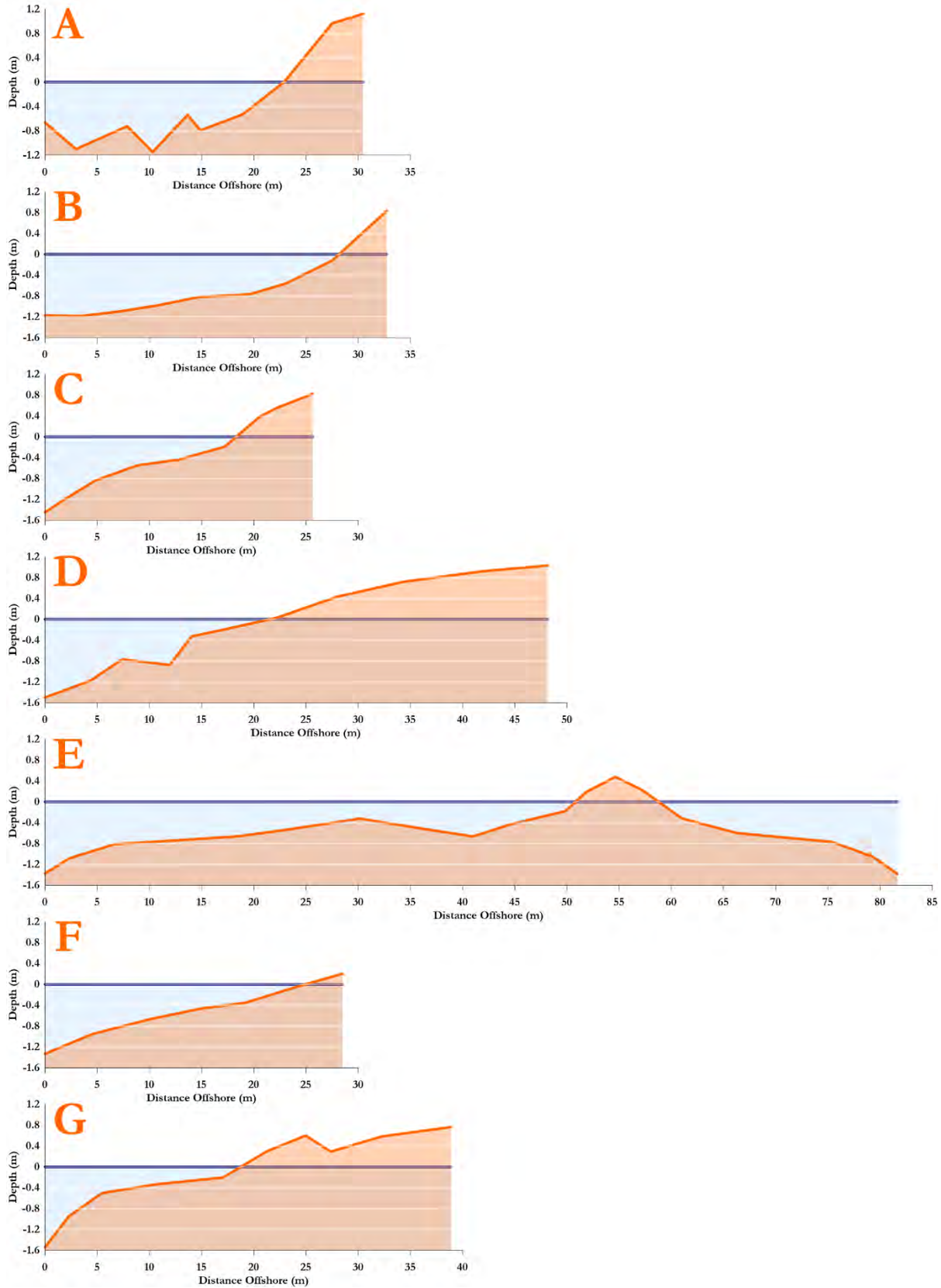


Figure 2.5 Beach profiles highlights from the data collection exercises.

Profiles A through D were obtained from Jumby Bay. Profiles A and B display a similar overall shape, exhibiting an average beach slope of 1(V):8(H). Profile C features a shallower foreshore, with a 10m wide zone at a depth of approximately 0.5m below MSL, resulting in a gentler slope of 1(V):12(H). Profile D, taken from the center of the public beach area, emphasizes the small rock platform at a depth of around 0.8m and has a beach slope of about 1(V):14(H).

Profiles E through G were collected from Maiden Island. Profile E, the longest profile, was extracted due to the ability to traverse from the western side of the peninsula to the eastern side. This profile distinctly demonstrates that the western bay area is shallower than the eastern region, with the beach slope on the western side being exceptionally gentle at 1(V):40(H).

Profile F reveals the shallow area at the base of a man-made scarp and has a beach/nearshore slope of 1(V):20(H). Profile G, taken between two revetment structures along the southern coast, displays three distinct beach slopes. The beach area, comprised of pebbles (approximately 5cm diameter stones), exhibited a beach slope of 1(V):10(H). In the foreshore, there was a platform with a gentle slope of 1(V):15(H), while beyond the platform, the slope steepened to 1(V):5(H) until the end of the profile.

Beach profile measurements provided critical information in the wading coastal area, which is typically difficult to obtain with SDB datasets. Moreover, the LiDAR sensor is only able to measure elevations on dry land areas. Utilizing measured beach profiles helps to bridge the gap between the dry beach and nearshore regions, ensuring a comprehensive understanding of the coastal environment.

2.2 Seafloor Classification

Seafloor classification, which was derived from satellite imagery, offers a range of advantages that span across various applications. These benefits include improved habitat mapping for conservation planning and resource management, an enhanced understanding of marine ecosystems to monitor ecosystem health and predict potential impacts of human activities or climate change, and informed coastal development and planning. Additionally, seafloor classification data support marine archaeological studies, aid in navigational safety, contribute to better sediment transport modelling, and assist in fisheries management by identifying essential habitats and spawning grounds. Overall, seafloor classification promotes a better understanding of marine ecosystems, supports informed decision-making, and contributes to the sustainable management of coastal and marine resources.

Seafloor classification (SFC) data was obtained from multiple satellite images provided by EOMAP®. The images were captured in the years 2003, 2009, 2012, 2015, 2017, and 2022. The distribution of the datasets varied from year to year, as the extent of a given year's data depends on the clarity of the image and water depths. As previously mentioned, the maximum water depth that can be calculated is 16m, which is also the maximum depth for producing seafloor classification results.

Data extracted for 2003 and 2009 had the smallest extents, with total areas of 16.8km² and 15.8km², respectively. The remaining years (2012, 2015, 2017, and 2022) had total areas ranging between 23.5km² and 28km². The difference in areas is attributed to the later years having more data to the northwest and west of the islands. The largest extent came from the year 2015, which likely had the clearest satellite image, resulting in a greater amount of extractable data.



In this analysis, the seafloor classification groups consist of coral-dominated, rock-dominated, seagrass-dominated (dense or sparse), and sediment-dominated categories. Data extracted for the years 2003 and 2009 are illustrated in Figure 2.6, while the data for 2012 and 2015 are presented in Figure 2.7. Figure 2.8 displays the datasets for the years 2017 and 2022.

When comparing the seafloor classifications between 2003 and 2009, the shared areas exhibit similar classifications. The northern coastline features a mix of all the classification groups, while the southern coastline is predominantly sediment-dominated. Differences in the overall pattern can be attributed to each dataset having a unique extent. For instance, the 2009 dataset exhibits a higher area of coral cover (34% compared to 31% in 2003); however, this is due to a larger portion of the coral platform northeast of Jumby Bay being classified in 2009.

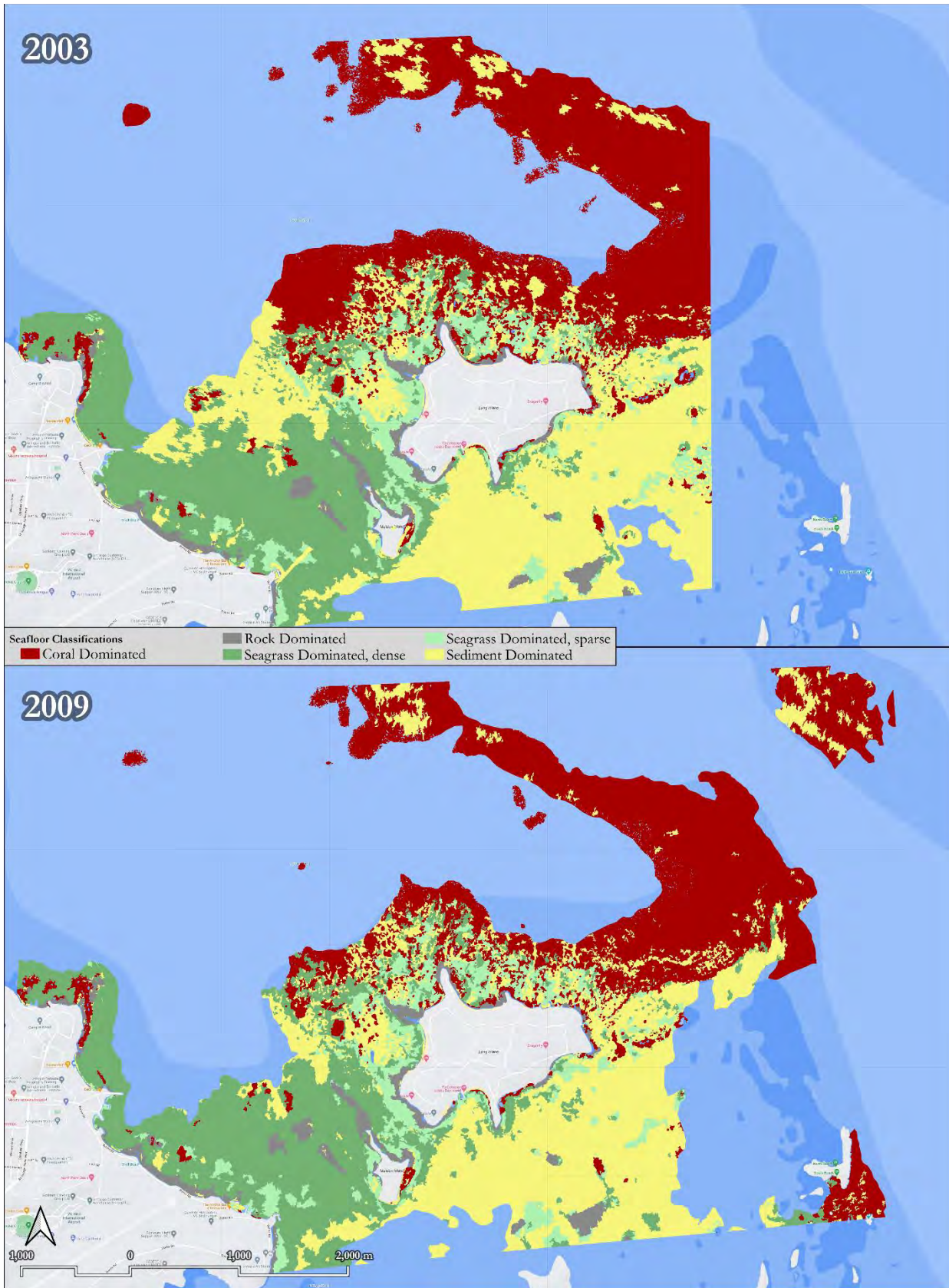


Figure 2.6 Seafloor classification data for the years 2003 and 2009.

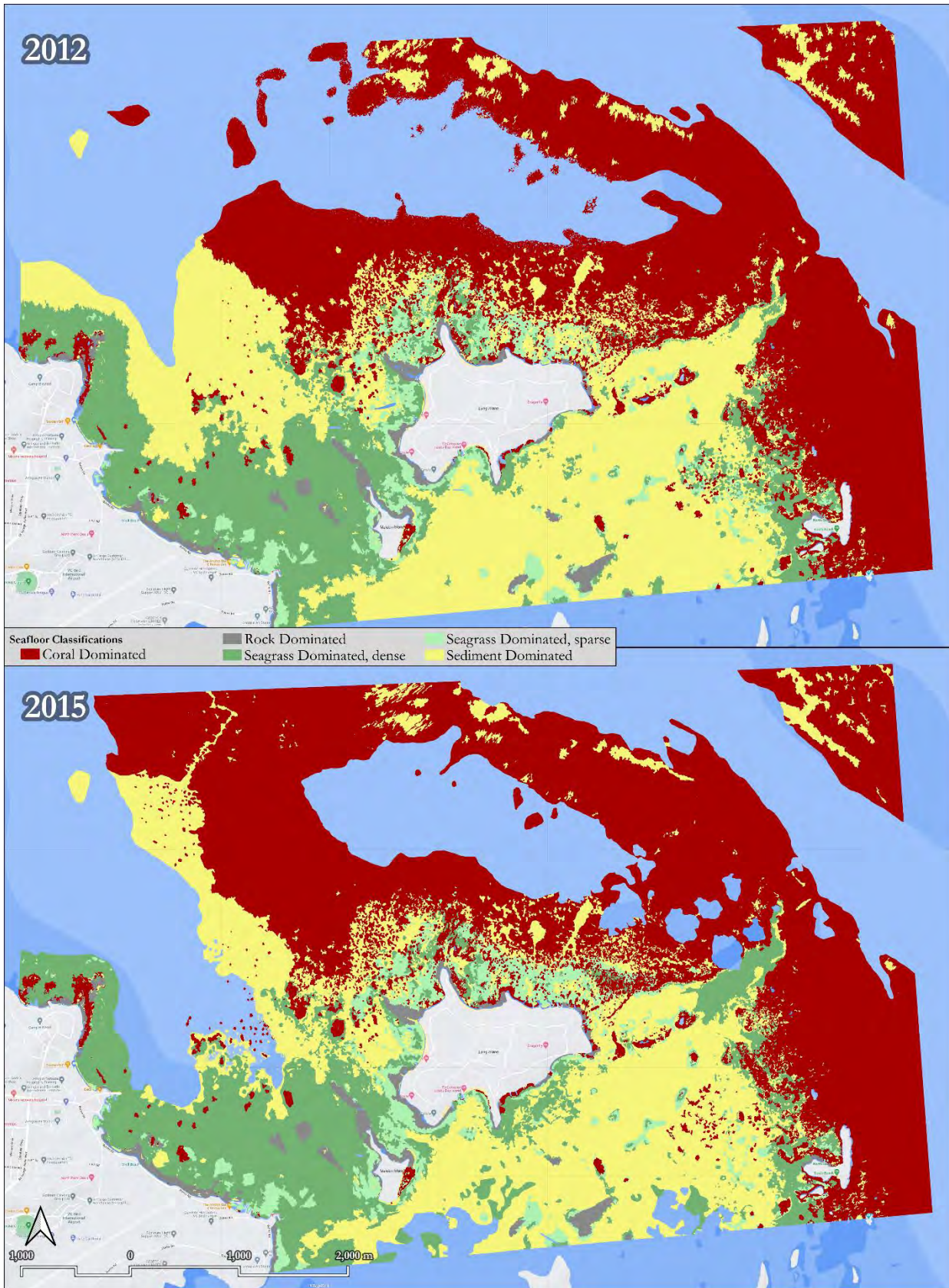


Figure 2.7 Seafloor classification data for the years 2012 and 2015.

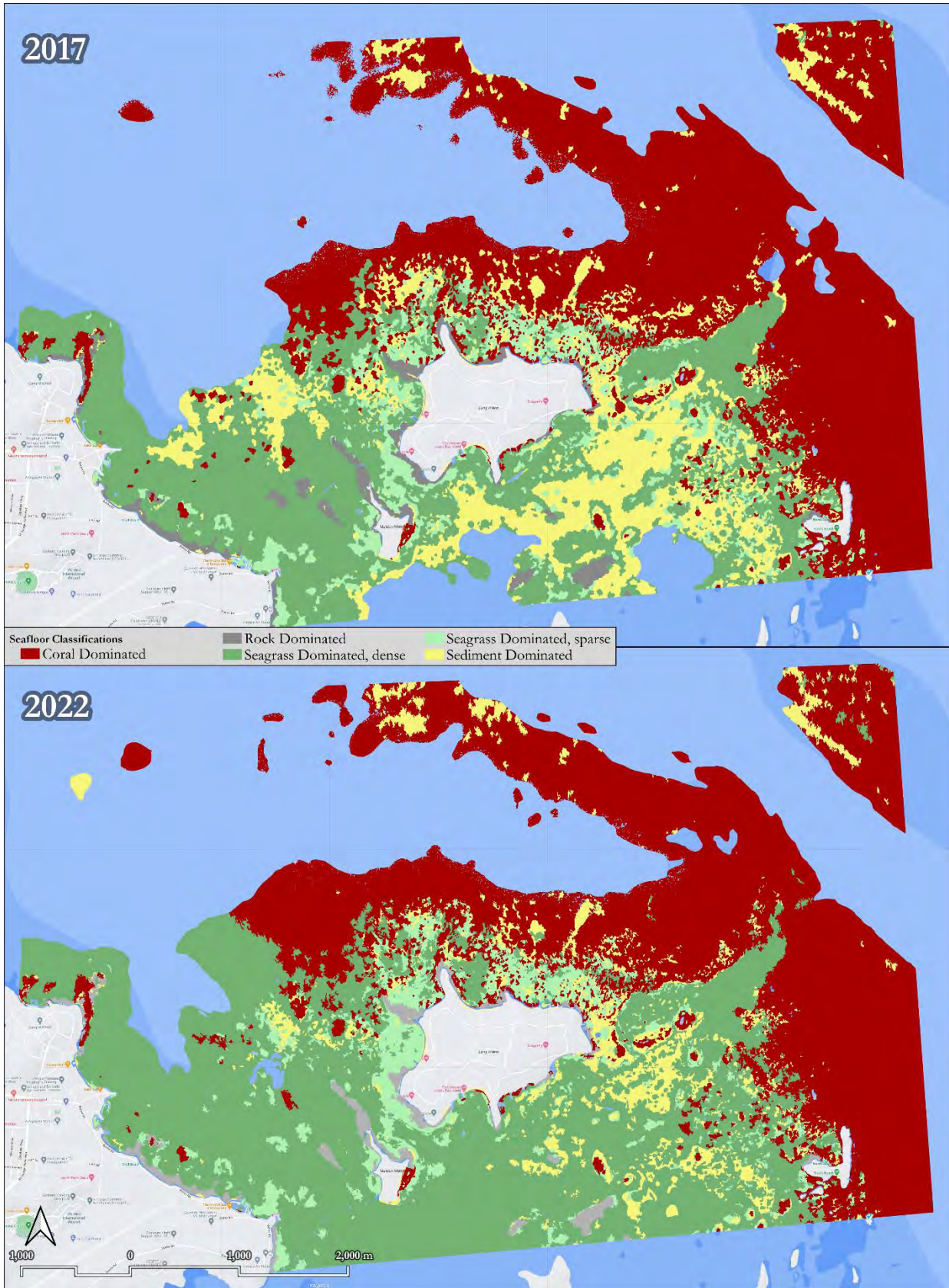


Figure 2.8 Seafloor classification data for the years 2017 and 2022.



In 2012, the satellite image appeared to be quite clear, enabling the extraction of classification data from the North Sound to the eastern drop-off. The classifications from 2009 and 2012 were similar in shared areas, with general patterns displaying coral dominance to the north, sediment dominance to the south, and seagrass dominance to the west.

The datasets for 2012 and 2015 had similar overall areas. However, the 2015 seafloor classification data included more results to the northwest compared to the 2012 dataset. The overall shape of the coral cover areas remained consistent, indicating a stable environment. Western offshore areas exhibited similar distributions for both years. The southern offshore area, which was dominated by sediment in 2009 and 2012, transitioned to a mix of seagrass and sediment in 2015. This change is particularly noticeable in the offshore area southeast of Jumby Bay.

Classification datasets for 2017 and 2022 were similar in area and distribution, as shown in Figure 2.8. The 2017 results revealed a significant increase in seagrass dominance along the southern area, with seagrass and sediment areas nearly equally distributed. Seagrass was observed along the shoreline of Jumby Bay and adjacent shallow platforms, leaving a narrow area of sediment-dominated pavement in between. The northern shoreline experienced an increase in seagrass density, with areas classified as sparse in 2015 being classified as dense in 2017. The coral-dominated zone to the northeast remained consistent with previous years (2015 and 2012).

The 2022 dataset showed another substantial increase in seagrass dominance on the seafloor. The area south of the island was predominantly covered by dense seagrass, with minimal sediment or coral areas. Fortunately, the coral areas to the south from the 2017 dataset persisted in the 2022 dataset. In the north, seagrass area and density also increased, with sediment dominance becoming negligible.

The proliferation and growth of seagrass may be associated with large-scale climate change impacts. Warmer temperatures and seas foster nutrient-rich environments that promote the growth of benthic plants such as seagrass. During the site visit, dense seagrass was observed at multiple shoreline locations, validating the nearshore classification. However, for offshore projects, it is recommended that the classification data be verified through a ground-truthing exercise.

2.3 Beach Sediment

Coastal sediment analysis offers valuable insights into coastal processes and plays a crucial role in evaluating the aesthetic appeal and comfort of beach or coastal zones. In Jumby Bay, several properties have imported sand to create beach cells that were not present originally. Based on client interviews, it was determined that the western side of the island predominantly features natural beaches, while other beaches have been constructed.

Maiden Island, formed from dredged material originating from the nearby channel, exhibits a sediment composition of sand, shell, and coral fragments. Coral fragments measuring 0.05m to 0.1m in length are abundant along the eastern coast, where they form a large, stable scarp. Figure 2.12 shows this scarp and other significant features.

A total of 20 sediment samples were collected from both islands for sediment type classification. Samples SS1 through SS13 were obtained from various beach cells on Jumby Bay, while samples SS14 through SS20 were collected from Maiden Island. These samples were sent to the University of the West Indies (UWI), Mona's geotechnical lab, where they underwent visual inspection, air-drying, and standard dry sieve analysis to determine grain size distribution and other characteristic parameters.

The locations of the sand samples, along with their mean grain size diameter, are presented in Figure 2.9 (Jumby Bay) and Figure 2.11 (Maiden Island). Except for sample SS5, which was collected from the back of the beach area, all other sediment samples were taken from the swash zone, the area where waves break along the beach. On Jumby Bay, the mean grain sizes ranged from 0.242mm to 0.75mm, with all samples classified as light brown sand (Table 2-1). Samples from the southern coast (SS6 to SS11) were generally finer, featuring median diameters (D50) up to 0.35mm, an optimal size for aesthetics and walking comfort.

The north-eastern sector of the island, most exposed to wave activity due to prevailing trade winds, exhibited sediment samples with mean diameters of 0.32mm and 0.42mm. This can be attributed to stronger waves stirring up larger sediment particles in the swash zone. Sample 3, an outlier on the island, had the largest grain size. Interviews revealed that this sand was imported to the island, with numerous shell fragments contributing to the increased mean diameter.



Figure 2.9 Location of sediment samples taken on Jumby Bay.

Table 2-1 Grain size distribution for all samples taken on Jumby Bay.

| Specimen | Type | Diameters (mm) | | | | | % Gravel | % Sand | % Silt Clay |
|----------|------------------|-----------------|-----------------|-----------------|-----------------|-----------------|----------|--------|-------------|
| | | D ₅₀ | D ₉₀ | D ₆₀ | D ₃₀ | D ₁₀ | | | |
| SS1 | Light Brown Sand | 0.332 | 0.670 | 0.376 | 0.249 | 0.168 | 0.1 | 99.9 | 0 |
| SS2 | | 0.513 | 0.855 | 0.585 | 0.386 | 0.291 | 0.2 | 99.8 | 0.1 |
| SS3 | | 0.750 | 1.789 | 0.910 | 0.495 | 0.252 | 3.5 | 94.3 | 2.1 |
| SS4 | | 0.340 | 0.451 | 0.362 | 0.298 | 0.245 | 0.1 | 99.7 | 0.2 |
| SS5 | | 0.233 | 0.428 | 0.272 | 0.182 | 0.140 | 0.7 | 99.3 | 0 |
| SS6 | | 0.269 | 0.456 | 0.306 | 0.201 | 0.151 | 0.5 | 99.5 | 0 |
| SS7 | | 0.293 | 0.761 | 0.340 | 0.209 | 0.153 | 2.1 | 97.8 | 0.2 |
| SS8 | | 0.351 | 0.675 | 0.388 | 0.284 | 0.190 | 0.8 | 99.2 | 0 |
| SS9 | | 0.242 | 0.537 | 0.286 | 0.185 | 0.143 | 0.4 | 99.3 | 0.3 |
| SS10 | | 0.317 | 0.447 | 0.343 | 0.264 | 0.180 | 0.1 | 99.6 | 0.3 |
| SS11 | | 0.680 | 0.508 | 0.310 | 0.194 | 0.140 | 0.5 | 99.5 | 0 |
| SS12 | | 0.421 | 0.786 | 0.481 | 0.336 | 0.255 | 0.1 | 99.9 | 0 |
| SS13 | | 0.325 | 0.534 | 0.358 | 0.261 | 0.175 | 0 | 100 | 0 |

Sediment sizes on Maiden Island were generally large (Table 2-2), which can be attributed to the presence of sizable coral fragments (10cm and above) scattered across the island. The origin of these fragments is believed to stem from two sources: dredging works conducted for the access channel and unsuccessful reef ball experiments.

Consequently, only three of the seven samples collected (SS14, SS16, and SS20) could undergo full sieve analysis. The remaining samples required separation, with only grain sizes smaller than 4mm being analyzed. This was particularly true for Sample 18, collected from the cobbly beach to the south, which exhibited the largest grain size (1.01mm) in the entire analysis.

Several reef ball structures can be observed in the nearshore area of the island. On the eastern side of the peninsula, two points feature reef ball structures that connect to the shoreline, creating enclosed seawater pools. Due to the presence of grey and white coral fragments in this area, no samples were collected for analysis.



Figure 2.10 Image of typical sediment along this shoreline.



Figure 2.11 Location of sediment samples taken from Maiden Island.

Table 2-2 Grain size distribution for all samples taken on Maiden Island.

| Specimen | Type | Diameters (mm) | | | | | % Gravel | % Sand | % Silt % Clay |
|----------|------------------------|-----------------|-----------------|-----------------|-----------------|-----------------|----------|--------|------------------|
| | | D ₅₀ | D ₉₀ | D ₆₀ | D ₃₀ | D ₁₀ | | | |
| SS14 | Light Brown Sand | 0.391 | 1.050 | 0.369 | 0.306 | 0.202 | 4.5 | 95.5 | 0 |
| SS15 | | 0.492 | 2.980 | 0.623 | 0.352 | 0.245 | 12.6 | 87.4 | 0 |
| SS16 | | 0.432 | 1.930 | 0.506 | 0.344 | 0.369 | 9.3 | 90.7 | 0 |
| SS17 | | 0.581 | 1.845 | 0.685 | 0.408 | 0.296 | 8.2 | 91.8 | 0 |
| SS18 | | 1.010 | - | 1.470 | 0.724 | 0.535 | 32.9 | 66.5 | 0.6 |
| SS19 | | - | - | - | - | - | - | - | - |
| SS20 | | 0.275 | 0.614 | 0.320 | 0.200 | 0.150 | 1.5 | 98.5 | 0 |

Sample 19 (SS19) was collected to gain a deeper understanding of the sediment on the eastern side of the island, with the sample and location depicted in Figure 2.12. This sample contained whole shells and coral fragments, found at the base of the scarp along the south-eastern shoreline. It is important to note that the scarp was artificially created using heavy machinery, with the intention of constructing a more tranquil beach area on the landward side. Signs of undercutting can be observed on the scarp, which may be a consequence of extreme events, such as hurricanes and swells.



Figure 2.12 Images of SS 19 and conditions around it (scarp and coral fragments beach).

2.4 Land Use Changes

The primary island of Antigua exhibits a variety of land use classifications that correspond to the distribution of human settlements and commercial activities. In contrast, the smaller offshore islands of Jumby Bay and Maiden Island predominantly feature woodland and forest classifications (PGDM, 2010). A thorough examination of historical satellite images reveals a noticeable decline in forest cover, accompanied by an increase in grasslands and development across the main island, Jumby Bay. This development is characterized by low-density housing, which allows for the preservation of its natural vegetation. Temporary reductions in vegetation on this island can be attributed to renovation or construction projects.

2.5 Rainfall Patterns

The hydrological regime of Jumby Bay and Maiden Island is predominantly governed by rainfall, evapotranspiration, and oceanic tidal influences. The basin primarily acquires water through infrequent rainfall events, which infiltrate the sandy soil and recharge the underlying groundwater. This groundwater eventually discharges into the ocean or surface water bodies, such as ponds.

Two distinct types of flooding must be considered: riverine flooding and pluvial flooding, otherwise known as precipitation flooding. Riverine floodplains possess easily identifiable drainage paths, including rivers, streams, roadways, or engineered channels. Riverine flooding occurs when stormwater runoff volume surpasses the capacity of these designated drainage paths.

In contrast, pluvial flooding results from inconspicuous depressions in the landscape that may not be easily discernible. Overflow from these depressions can lead to flooding. A typical example of pluvial flooding arises when natural drainage paths become obstructed, rerouting runoff, and subsequently causing floods. Another instance involves sinkholes, which can create ponding in the surrounding area during heavy precipitation events.

The watersheds within the project site are characterized by low-lying terrain and lack rivers or significant flow paths. Consequently, the islands are susceptible to pluvial flooding. To quantify this flood risk, it is crucial to analyse rainfall patterns over time. Antigua typically experiences 127 rainy days and 238 sunny days per year. Rainfall data from 1981 to 2021 was obtained from the NASA Langley Research Center (LaRC) website (Figure 2.13). Elevated precipitation levels are observed during September, October, and November, which correspond with the conclusion of the hurricane season.

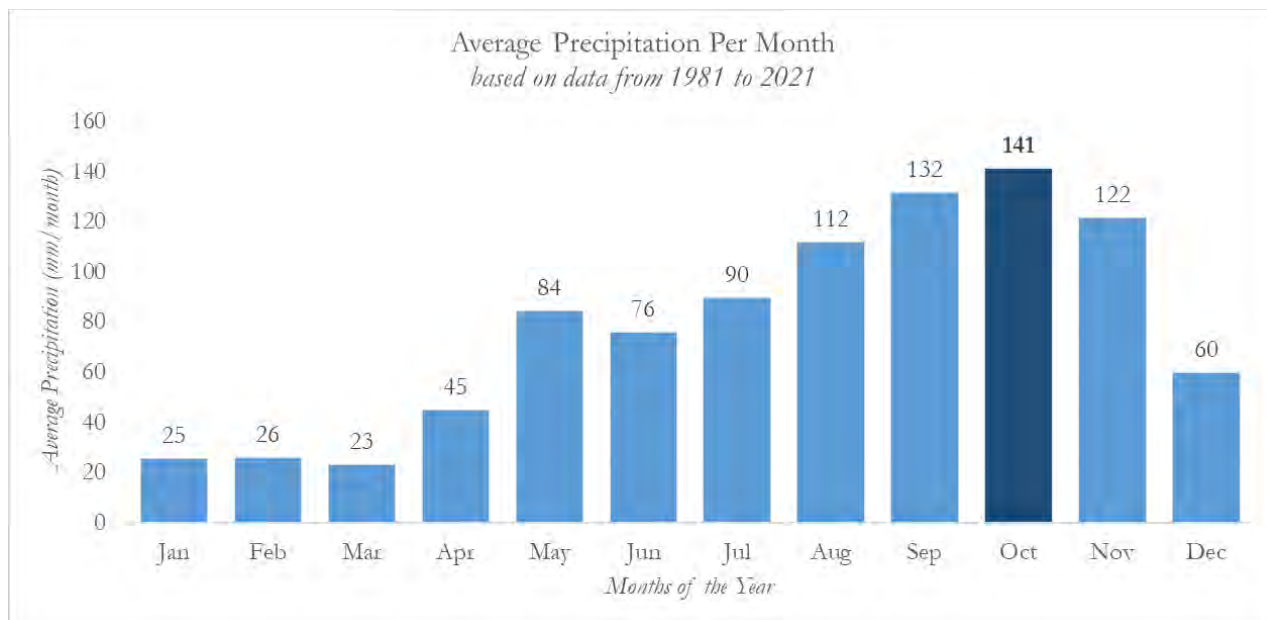


Figure 2.13 Average monthly rainfall for the period of 1981 to 2021 (data source LaRC).

The assessment of average daily precipitation values provided insights into their variability across different years. This analysis also highlighted anomalies, illustrating the deviation of a specific year's precipitation from



the long-term average daily rainfall. Over the forty-year period, these anomalies ranged between -1.2 mm/day and 2.1 mm/day. Notably, an exceptional rainfall anomaly occurred in 2011, which fell within a four-year timeframe (2010-2013) characterized by heightened precipitation levels.

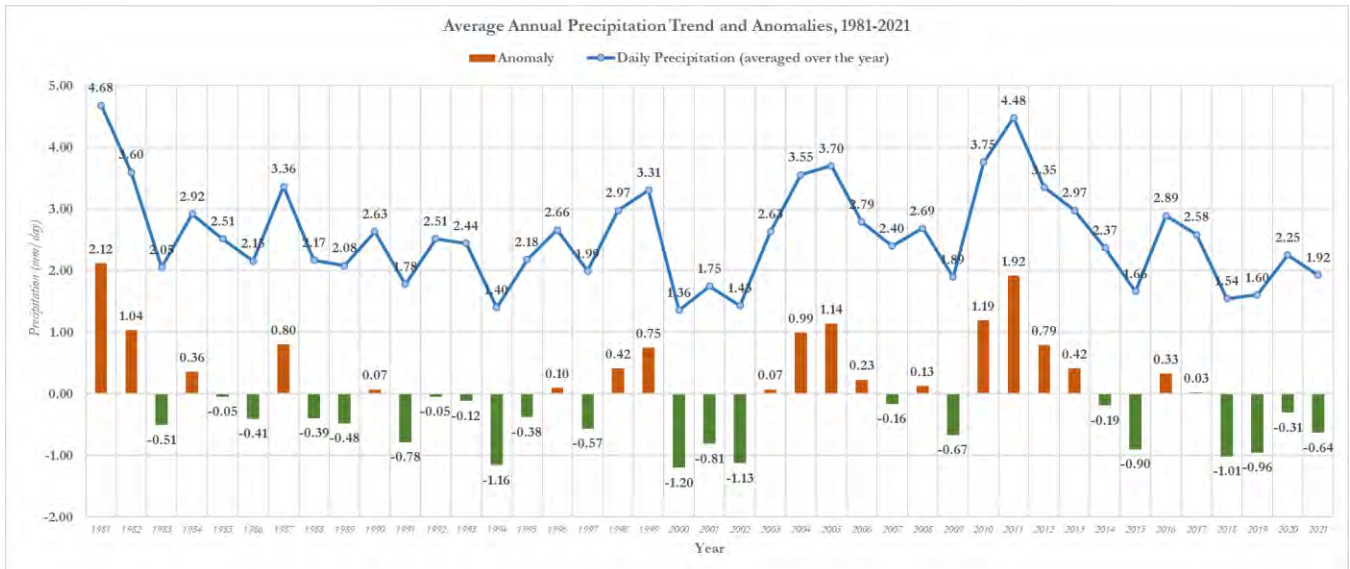


Figure 2.14 Average daily rainfall and average daily rainfall anomalies for the years 1981 to 2021 (data source LaRC).

A more in-depth examination of the 2011 rainfall patterns was conducted based on the anomaly findings. Within the studied period, 2011 recorded the second-highest annual rainfall, with four months - July, August, September, and November - registering total rainfall depths exceeding 200mm. The increased precipitation during these months could be attributed to the passage of two tropical storms in September and one in August.

Tropical storms and other weather systems can deliver substantial rainfall within a brief period. Such events are typically further categorized as rainfall events with specific return periods. Daily rainfall data was employed to conduct extremal statistical analyses for identifying design events. The outcomes of this analysis for peak hourly rainfall intensity are presented in Table 2-3.

Table 2-3 Calculated 24-hour rainfall intensities.

| Rainfall Event | Peak Hourly Rainfall Intensity (mm/hr) |
|----------------|--|
| 2-year | 12.9 |
| 10-year | 19.8 |
| 10-year | 25.0 |
| 25-year | 32.0 |
| 50-year | 37.2 |
| 100-year | 42.4 |

2.6 Stakeholder Identification

Jumby Bay Island Company (JBIC) Ltd enjoys a strong reputation across Antigua. Operating as a self-regulating island, it boasts local utilities and personnel. The island employs approximately 600 individuals in various roles, including property management, restaurant staffing, ferry operations, and security, as well as support positions in the canteen, laundry, and large-scale clean-up facilities.

Property owners are typically represented by JBIC, which unifies them as a collective entity. It can be inferred that any prospective construction activities would be spearheaded by JBIC on the property owners' behalf. As the representative of the owners and being heavily reliant on local staff, JBIC is regarded as the primary stakeholder in any future projects. It is crucial to preserve the island's luxurious ambiance and friendly culture as it continues to develop.

The Department of Environment (DoE) of Antigua and Barbuda serves as the principal environmental regulator on the island. They mandate that any implemented works do not result in long-term detrimental impacts on the property or its adjacent nearshore areas. The islands feature low-density housing, managed by a cohesive group of owners. Consequently, there is less emphasis on potential impacts on neighbouring properties. This is because properties are situated at a reasonable distance from both the shoreline and adjacent properties. Nevertheless, the DoE remains deeply committed to ensuring that any future projects do not adversely affect the marine environment. This commitment can be demonstrated through monitoring marine life populations and conducting coastal process modelling.



2.7 Coastal Structures Inventory

During two comprehensive site visits, a thorough survey of all coastal structures on the islands was carried out by our team of coastal engineering experts. Each structure was meticulously assessed and documented, taking into account the type, construction material, and approximate dimensions. In addition to these details, we also assigned a quality grade ranging from 1 (Very Good) to 5 (Very Poor) to each structure.

The grading scheme employed is rooted in two key factors: the presumed stability of the structure and its ability to endure wave attack, as determined by the appropriateness of its dimensions. Our assessment, accompanied by the full inventory of coastal structures, can be found in Appendix B. This detailed information will serve as a valuable resource for future analysis, monitoring, and planning of coastal infrastructure projects on the islands. Table 2-4 gives a brief description of each group.

Table 2-4 Classification scheme for structures on the island.

| Grade | Label | Description |
|-------|-----------|--|
| 1 | Very Good | Cosmetic defects that will have no effect on performance |
| 2 | Good | Minor defects that will not reduce the overall performance of the asset |
| 3 | Fair | Defects that could reduce performance of the asset |
| 4 | Poor | Defects that would significantly reduce the performance of the asset. Further investigation needed |
| 5 | Very Poor | Severe defects resulting in complete performance failure |

In general, coastal structures that received a grade of 1 exhibited superior quality and stability, such as well-maintained docks with securely fastened planks and boulder structures exhibiting minimal signs of dislodgement. At the other end of the spectrum, dilapidated groynes and remnants of old construction, which no longer serve their intended purpose, were assigned a grade of 5.

Over the years, the islands have seen numerous structures being constructed and subsequently removed, leading to a mix of varying quality and stability. During our survey, we assessed a total of 74 structures, with the majority receiving a grade of 2 or 3, indicating moderate to satisfactory conditions.

To provide a comprehensive overview, we have tabulated the counts for each grade and the corresponding locations of these structures. This information can be found below in Figure 2.15.

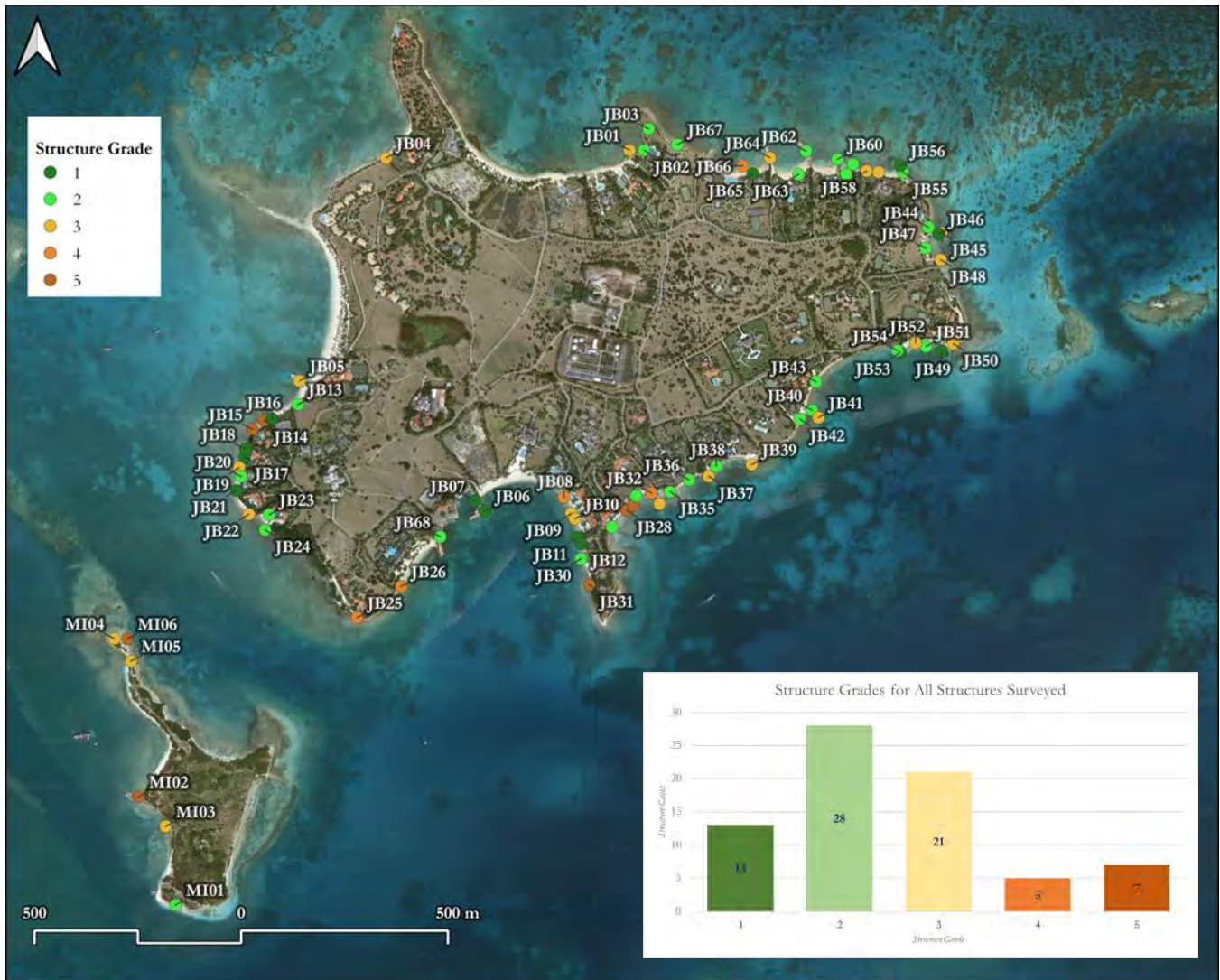


Figure 2.15 The location of the structures that were surveyed and their overall scores.

On Jumby Bay numerous boulder structures can be observed, with most of the properties featuring some form of armour structure. Our survey covered 21 boulder groynes and 21 boulder revetments, revealing varying degrees of stability and effectiveness among these structures.

Notably, the groyne structures on the eastern side of the island were found to be less effective in sediment retention relative to their lengths. Conversely, groyne structures on the western side, despite being generally smaller, demonstrated a greater capacity to hold sediment in place.

This information on the island's coastal structures, combined with an analysis of the local wave climate, will prove invaluable in informing future coastal engineering works.

3 Evolution of Coastal Areas

The coastal environment is dynamic, and this can be seen in multiple ways. As wave conditions vary over a year or even a decade, the responses of beach and marine life vary as well. This section of the report will highlight the progression of the shoreline, bathymetry, and benthic resources. The analysis is based on six years of data and the changes that occurred between each year.

3.1 Shoreline Changes

Analysing shoreline changes along beaches and erodible shorelines offers numerous advantages for coastal zone management, as it helps identify trends, assess risks, and inform decision-making for sustainable development. Some of these advantages include:

- Erosion and accretion detection: By monitoring shoreline changes, coastal managers can identify areas experiencing significant erosion or accretion, enabling them to prioritize intervention measures and allocate resources effectively.
- Understanding sediment dynamics: Analysing shoreline changes provides insights into sediment transport processes, which are crucial for designing effective coastal protection and restoration strategies, such as beach nourishment or sediment bypassing.

Long-term erosion and accretion patterns were estimated by performing a historical shoreline analysis along the islands' beach front. This process involves retrieving as many years as possible of satellite data for the location and having those images georeferenced to the same horizontal coordinate system. Afterward, each shoreline is digitised by using an algorithm that delineated where the blue water changes to light sand. Since the line digitised may be considered as always wet, these lines are used to represent the progression of the low water mark over time.

3.1.1 Jumby Bay

Beach profiles (sections highlighted earlier in Figure 2.5) show that there are gentler slopes on beaches to the west and south-west of Jumby Bay. In this area the average beach slope is 1(V):13(H). This indicates that over the tidal signal (0.6m) there may be up to an 8m shift in the waterline, which is considered as the error range for this analysis. The steep slopes to the north and east have a narrower error band of 5m.

It is important to note that this analysis highlights a few instances of a dynamic process and generalises periods of sediment transport. The analysis used requested satellite imagery that had an irregular frequency in the time between images. The satellite images were from 2003, 2009, 2012, 2015, 2017, and 2022. Three satellite images (2003, 2015 and 2017) were taken in the swell season between November and February. At this time there are typically higher energy waves, which may result in a narrower beach. The 2009 image was taken during the hurricane season of that year, but the season was not particularly active for Antigua. The other images were taken under the usually calmer summer conditions.

The results of the analysis are shown in a plan format and at measurement profiles. The profiles were drawn at mainly sandy locations as these were the most dynamic. After the profiles were drawn the differences in beach width over a year were calculated and then normalised by the number of years that had passed between the satellite images being taken. This formed the main result of beach change in meters per year. This rate is useful as it interpolates to indicate long-term trends.

Sections of shoreline with hard pavement, mangrove and structure were analysed with shoreline position only. Historical shorelines on Jumby Bay mainly highlighted the change in structures over time. Beach areas that experienced a fluctuation in width were mainly related to nourishment activities which were out of sync with the long-term trends. The full shoreline analyses are shown in Figure 3.1 to Figure 3.4. On an island-wide scale, it can be seen where the latest shoreline position (2022) is further back than other shorelines in the northern and western long beach areas.

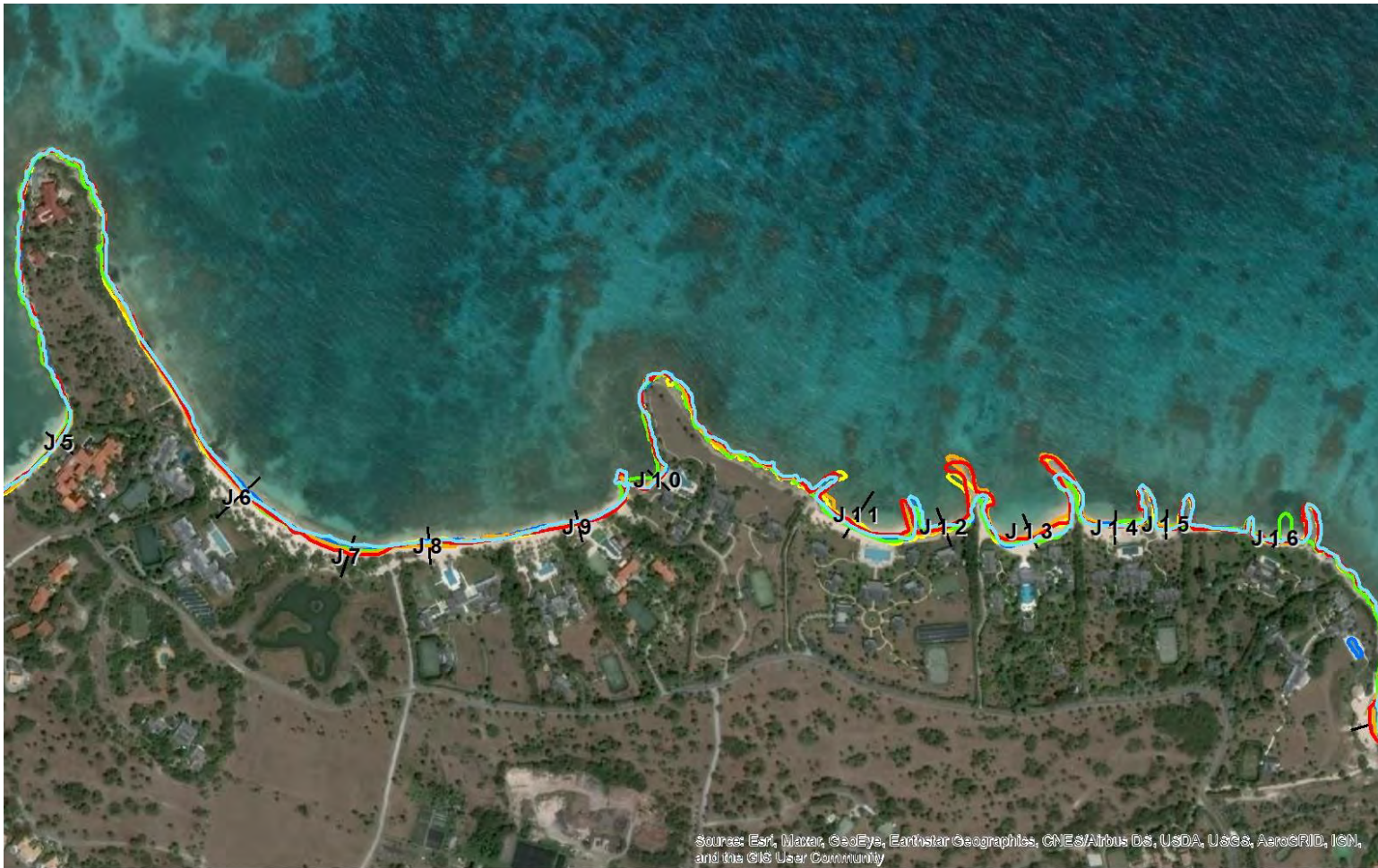
Shorelines plotted on the north-eastern corner of the island show the structures that have been built and extended with time. One structure that was present in 2003 was removed by 2009 with two other groynes put in place nearby. Two groynes (by profile J13) were extended a few times over the analysis period and are now twice the length that they were in 2003. The groyne west of J11 had the most fixed position up to 2017. The structure was later demolished and as such did not show up in the 2022 image or in the coastal structure inspection.

The eastern coastline is mainly rock platform and thus there was only a small recession of the shoreline over the analysis period.

The southern coastline has two different regimes, the southeast is quite exposed and as such has few natural beaches. This area has small beaches (30 to 50m of beach front) that are being maintained by groyne structures. The placement of four groynes on the southeast corner has allowed for some accretion of sediment. The southwestern portion of the island has a much calmer wave climate and gentler beach slopes. This area showed a stable beach cell with little sediment movement. Five groyne structures in this bay have helped to keep the bay stable and produced small salients.

The western coastline has a few built up beaches along six properties, and the main beach area that is used by the resort is also on the western coast. The western coast properties had small wedge type beaches that were contained by small groynes to form a triangular shape. The beaches in this area were generally stable with small rates of accretion and erosion over the analysis.

An aerial view of the shoreline progression is further supported by doing a profile beach measurement analysis. Profile measurements will show the changes in beach width and give an idea of whether the beach is stable, accreting or eroding. For this analysis, similar zones are used as before. These zones are north, east, west, and south. The northern section has profiles J6 through to J16 and the eastern section has J17. The eastern section has one profile because the remainder was hard pavement or structures. The southern section has profiles J18 through to J30. The western section was assessed with eight profiles (J1 to J5 and J31 to J33).



**Antigua - Long Island
 Shoreline Change**

LEGEND

- 2003
 — 2012
 — 2017
 — Measured point
- 2009
 — 2015
 — 2022

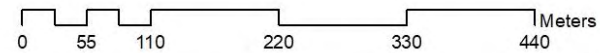


Figure 3.1 Shoreline position analysis for the northern section of Jumby Bay.



**Antigua - Long Island
 Shoreline Change**



LEGEND

- 2003 — 2012 — 2017 — Measured point
- 2009 — 2015 — 2022

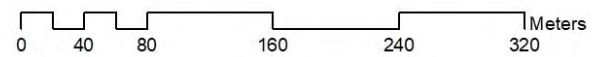


Figure 3.2 Shoreline position analysis for the eastern section of Jumby Bay.



Sources: Esri, Maxar, GeoEye, Earthstar Geographics, CNES/Airbus DS, USDA, USGS, AeroGRID, IGN, and the GIS User Community

Antigua - Long Island Shoreline Change



LEGEND

- 2003 — 2012 — 2017 — Measured point
- 2009 — 2015 — 2022

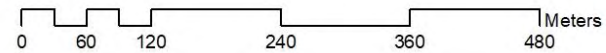
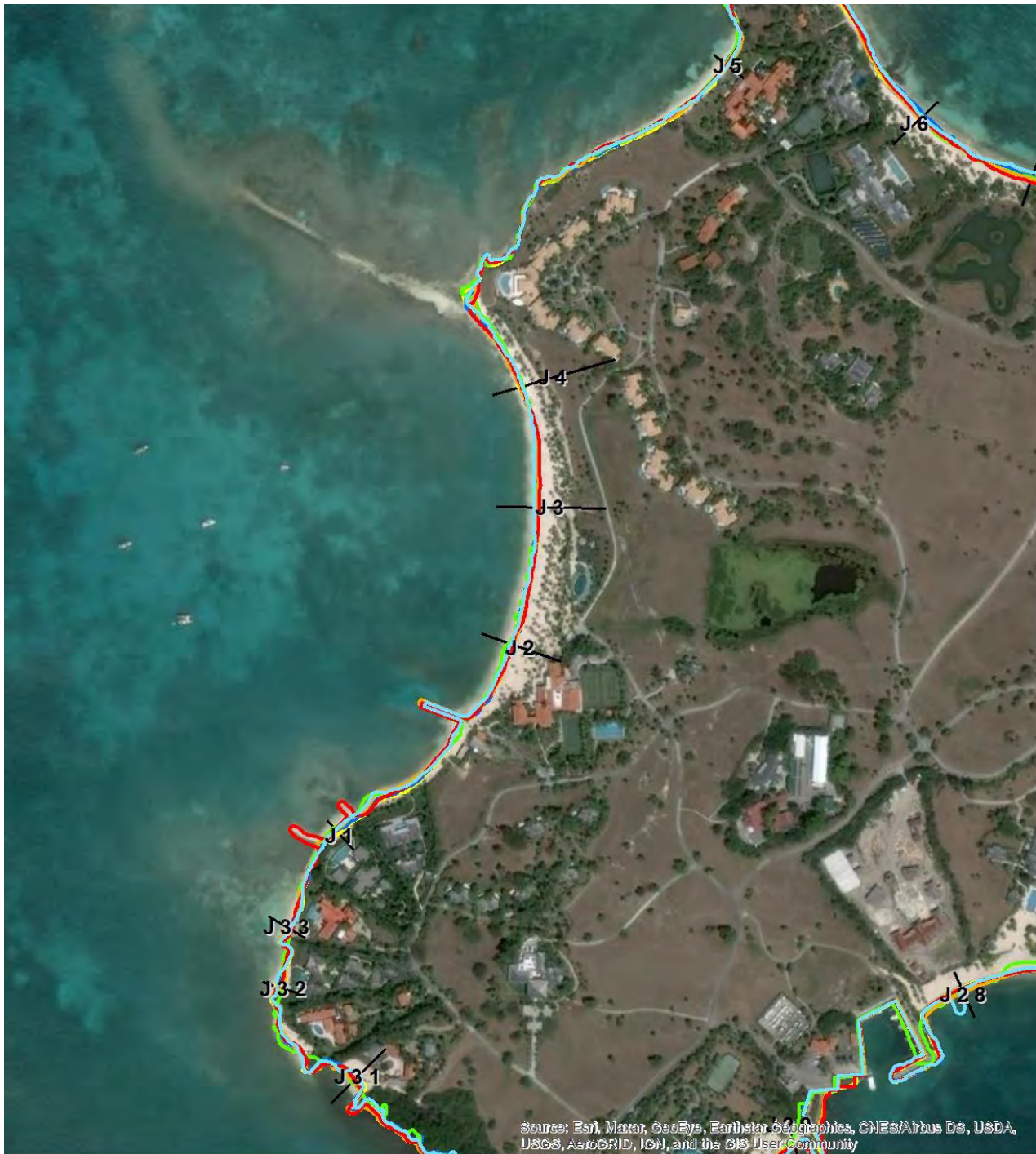


Figure 3.3 Shoreline position analysis for the southern section of Jumby Bay.



Antigua - Long Island Shoreline Change



LEGEND

-
 2003
 2012
 2017
 Measured point

-
 2009
 2015
 2022

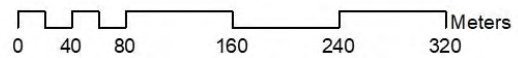


Figure 3.4 Shoreline position analysis for the western section of Jumby Bay.



3.1.1.1 Northern Zone

The northern narrow long beach had fairly stable beach widths as is characterized by a yellow-coloured short bar in graphs for J6 through J10 (Figure 3.5). An outlier in this case was profile J7 which was showing an erosion trend from 2009 to 2017. There may have been a localised nourishment activity in/around 2009 which was eroded in the subsequent years; thereby returning to a beach width similar to the start in 2003.



Figure 3.5 Profile analysis results for the northern section of Jumby Bay.

Profiles J11 through to J16 were taken to the north-eastern corner of the island which has had multiple groynes. Profiles J11, J12 and J13 had localised accretion which did not match the other results in this area. It is therefore hypothesized that beach nourishment works were done at these instances. Profile J12 showed a large erosion trend between 2009 and 2012. During this period a quasi-curved groyne was built to the west of the profile location, as a result there was erosion to the east of this structure. By 2017, the groyne was removed and the property line setback to create a wider beach area. This corresponds to the accretion trend shown by 2017. Profile J14, J15 and J16 showed little beach change over the analysis period. Beach cells in this area had narrow beaches with little fluctuations. The beach widths were much narrower when compared to the length of groynes which suggests that the structure type could be optimized.

3.1.1.2 Eastern Zone

The single measurement profile for the eastern coast is shown in Figure 3.6. The profile was taken in a beach cell that is bound by two groynes of different lengths. The profile shows a pattern of erosion for most of the analysis. The beach cell seemed to have been nourished between by/around 2009, however the exposed nature of the beach cell led to erosion after the sand was placed. The property has a loosely packed revetment which has acted as a last line of defence that was in place by 2017. The erosion calculated by 2017 showed the waterline at the base of the revetment which may have been related to the swell season.

A limitation of analysis for profile J17 was the presence of large sargassum mats that filled up the bay in some satellite images. The presence of these mats could artificially recede the shoreline as the digitisation is done based on a change in colour. Large sargassum mats became a hinderance in the analysis after the year 2015 in which there was a large onslaught of sargassum mats.

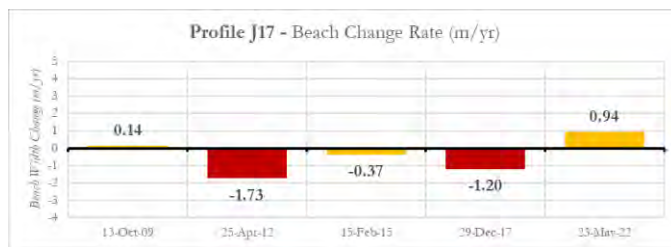


Figure 3.6 Profile analysis result for the eastern section of Jumby Bay.

3.1.1.3 Southern Zone

Profiles J18 through to J25 were taken from the south-east corner of the island. Profiles J18 and J19 were taken from the eastmost beach cell. The area has four structures which act to trap sand. Images show that the area was nourished early in the analysis and has become a dynamically stable beach. The beach widths have increased and decrease throughout the analysis with no distinct trend in either direction. The lengths of the groynes in this area are providing satisfactory sediment trapping.

Profile J20 showed significant erosion by 2015 linked to a possible highwater event in which the waterline was at the vegetated area. A review of the wave data shows an easterly event was taking place at the time, this may have led to higher water levels at the shoreline. After 2015, a perched beach with revetment was built out which corresponds to the increase in beach width. The revetment has kept the shoreline stable since the waterline is at the structure face. It is worth noting that, almost all profile results for the south-eastern component were negative in 2015. It is hypothesized that this is related to the passage of the easterly event with offshore waves of up to 2m.

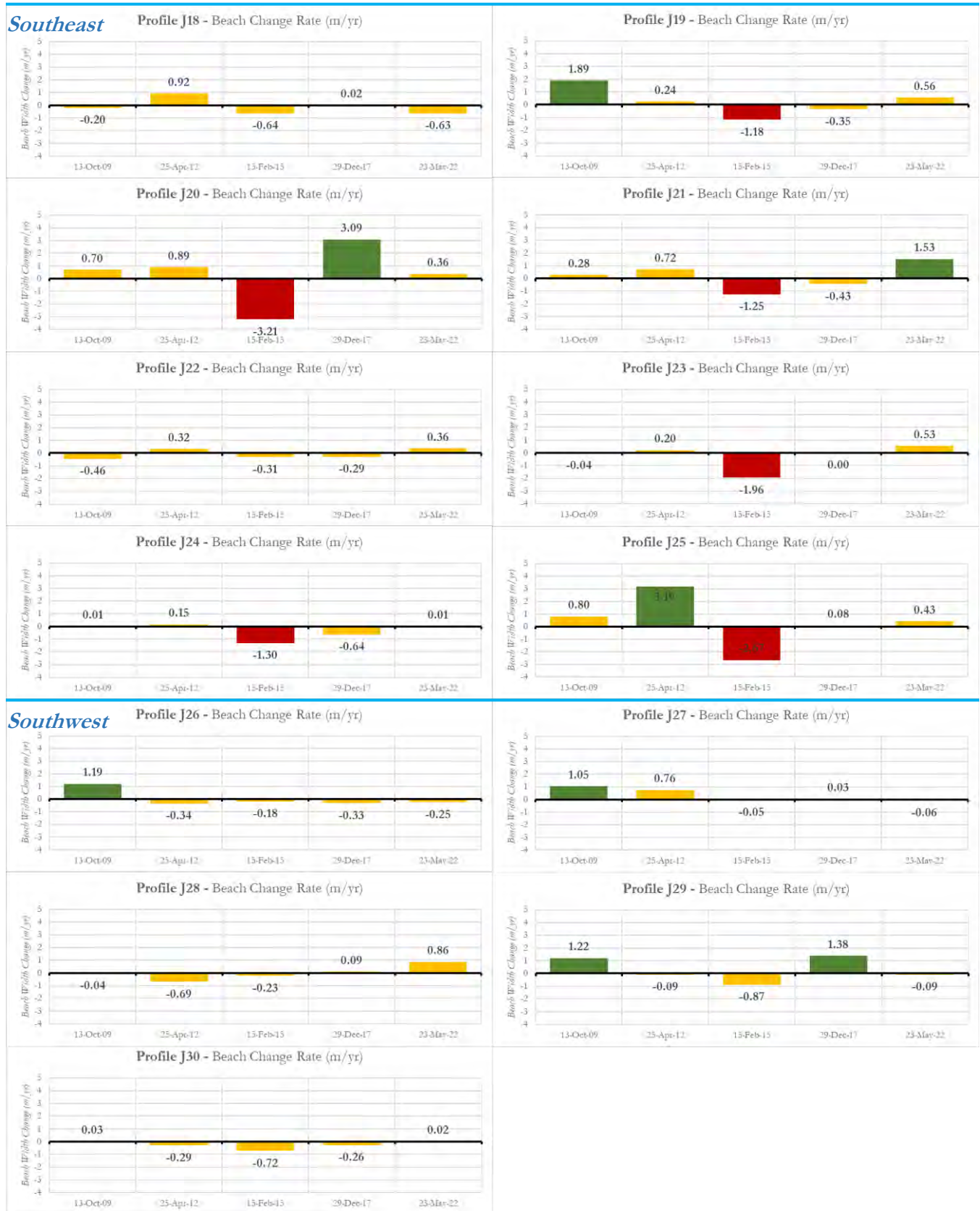


Figure 3.7 Profile analysis results for the southern section of Jumby Bay.

Profile J21 was taken in a small built beach area in between two groynes, the beach area was small as the larger groyne seemed to be mainly used for docking. The smaller groyne was removed by 2017 which increased erosion in the area. By 2022, the beach was nourished with a revetment put in place to hold the sand in a stable position.

Profile J25 had a similar case as J20 where the increase in beach width is linked to a built out perched beach that is supported by a rock revetment. All other profiles were stable outside of the retreat that was calculated for 2015.

Southwestern profiles showed stable results for this analysis with little fluctuations being seen. Profile J26, J27 and J28 were taken in the very calm bay beside the public dock. The bay was nourished between 2003 and 2009 which is why accretion is shown for the period ending in 2009. Small but constant retreat can be seen on profile J26 which may indicate that the structures in this area need to be repaired to better hold sand and protect the property. Other sections of the bay have been stable since the initial beach nourishment.

Profiles J29 and J30 were taken from a southern villa lot. The profiles show an initial increase in beach with which was related to the building out of a curved groyne and the area being nourished with sand. It is further hypothesized that between 2015 and 2017, the groyne structure was widened, and more sediment added to the beach area. This corresponds to the increase in beach width seen by 2017. Profile J30 is fairly stable with a small lean towards retreat which may be handled by regular nourishment as is practice on the islands.

3.1.1.4 *Western Zone*

Profiles J2 through to J4 were taken along the main public beach. J1, J5 and J31 to J33 are located on the sandy areas of private properties. The public beach area has net shoreline retreat in the profile results. Particularly in profile J3, there was an average retreat of 0.5m from 2012 to 2017. In this case, the beach receded by 2.5m over 5 years. Accretion was seen for the last period on profile J3 and J4. When reviewing the images, there is evidence of beach nourishment between 2017 and 2022 which would explain the accretion result.

J4 was taken at the north end of the public beach. This area was very dynamic over the analysis because of the presence of a wide platform area that kept the sediment in place under calmer conditions. Erosion of 1m per year from 2015 to 2017 was shown in the results which may have been recorded in the aftermath of the passage of Hurricane Irma in September 2017. Imagery shows that after the event the typically wider beach section at the north was eroded to the vegetation line.

Profiles taken along the south-western built beach cells (J1, J31 to J33) highlight the beach nourishment that was done for these properties and how the placed sediment moved with time. Profile J1 was not built up in the 2003 imagery and a very narrow beach area. Following, imagery suggests that a small beach area was built out with a submerged groyne used to keep sand in place. By 2017, there was erosion of the beach area which led to the construction of two new groynes. Unfortunately, the placement of the groynes reduced the sediment present for nearby shorelines. The groynes were subsequently removed by 2022 and a loose revetment used to hold sediment.

Profiles J31 to J33 also did not have developments in the 2003 image but rather had a narrow beach area. Between 2003 and 2009 the properties were developed, and some beach areas were experiencing erosion. The



properties were then outfitted with groynes by 2012 which helped to stabilise some beach widths. This is shown by the smaller movement from 2015 onwards in the graphs for these profiles.

Profile J31 used shows that the property owner in this area used some property area for their beach. A groyne was placed which helped to keep sediment and produce a stable beach. This is why such a large value of accretion was calculated for the period between 2009 and 2012. Following the beach creation, the cell has been stable.

Profile J32 shows a trend that moves from accreting to eroding in recent years. The beach cell has a transient nature which would affect the profile results. The beach cell is typically wider by the southern groyne and very narrow elsewhere. In the periods of small accretion there was some sediment on moving in the middle of the beach cell where the profile was taken. In recent years, the sediment has moved to be by the southern groyne and not in the middle of the beach cell. This would show that there is more erosion to the north that accretion to the south which produces net erosion.

Profile J33 was calculated as being a stable beach cell with one outlier of almost 1m/yr of erosion in the period 2015 to 2017. This result may be linked to the passage of Hurricane Irma in 2017 causing erosion in western shorelines as was the case with profile J4. Additionally, while reviewing the images available dredging works were observed 30m away from the beach area in 2017. This may have affected the stability of the beaches nearby by creating a sink in the nearshore.

Profile J5 is located on the lee side of the north-west peninsula and shows a fluctuating pattern in the historical shoreline analysis. There was a high variability in the beach width in this area. The overall trend showed net erosion over the analysis. Evidence of beach nourishment could not be confidently identified in the satellite images.



Figure 3.8 Profiles analysed for the western section of Jumby Bay.

3.1.2 Maiden Island

Historical shoreline analysis results for Maiden Island were more typical of a standard analysis as the changes in beach width were mainly due to wave action and less so to structures. Beach profile results for Maiden Island show that there are generally steep beach slopes around most of the island. The only exception to this is along the northern spit which has a very gentle beach profile. In this area the beach slope was calculated as 1(V):40(H) which would correspond to an error range of 24m. The rest of the island had an average beach slope of 1(V):10(H) which over the tidal signal would correspond to a 6m error range.

This shoreline analysis was done using a traditional digitising routine in GIS software. The images were retrieved from Google Earth engine and georeferenced based on the few fixed features on the island. For

Maiden Island, more satellite images were available for the analysis which helped to better describe the shoreline progression.

As with Jumby Bay, the satellite images were not regularly spaced and represent snapshots in time. The satellite images were from 2003, 2012, 2015, 2017, 2018, 2019, 2020, 2021 and 2023. Six satellite images (2003, 2015, 2017, 2018, 2019 and 2021) were taken during the typical swell season between November and February. The swell season typically has energetic wave events which result in a narrower beach during the season. The other images were taken under typically calmer summer conditions. Some other images were available but could not be digitised due to either cloud cover or the images being too bright to see the swash zone.

Figure 3.9 shows the aerial plan with the digitised shorelines and measurement points. Generally, the analysis shows that the whole island was a different shape in 2003. The boat channel to the west of the island was dredged and used to build out the island around this time. Also, a long breakwater was built in 2005 to the southern tip of the island. This structure was built to hold the dredge material in place and prevent it from sinking into the boat channel. Following this period, the shoreline has had a similar shape from the 2012 image onwards.

The northern tip/spit of the island showed erosion over time with spit getting narrower. A large concrete foundation has been (unintentionally) acting as a groyne that holds the spit since around 2004. A revetment was added to narrowest part of the spit between 2005 and 2012 which has helped in maintaining the narrow and low part of the spit.

Western beach widths have fluctuated significantly when compared to initial image in 2003. There was about a 10m difference between the widest beach width in 2003 and 2012 and the narrowest in 2019. Eastern coastal areas did not have as many changes in beach width following the initial dredge works in 2003.

The presence of sargassum mats on the eastern shorelines may affect the results on these beach areas. The digitised beach widths may be reduced as the sargassum mats sit on the dry beach area and cover the waterline. The south-east coast of Maiden Island had both dried and alive sargassum in the area on the 2023 image. For this zone, the shoreline was digitised as a best guess of the waterline position based on the colour of the sargassum.

Five measurement profiles were used to capture the changes in beach width from one year to the next. These are presented in Figure 3.10.



Maiden Island Shoreline Change

LEGEND

- 2003 2017 2020 2023
- 2012 2018 2021
- 2015 2019 2022

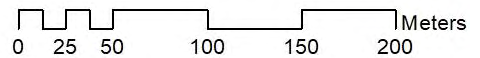


Figure 3.9 Whole island shoreline position analysis for Maiden Island.

Profiles M1 and M2 were taken along the western side of the island. Both profiles show an erosion trend from 2012 to 2019. The years following were typically accreting. The results that showed accretion were for 2020 and 2023 which were taken in the summer which usually has a wider beach area. In this analysis, erosion trends were calculated for images that were extracted in the swell season. This result indicates that there may be a high intra-annual (within a year) variability in the beach width for these areas.

Profile M3 was extracted from the southern coast that was filled with dredged material between 2003 and 2012. This corresponds to the large accretion rate at the start of the analysis. Following this, a triangular section of beach was formed from dredged material. Reviewing the images showed that during the analysis, this beach area moved either wholly to the north or wholly to the south along the breakwater. In the last five years of the analysis, there was a clear link between erosion during the swell season and accretion in the calmer months.

Profile M4 was taken on the eastern coast of the island and generally shows shoreline retreat. This profile currently has a 1.5 to 2m high scarp and sediment at the base. Interviews with the client show that the scarp was intentionally excavated to create a wider beach. Unfortunately, the trend of erosion has only increased since the works in 2005. The last result in the profile analysis for 2023 shows that there is accretion. However, this result was affected by the presence of large sargassum mats and should only be used as a guide.

Profile M5 was extracted along the north-eastern coastline and shows a trend of erosion. Higher erosion rates were mainly recorded during the swell season as was the case for other profiles. Similar to profile M4, accretion was shown for the period between 2021 and 2023. This may also be related to the presence of dark sargassum mats on the image.

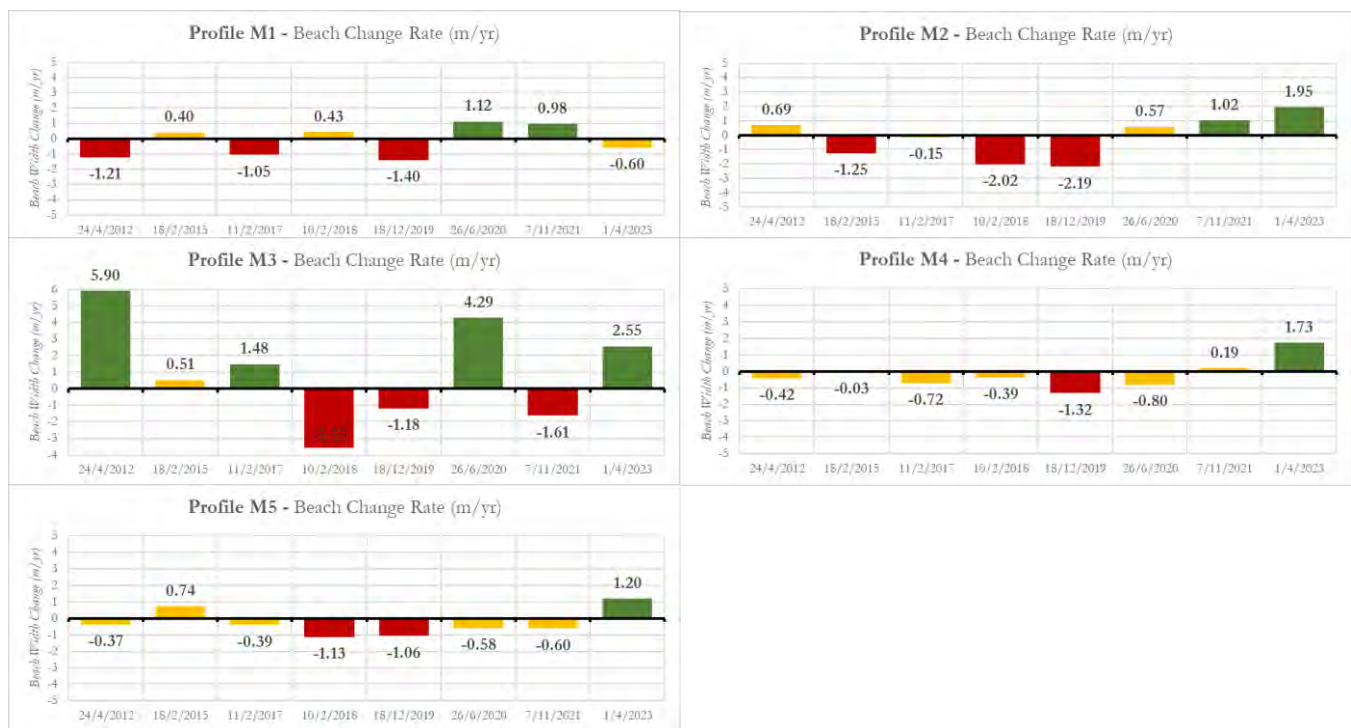


Figure 3.10 Profile analysis results for Maiden Island.

The general results for all profiles are summarised below in Figure 3.11. Twenty profiles of the thirty-eight assessed showed a trend of erosion while the remainder indicated accretion. A few profiles had very low beach width change which could be characterized as stable. These included J3, J9, J12, J28 and M2.

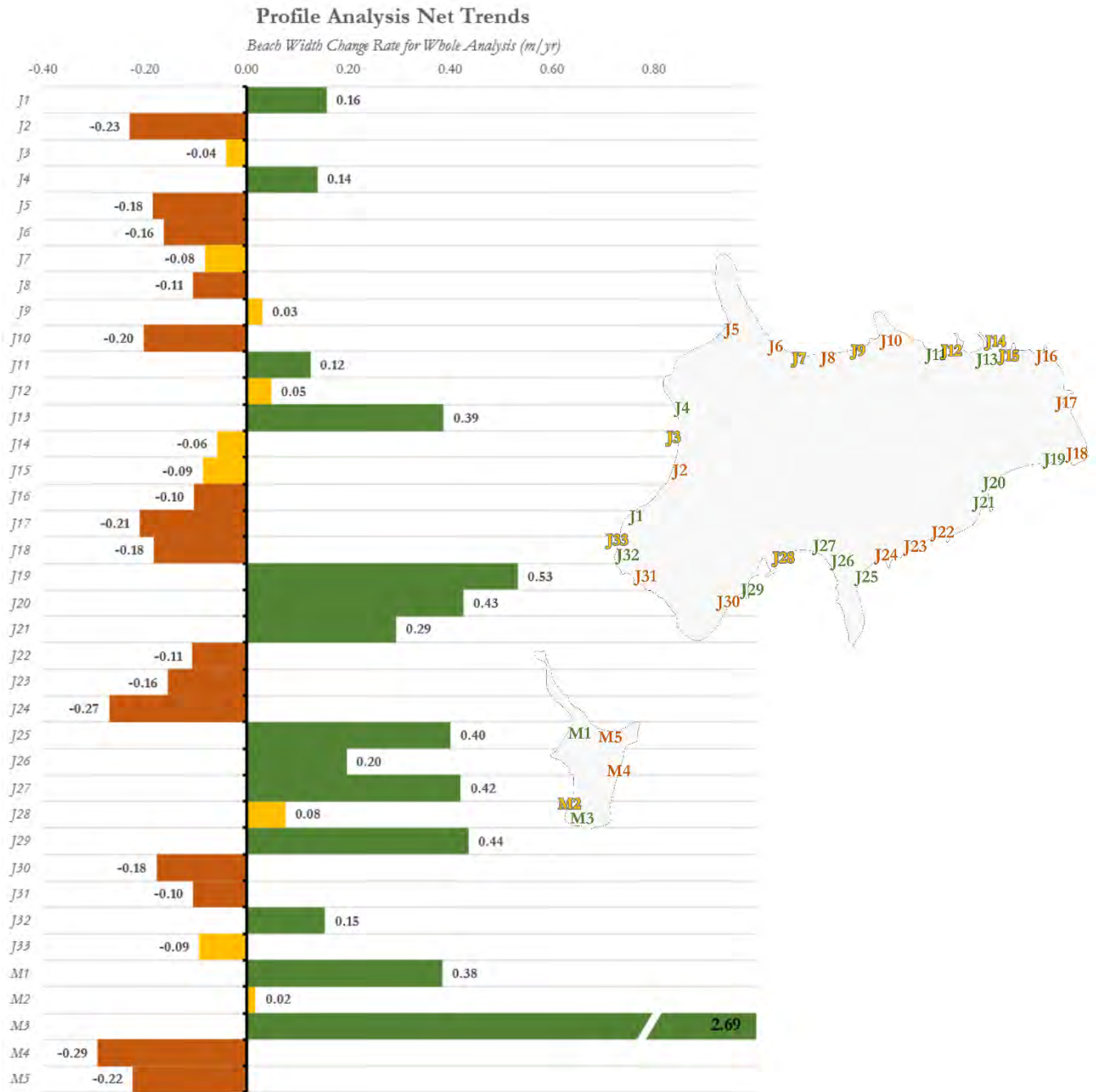


Figure 3.11 Summary of profile analysis results for the entire exercise.

3.2 Bathymetry Changes

Using satellite-derived bathymetric (SDB) data, our team conducted a comparative analysis of bathymetric changes between the years 2003 and 2022. A two-dimensional difference plot was generated to illustrate depth variations over the period. It is essential to note that, given the negative bathymetry values used in our calculations, the interpretation of the data is as follows:

- Negative values signify shallower waters, indicating a reduction in water depth, whereas positive values represent deeper waters, signifying an increase in water depth. Our analysis revealed that water depth changes occurred within a range of ± 4 meters.

Bathymetry changes from 2003 to 2009 have been shown in the top inset of Figure 3.12. This image and all other result images have a red colour for deeper water and green for shallower water. There are a few contour lines to indicate the magnitude of the depth changes. The bathymetry difference between 2009 and 2003 show shallower depths with a difference of 0 and 0.5m to the north of Jumby Bay. To the east of Maiden Island and south of Jumby Bay the water depths were also shallower by about 1m. West of Jumby Bay has an increase in water depth by around 0.2m.

Bathymetry changes from 2009 to 2012 have been shown in the bottom inset of Figure 3.12. For this period, there was mainly deeper water by about 0.2m around both islands. The water depths to the south-east of Jumby Bay were deeper by 0.5 to 1.5m. The reef area to the north-east of both islands has shallower depths with a difference of around 1 to 1.5m.

Differences in bathymetry between 2012 and 2015 have been presented in the top inset of Figure 3.13. Results were mixed across the area that was used. Deeper water was seen along the north and eastern areas of Jumby Bay. Water was also deeper to the north of Maiden Island. The area just south of each island has shallower water with a difference of 1m to 2m.

Differences in water depth between 2015 and 2017 have been presented in the bottom inset of Figure 3.13. Generally, there was deeper water in the southern and north-western offshore areas of the islands. A section 2km to the east of Jumby Bay was an average of 2m shallower in 2017 than in 2015. In the nearshore of both islands the depths were slightly shallower with an average change of 0.4m.

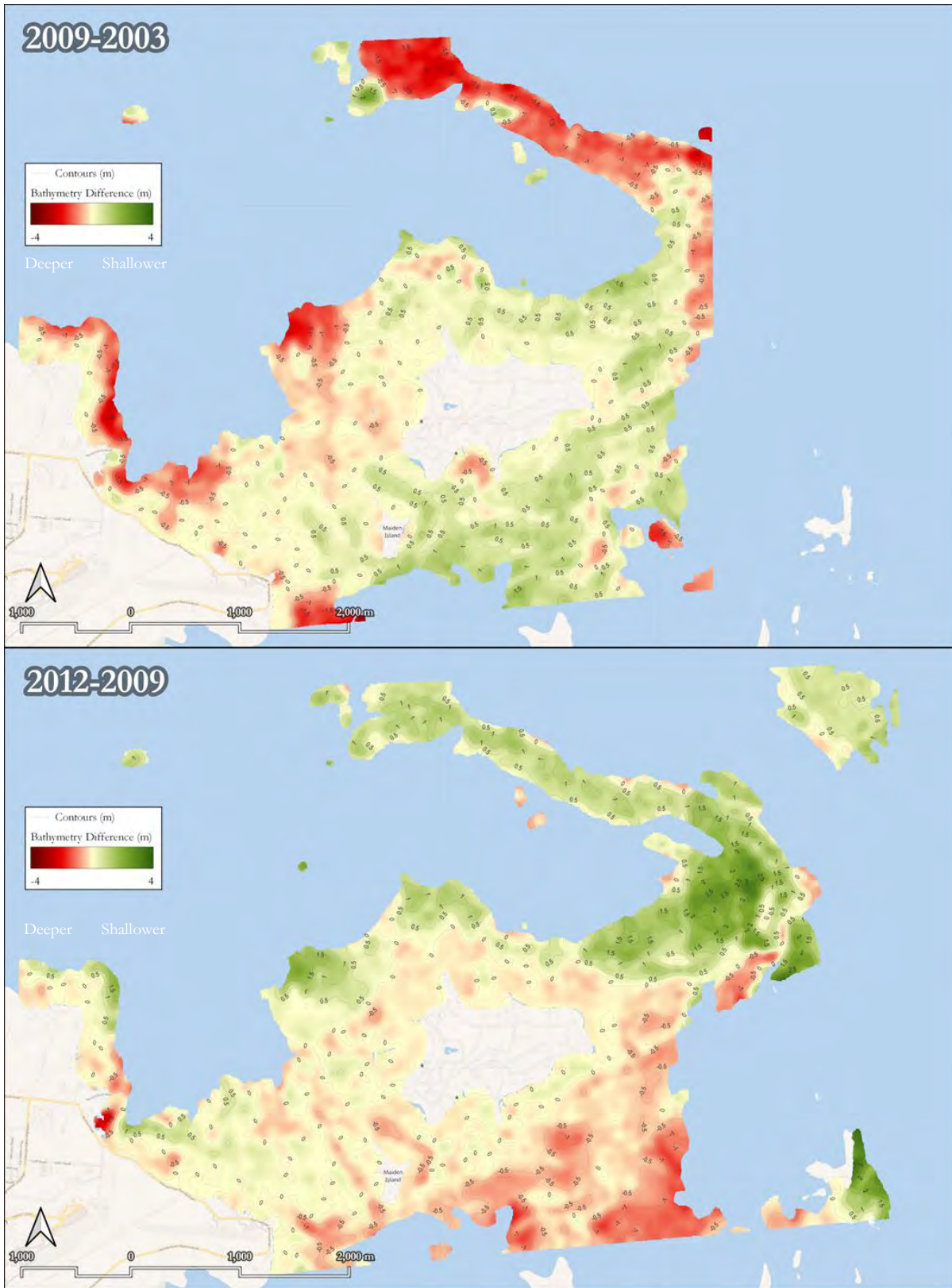


Figure 3.12 Bathymetry changes between the years 2009 & 2003 and 2012 and 2009.

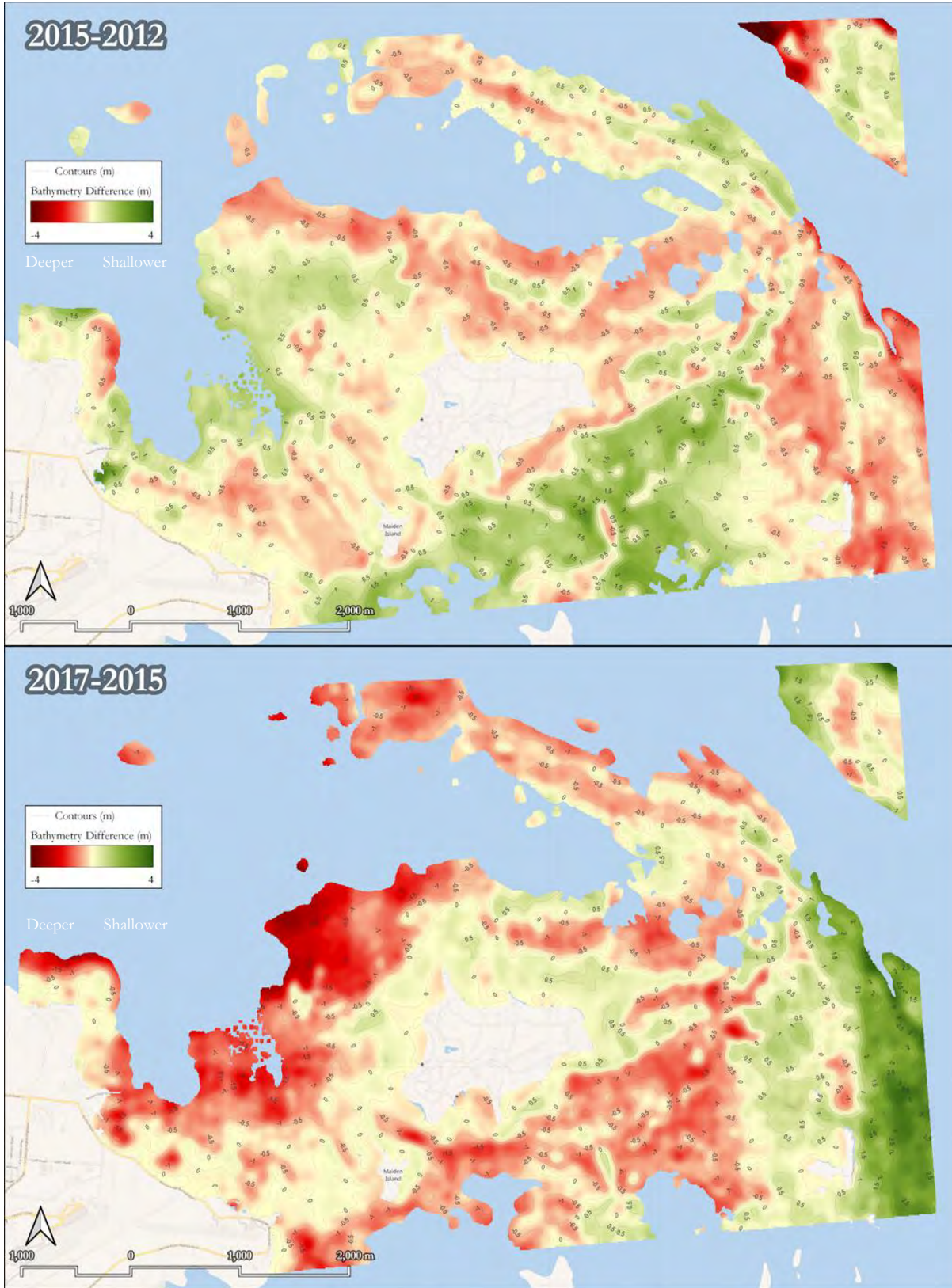


Figure 3.13 Bathymetry changes between the years 2015 & 2012 and 2017 & 2015.

In the northern area of the study zone, positive values were observed, which suggests that the waters were shallower in 2022 compared to 2017. On average, the water depth in this area decreased by approximately 0.5 to 1m. Further, the southern nearshore areas also exhibited shallower waters in 2022 compared to 2017, by 0.5 to 1.5m. Conversely, the eastern and south-eastern offshore regions experienced an increase in water depth over the 5-year period, with an average increase of 1.5m.

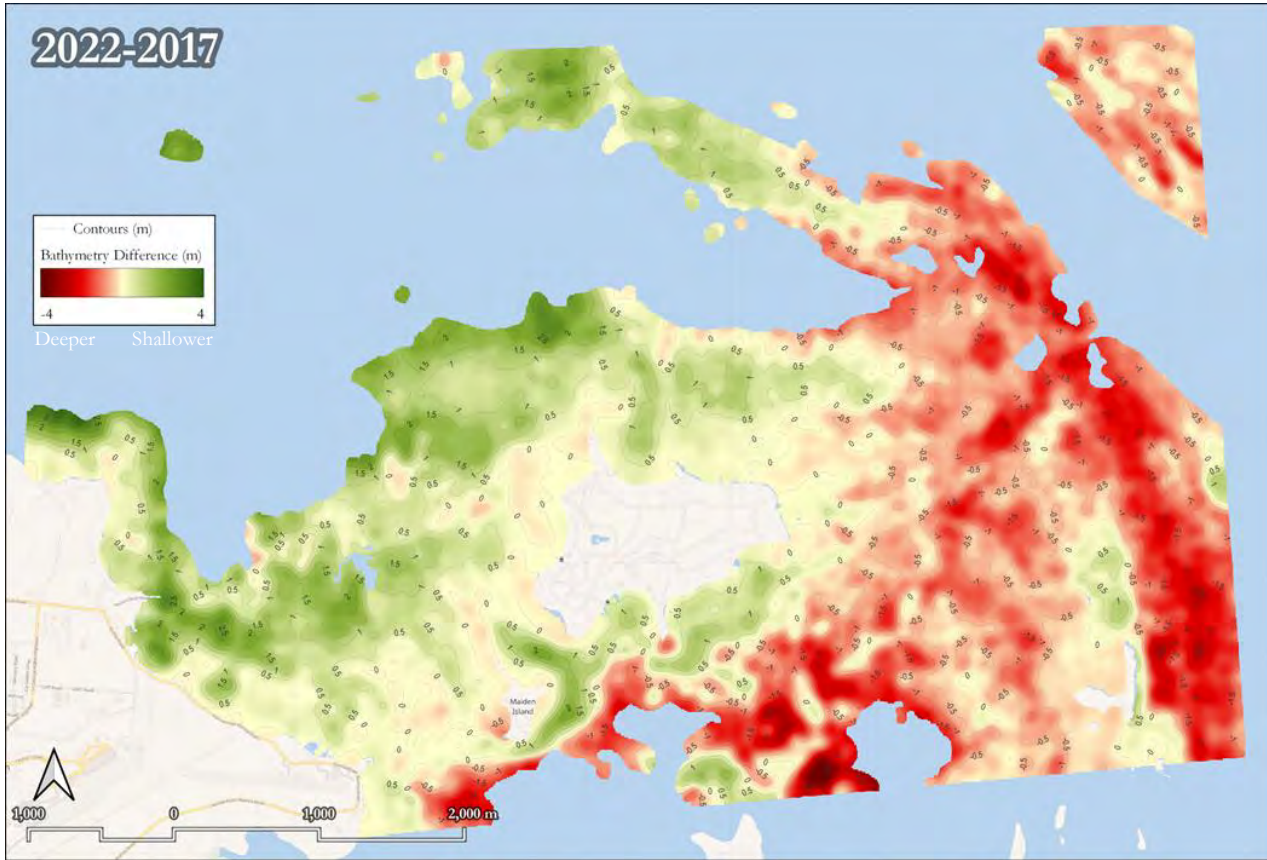


Figure 3.14 Bathymetry changes between the years 2017 and 2022.

This in-depth analysis of bathymetric changes provides valuable insights into the evolving marine environment, with potential implications for coastal management, infrastructure planning, and ecological conservation efforts.

3.3 Seafloor Classification Changes

Our team evaluated six years of seafloor classification (SFC) data to identify trends in the distribution of benthic resources over time. We generated summary images to illustrate the changes between the first year of data (2003) and the most recent data available (2022). Figure 3.15 presents the changes in coral-dominated pavement. In 2003, the coral coverage had a narrower extent than in 2022, which is evident by the straight line to the east of Jumby Bay. The brighter red shading indicates areas where coral cover was consistently maintained over the 19-year period. The analysis reveals that coral habitats remained relatively stable, with observed differences primarily due to changes in data extents rather than alterations in seafloor features.

To round out this analysis, a general summary of the change in seafloor classification is presented. The analysis involved reducing the years of the seafloor classification data to a shared area, defined by a curved shape outlining a zone around the islands where SFC data were available for every year. This zone was at a 700m offset of Jumby Bay and extended 2km west of Maiden Island.

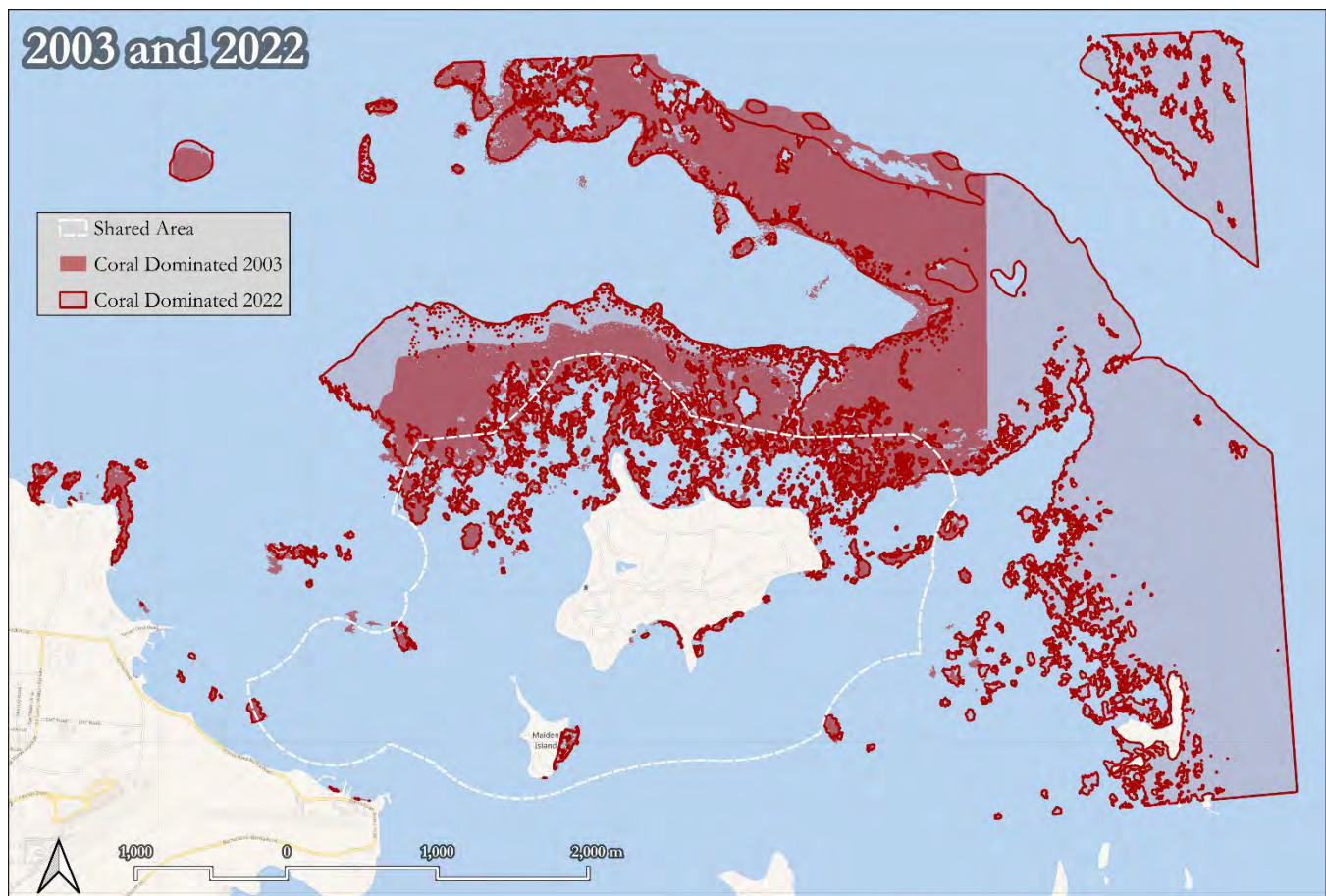


Figure 3.15 Comparison of coral dominated seafloor in 2003 and 2022.

Figure 3.16 examines the changes in seagrass dominance over the same period. The extent of seagrass cover increased significantly during the analysis period. The outlined areas represent the seagrass cover in 2022, while the shaded areas depict the coverage in 2003. Initially, seagrass dominance was predominantly observed to the west of Maiden Island, with some patches to the north of Jumby Bay. By 2022, seagrass had expanded southward, enveloping the islands, and the patches to the north had become denser. Consequently, the overall seagrass cover nearly doubled throughout the analysis period.

Understanding these changes in benthic resources is crucial for coastal and marine ecosystem management, as it informs conservation efforts and sustainable development planning in response to the evolving coastal environment.

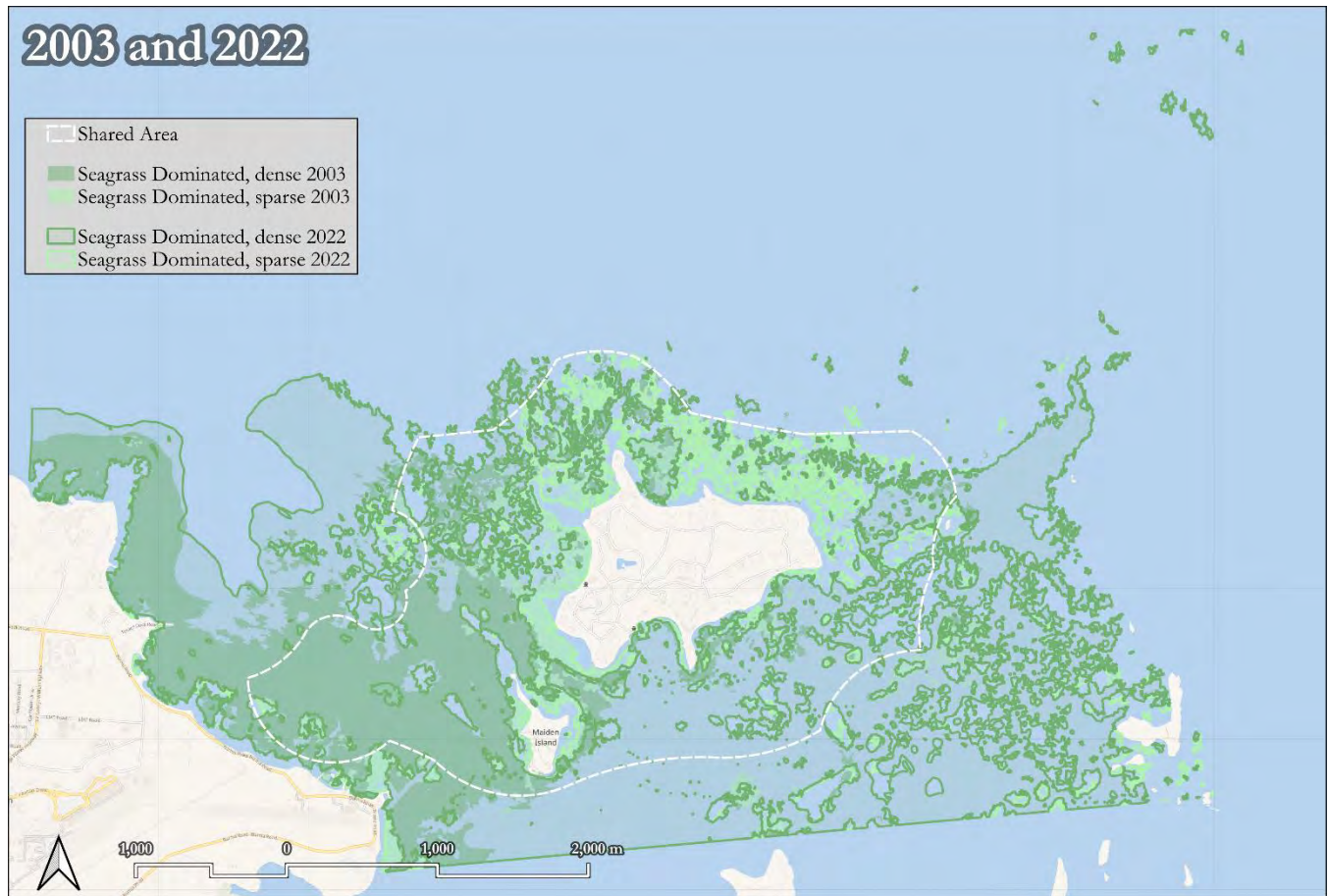


Figure 3.16 Comparison of seagrass-dominated seafloor in 2003 and 2022.

Figure 3.17 provides an overview of the changes in sediment-dominated seafloor between 2003 and 2022, in response to the increased seagrass dominance described in Figure 3.16. The areas previously dominated by sediment were significantly reduced as the seagrass cover expanded from west to east. The brighter yellow outlined areas represent zones that remain sediment-dominated, including a few small patches to the north and a narrow zone to the southeast of Jumby Bay.

The changes in sediment-dominated seafloor have implications for benthic habitats and the broader coastal ecosystem. Sediment-dominated seafloor habitats are typically characterized by low species diversity, whereas seagrass-dominated habitats support a more diverse and productive ecosystem. The observed shift from sediment-dominated to seagrass-dominated seafloor is, therefore, likely to have positive ecological implications, such as supporting fisheries, improving water quality, and enhancing the overall health of the coastal ecosystem.



Figure 3.17 Comparison of sediment dominated seafloor in 2003 and 2022.

Figure 3.18 shows the changes in dominant seafloor cover over time. The coral cover remained relatively constant at around 12.5%, while rock-dominated areas had a consistent cover of 4% for all years. However, sediment-dominated areas reduced significantly from 38% in 2003 to 10% in 2022. Notably, the sediment cover was relatively stable until 2015, after which it was halved in 2017 and then again in 2022.



The key finding from the summary chart is the substantial increase in seagrass cover, particularly in dense seagrass areas. Sparse seagrass areas had minimal increases over the analysis period, with an average cover of 14% for the years 2003, 2009, 2012, and 2015, slightly increasing to 17% for the years 2017 and 2022. However, the dense seagrass cover increased significantly from 30% in 2003 to 57% in 2022 within the shared area. Notably, the year 2015 appeared to act as a tipping point for seagrass growth, coinciding with a large sargassum bloom, which was linked to increased nutrients in the water column. Further marine studies may be required to investigate possible environmental factors that could influence seagrass growth.

The changes in seafloor classification highlighted in our analysis have important ecological implications, including impacts on benthic habitats, fisheries, and water quality. These findings underscore the importance of ongoing monitoring and assessment to inform sustainable coastal management strategies that preserve and protect valuable coastal ecosystems.



Figure 3.18 Historical comparison of dominant seafloor cover in the shared area around Jumby Bay and Maiden Island.

Overall, our analysis of the changes in benthic resources highlights the dynamic nature of coastal environments and the importance of ongoing monitoring and assessment to inform sustainable coastal management strategies.

4 Hazard Exposure

Coastal hazard exposure refers to the risk of damage or harm to people, infrastructure, and the environment that could result from natural hazards occurring in coastal areas. Typical hazards in the Caribbean and North Atlantic basin include storms, hurricanes, sea-level rise, saltwater intrusion, erosion, and flooding. Coastal areas are particularly vulnerable to these hazards because of their proximity to the sea and exposure to the forces of wind and water. With the effects of climate change, and as sea levels rise and weather patterns become more extreme, the risks associated with coastal hazards are expected to increase.

Planning guidelines must strike the right balance that protects lives, the environment, and important infrastructure. Future planning should also ensure that economic development is not stifled by overly protective measures and buffers.

4.1 Scenario Selection for Planning Development

For appropriate planning guidelines, there are three main parameters that need to be evaluated:

- Planning Time Horizon - which defines how long into the future is being planned for.
- Extreme Event Return Period – this describes the severity of natural hazards which is typically analysed through a statistical risk occurrence.
- Climate Change Scenario – or emission pathway that describes a range of impact magnitudes (normally represented by an RCP or SSP).

Of these, the planning time horizon is the most important. When planning guidelines contend with extreme events such as coastal flooding, which are infrequent but damaging events, a statistical approach is typically adopted. Doing this within a framework of uncertainty that is exacerbated by climate change brings additional challenges. The different scenarios of potential climate change, and in particular global sea level rise, vary considerably.

Adopting an overly optimistic climate change scenario; one that relies on global emissions rapidly dropping, may result in lives, ecosystems, and assets being exposed to unacceptably high risks if that pathway is exceeded. Conversely, a more pessimistic outlook on global emissions may result in unnecessarily high costs for economic development and may appear to be overly conservative for the next few decades, as conditions are not as bad as planned for.

4.1.1 Extreme Event Return Period

For engineering design purposes, the selection of an appropriate return period looks at the consequence of failure and then balances the initial capital cost against future possible maintenance costs. Typically, for shoreline protection and other non-critical infrastructure, a return period of 50 years is recommended so that the initial capital costs are reasonable. A larger design return period is considered if the design involved critical infrastructure such as port facilities, power generation, essential transportation links, water supply or facilities that may require a longer design life.

For planning purposes, extreme events that have a higher return period of at least 100 years are being recommended more often. This is to avoid development of infrastructure in greenfield sites (or redevelopment of existing infrastructure) that may be overly exposed to the effect of climate change in the foreseeable future.

Representative extreme events are typically defined by projecting historical climate data into the future. Recent findings have suggested that for flooding events, climate change will result in today’s predictions of extreme events becoming more common. What is estimated today as a 100-year flood event is predicted to occur more frequently in the future, such that it will eventually be considered a 30-year event, and eventually a 10-year event, and possibly an annual occurrence.

The following figure from IPCC (2019) Special Report on the Ocean and Cryosphere depicts how Historical Centennial Events (HCE’s, 100-year return period events) are predicted to transition to annual events (1-year events). The data near Antigua appears to suggest this transition will occur in approximately 2045-2055 for both the RCP 2.6 and RCP 8.5 emission scenario.

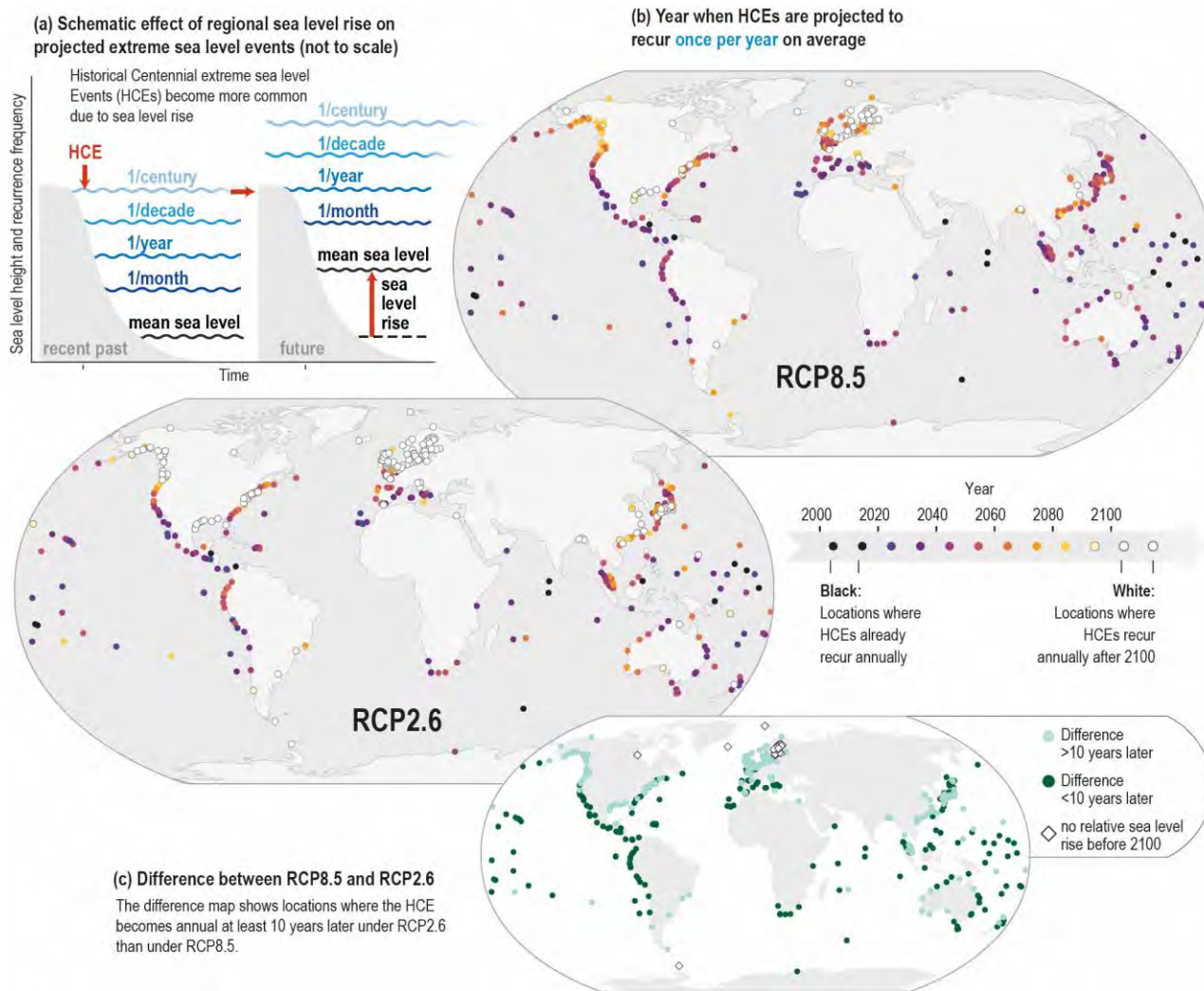


Figure 4.1 Graphical description of transition of Historical Centennial Events (HCE’s, 100-year return period events) to transition to annual events (1-year events)¹.

¹ IPCC, 2022: Summary for Policymakers [H.-O. Pörtner, D.C. Roberts, E.S. Poloczanska, K. Mintenbeck, M. Tignor, A. Alegría, M. Craig, S. Langsdorf, S. Löschke, V. Möller, A. Okem (eds.)]. In: *Climate Change 2022: Impacts, Adaptation, and Vulnerability*. Contribution of Working Group

In addition to increase return periods of storms, the concept of risk must be explored when planning. The latest IPCC report (AR6 Synthesis Report, 2023) provides guidance for the selection of appropriate scenarios for coastal flooding and erosion risk. Two important points are stressed and supported by published figures:

- Figure 4.2 indicates that between AR5 and AR6 new research has revealed that the risk/impacts for various “Reasons for Concern” have increased for the same level of global warming, or put another way, moderate to high risks/impacts are now predicted to occur at even lower global warming levels. Looking at extreme weather events, the newer science (2022 vs 2014) has revealed that high risks will occur at 1.5°C warming, whereas in the AR5, this was above 2°C.
- Figure 4.3 depicts projected global mean sea level rise until the end of the century and makes the point that jurisdictions that have the potential, desire, and/or capacity to respond have a risk profile that is potentially lower.

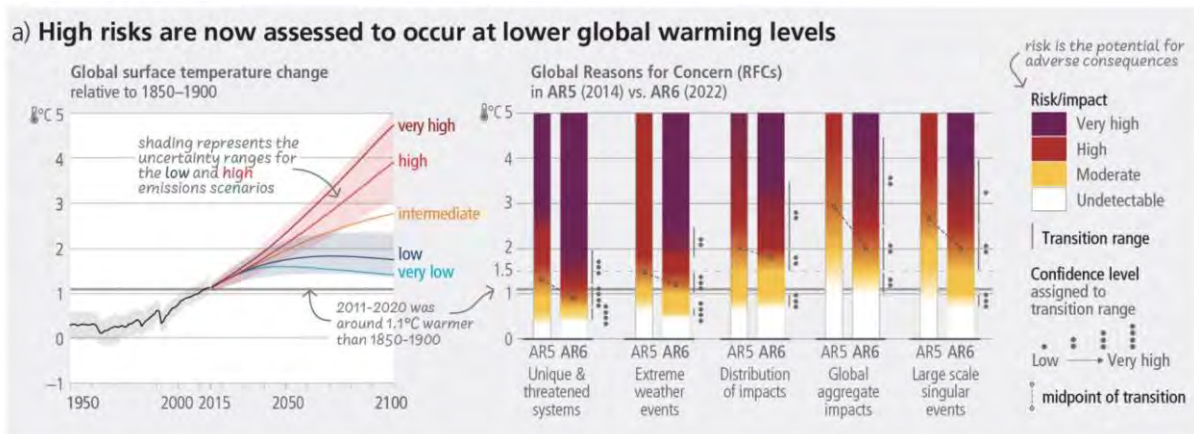


Figure 4.2 Increase in risk from IPCC's AR5 to AR6 reports for given global surface temperature change scenarios.

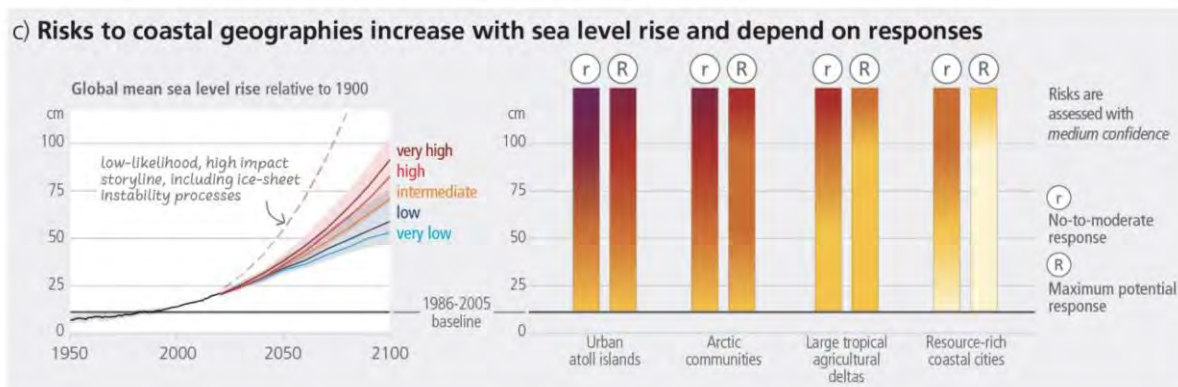
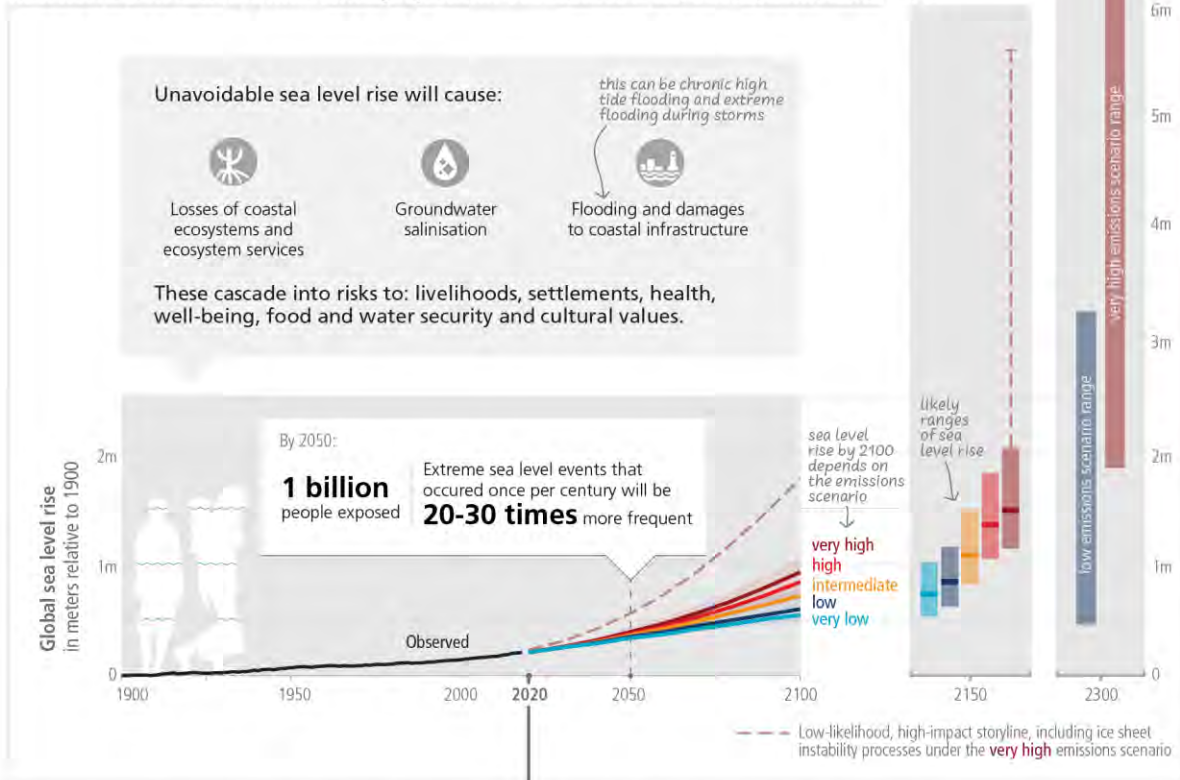


Figure 4.3 Risk profiles of jurisdictions based on response to sea level rise threat.

A comparison of the temperature and mean sea level rise between 1950 and 2100 shows a rather disturbing correlation – even if a low emission pathway occurs and global temperatures decrease in the latter half of this century, mean sea levels continue to increase, and will continue well into the next century and beyond. AR6 includes Figure 4.4, which accurately summarises the risks until the end of the century, and an assessment of the years beyond.

Sea level rise will continue for millennia, but how fast and how much depends on future emissions

a) Sea level rise: observations and projections 2020-2100, 2150, 2300 (relative to 1900)



Responding to sea level rise requires long-term planning

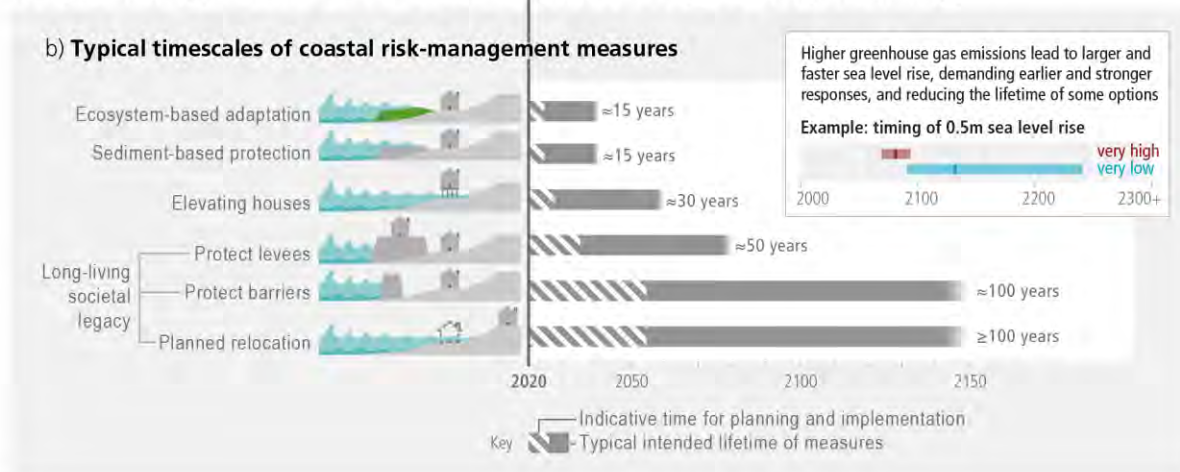


Figure 4.4 Summary of risks from sea level rise over the next century².

By the end of this century, the mean sea level is predicted to be at least 0.5m higher than its present value, for all climate change scenarios. The intermediate climate change scenario has a median level that rises to 0.75m above present in 2100 and then above 1.0m by the year 2150. The steadily rising sea level which appears to lag behind the rise in temperature suggests that a precautionary approach for sea level rise is appropriate. A long-term planning horizon should ideally consider 1m of sea level rise by 2100. If the rate of sea level rise is not as rapid as the latest scientific literature suggests, that buffer will be available for the future, as sea levels will continue to rise, possibly for centuries.

4.1.2 Climate Change Scenarios (Emission Pathways)

Sea level rise is one of the main impacts from climate change in the coastal area. This impact and others such as marine heat waves are quantified through the use of emission pathways. In the latest IPCC report (AR6), the trend used to describe climate change scenarios was changed from Representative Concentration Pathways (RCPs) to “Shared Socio-economic Pathways” (SSPs). SSPs are a new method of assessing future scenarios by combining the knowledge of the physical sciences of climate change with the resulting societal impacts. SSPs incorporate adaptation and mitigation research to create a more holistic approach to future projections.

SSP1 - 2.6 - ‘Sustainability’ Development Pathway

Under SSP1 – 2.6 global warming stays just below 2°C at the end of the century when compared to pre-industrial (pre-1900) levels.

SSP2 - 4.5 - ‘Middle of the Road’ Development Pathway

SSP2 – 4.5 corresponds to emissions reductions which are roughly in line with the upper bounds of the latest Nationally Determined Contributions and global warming of around 2.7°C at the end of the 21st century.

SSP3 - 7.0 - ‘Regional Rivalry’ Development Pathway

SSP3 – 7.0 corresponds with a medium-high development pathway. Under this SSP no additional climate change policy is put in place and there are high non-CO₂ related emissions. This pathway corresponds to a pathway that is roughly in the middle of the previous RCP6.0 and RCP8.5.

SSP4 - 6.0 - ‘Inequality’ Development Pathway

SSP4 – 6.0 describes a world with high investment in human capital that widens the gap between societal groups. There is little investment in mitigation and environmental policies focus on local issues for the upper class.

SSP5 - 8.5 - ‘Fossil Fuel Intensive’ development pathway

SSP5 – 8.5 corresponds to very high emissions, no additional climate policy and intensive fossil fuel dependent development which is the worst-case scenario pathway. (See Riahi et al., 2017 for more details on SSPs).

Sea level rise projections have been published for each of the SSPs listed. A simple calculation of global sea level rise under SSP2 and SS5 for three design horizons (20 years, 50 years and 100 years) is shown in Table 4-1.

² IPCC 2022. Figure 3.4.



Table 4-1 Sea level rise scenarios adopted for this study.

| Scenario | Time Horizon (yr) | Rate (mm/yr) | Source | Projected SLR (m) |
|------------|-------------------|-------------------------|-------------------------|-------------------|
| SSP2 – 4.5 | 20 | 5.4 | SSP2-4.5 Rate 2040-2060 | 0.11 |
| | 50 | 6.6 | SSP2-4.5 Rate 2040-2060 | 0.33 |
| | | | SSP2-4.5 Rate 2080-2100 | |
| 100 | 7.7 | SSP2-4.5 Rate 2080-2100 | 0.77 | |
| SSP5 – 8.5 | 20 | 6.6 | SSP5-8.5 Rate 2040-2060 | 0.13 |
| | 50 | 8.6 | SSP5-8.5 Rate 2040-2060 | 0.43 |
| | | | SSP5-8.5 Rate 2080-2100 | |
| 100 | 10.5 | SSP5-8.5 Rate 2080-2100 | 1.05 | |

In summary, the selection of an appropriate planning time horizon is the most important aspect when considering coastal erosion and flooding in the framework of climate change. The increased frequency of coastal flooding is affected by future sea levels, and by changes in the climate which affect the wind and waves. Different climate change scenarios affect the timing of the rising sea levels. Climate horizons indicate a planning timeline, however the longer the timeline the greater the extent of the impacts of climate change.

5 Wave Climate Analysis

This section outlines the existing coastal processes at the project site located along the coast of Long Island and Maiden Island, taking into consideration both the prevailing operational wave climate and the extreme (hurricane) wave climate. The coastline is subject to two distinct wave climates: (1) the operational wave climate, characterized by day-to-day waves generated by north-east Trade Winds and seasonal (winter) swell waves, and (2) the extreme wave climate, which involves occasional hurricanes producing significantly higher waves. The analysis of both wave climates is essential for informed coastal engineering design and is detailed in this section.

The operational wave climate refers to the daily variations in wave heights, periods, and directions for a given location. These wave conditions play a crucial role in sediment transport along the shoreline and are responsible for long-term morphological changes. In coastal engineering design, the operational wave conditions are typically employed to identify the most suitable design solution in terms of the types and arrangement of structures.

The extreme wave climate encompasses waves associated with tropical storms and hurricanes, events to which the Caribbean region is exposed each year from June to November. These storms can cause dramatic and sudden alterations to the coastline. Generally, coastal protection structures are designed to endure wave attacks from such extreme storm events. This includes selecting an appropriate armour stone size for a coastal structure or determining the design wave forces that might arise due to extreme waves. However, the stability of beach nourishment is typically not designed for these wave conditions. The severity of the design storm event (i.e., return period) is chosen based on the acceptable level of risk of damage or failure that the owner is willing to accept. A 50-year return period often represents a reasonable balance between capital investment and maintenance costs.

5.1 Operational Wave Climate

The operational wave climate at the project site can be divided into two primary components: day-to-day, relatively calm conditions, and seasonal winter swells occurring from December to May. The day-to-day conditions result from the influence of the north-east Trade Winds, typically generating moderate waves. In contrast, the seasonal winter swells are produced by north Atlantic cold fronts, with waves approaching from the north to north-west sector. Consequently, the north coast of Long Island (Jumby Bay) is exposed to these longer period and more energetic wave conditions on an annual basis.

Although these winter swells account for a relatively small percentage of the year, it is important to note that they have a more significant impact on the project site's shoreline compared to the daily wave conditions. This is due to their higher energy, which contributes to greater sediment transport and coastal morphological changes. Understanding these nuances in the operational wave climate is essential for effective coastal engineering design and management strategies.

5.1.1 Daily Wave Climate

The operational wave climate at the project site is characterized by two main components: day-to-day, relatively calm conditions, and seasonal winter swells (December to May). The day-to-day conditions are generated by the north-east Trade Winds, while the seasonal swells are produced by North Atlantic cold fronts and typically approach from the north to north-west sector.

The deep-water operational wave climate was determined using the Reanalysis v5 (ERA5) dataset, produced by the European Centre for Medium-range Weather Forecast (ECMWF). The ERA5 model reanalyses wave parameters, including significant wave height, wave period, and mean wave direction, as well as wind speed and direction every hour from 1979 to 2022. This dataset provides over 383,000 timesteps of data at an enhanced resolution of approximately 31x31km (or ~0.25 degrees) over the Caribbean region.

Figure 5.1 illustrates the wave height distribution and the location of the node selected for the project. The wind data extracted from the selected node indicates that winds primarily come from the east, with an average speed of 7m/s for most of the year. Model wind directions are in agreement with the literature review, which identifies the east Trade Winds as the predominant winds in the area.

Model data revealed that waves offshore Jumby Bay predominantly come from the northeast to east (87.8%) during the tourism period (November to April). The average wave height of the east-north-east waves is between 1.5-2.0m, with an average wave period of 9.0s as shown in Figure 5.2. The ERA5 database was also utilized to extract wind data, which showed consistency with the resulting wave data.

By presenting the wave and wind data, this analysis helps the reader better understand the complexity of the operational wave climate at the project site, which is crucial for effective coastal engineering design and management strategies.

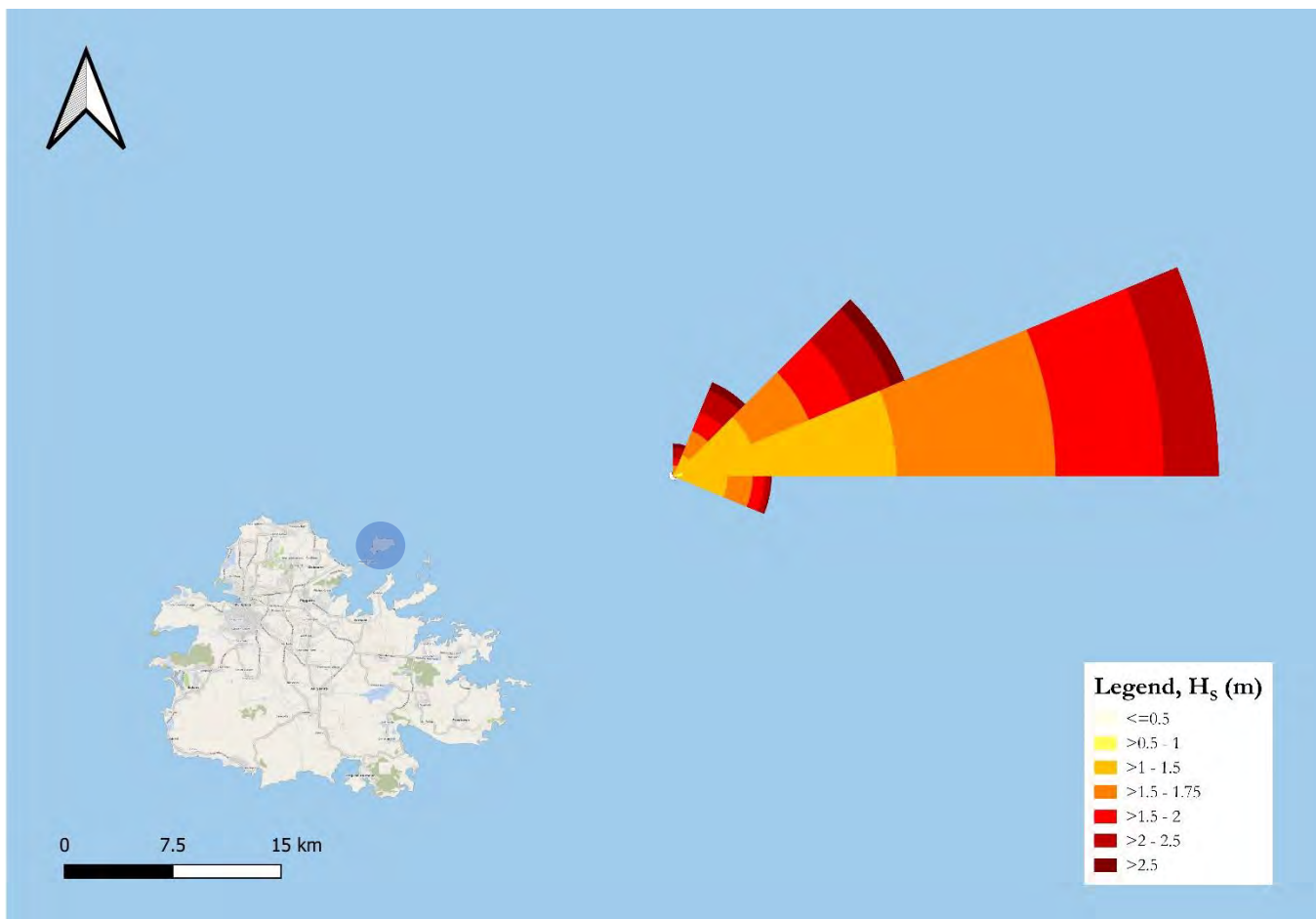


Figure 5.1 Offshore node location and wave roses showing wave heights and direction.

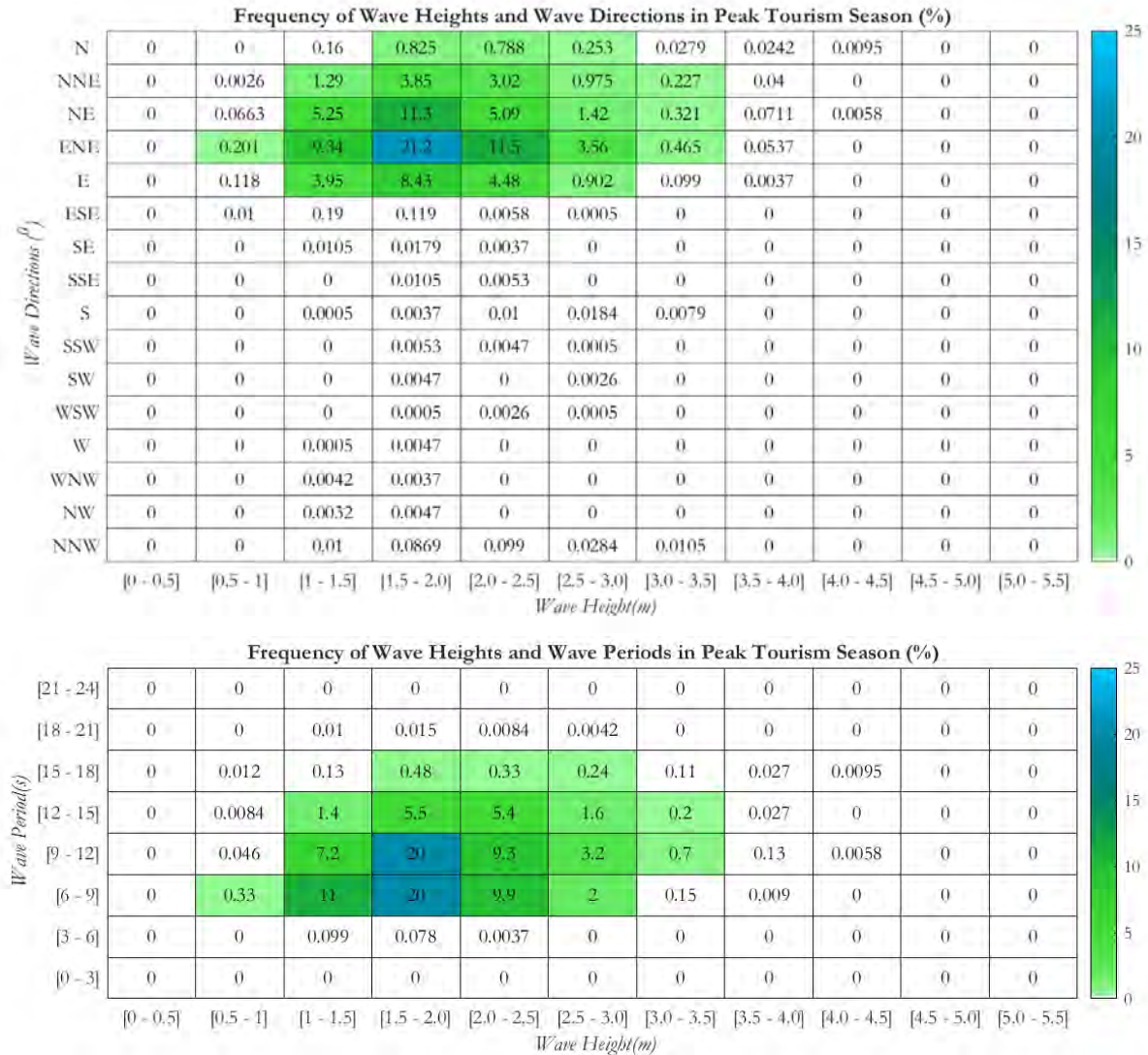


Figure 5.2 Frequency of wave height, wave direction and wave period during the peak tourism season.

The 43 years of wave data were analysed to assess the variation in offshore wave conditions across different months of the year. The results are presented in Figure 5.3. September exhibited a broad range of wave heights, including the highest wave height within the dataset. However, the average wave height (indicated by the blue line) was among the lowest, which could be attributed to the hurricane season potentially skewing the data significantly. The tourist season, spanning from November to April, experienced higher average wave heights.

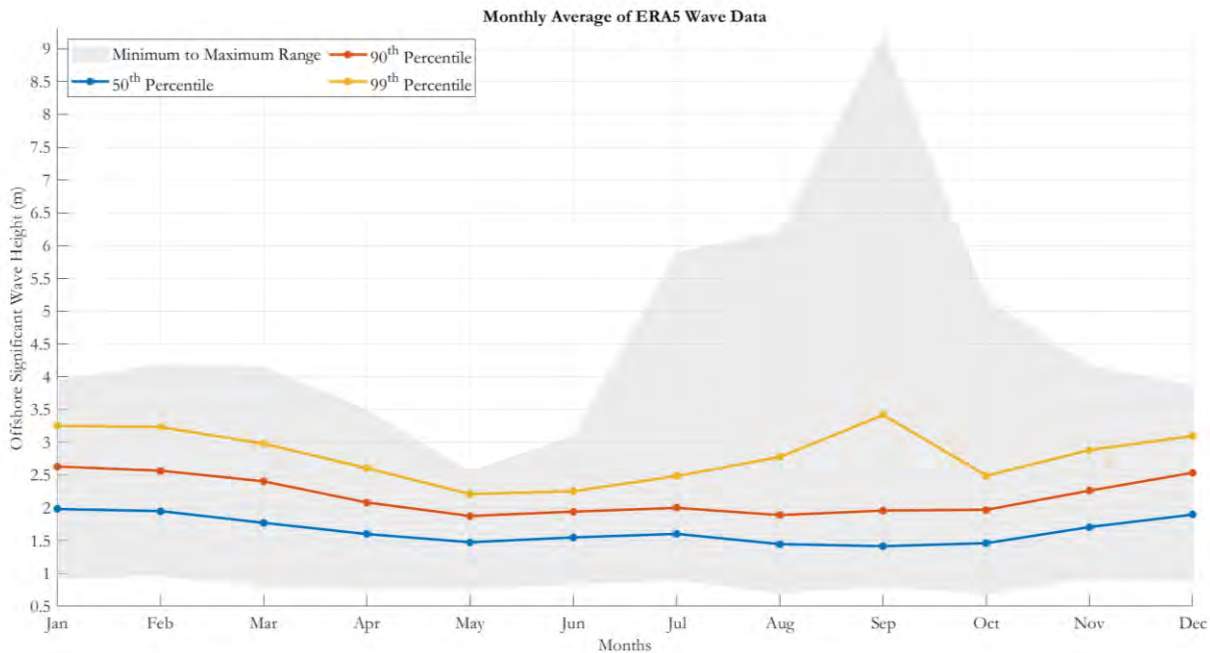


Figure 5.3 Monthly Statistics on offshore wave data.

5.1.2 The Nearshore Operational Wave Climate

The wave data obtained from the ERA5 node underwent a tri-variate frequency analysis of wave height, period, and direction, which is commonly referred to as "binning." This analysis categorized the wave data into 1124 distinct conditions or "events" based on a combination of wave height, peak period, and direction. Each event had a specific duration related to the number of occurrences over a 43-year period.

Although the ERA5 model is typically applied at spatial scales larger than 30km and outside the surf zone, it was not detailed enough to provide accurate nearshore wave data for Jumby Bay. Therefore, to develop the nearshore wave climate for the project area, a spectral wave model called MIKE 21 SW (described in Appendix A) was utilized. This model simulated waves approaching from the southeast, east, north-east, north, and north-west and moving over the deep water to the nearshore bathymetry of the island. The model was run in a semi-stationary mode with inputs of wave heights, periods, and directions along the boundaries of the model domain, which are shown in Appendix A.

The resulting nearshore wave climate data are displayed in Figure 5.4 as wave roses that demonstrate the variation of wave heights around Jumby Bay.

Figure 5.4 demonstrates the varying wave directions and intensities depending on the specific location along the coastline.

In the northern section of the island, waves predominantly approach from the north-northeast, exhibiting the highest wave energy directed towards the shoreline. Wave heights in this region range from 0.4-1.2m. At the eastern end, wave direction shifts to the northeast and east-southeast, with wave heights varying between 0.5 and 1.0m.

Moving to the southeast portion of the island, waves approach from the southeast and east-southeast directions, and the wave heights decrease to a range of 0.3-0.6m. The southwest end experiences the most protection from wave activity, thanks to the shielding effects of Maiden Island and Antigua. Here, waves approach from the southwest and south, and wave heights are observed to be between 0.3-0.5m.

Lastly, at the western end of the shoreline near Jumby Bay Resort, waves approach the coastline from the west-northwest. Further south along the same shoreline, waves shift to a northwest direction, with wave heights ranging from 0.3-0.6m.

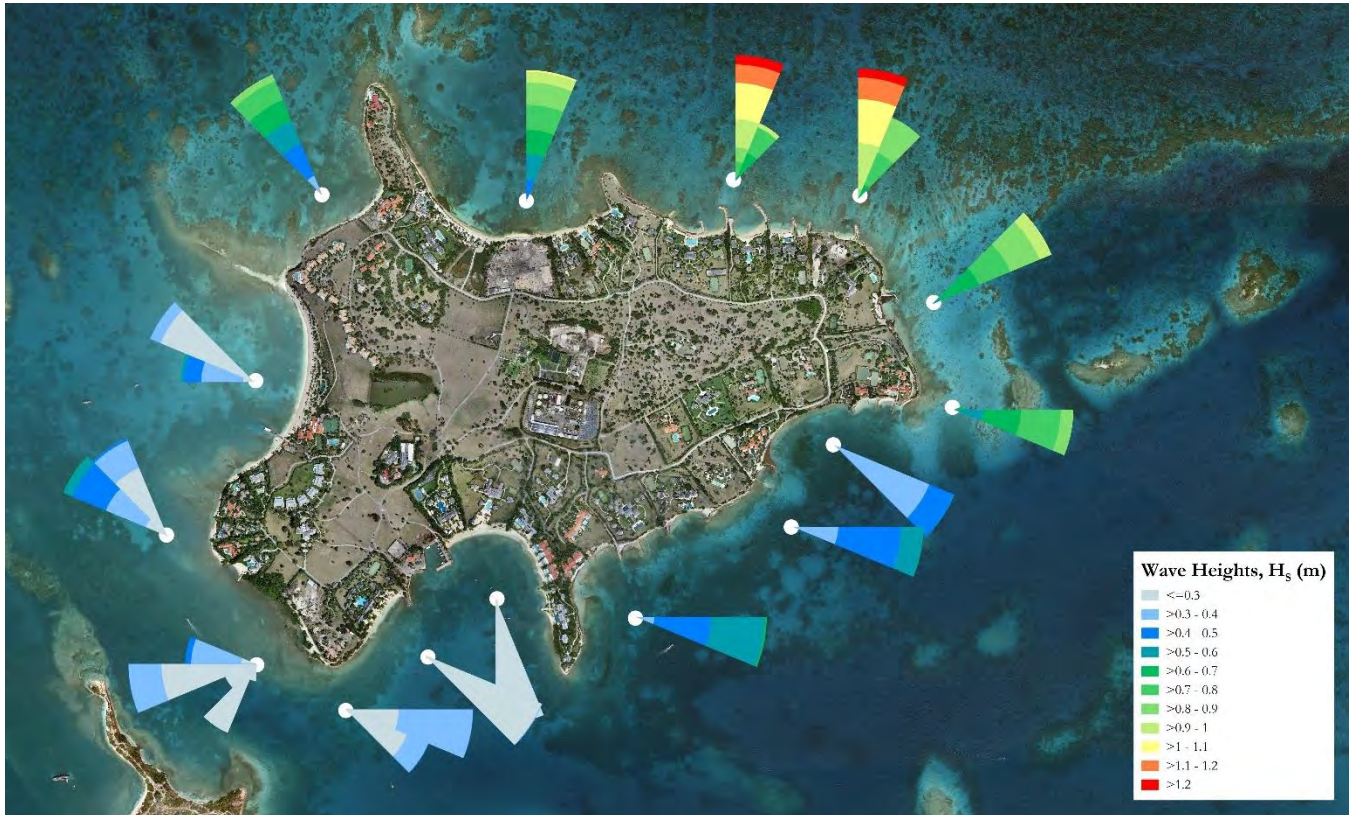


Figure 5.4 Nearshore wave roses along the shoreline of Jumby Bay.

Figure 5.5 presents the wave rose diagrams, which reveal minimal wave energy in the vicinity of Maiden Island. The low energy levels can be attributed to the island's geographical position and the protective influence of Jumby Bay. Throughout the year, wave heights surrounding Maiden Island typically range between 0.3 and 0.5m. The most significant waves tend to approach the island from the north-northwest to northwest directions, predominantly impacting the western shoreline of Maiden Island.



Figure 5.5 Nearshore wave rose plots for Maiden Island.

The wave roses, or directional distributions of wave energy, provide valuable insights into the potential for alongshore sediment transport at specific sections of the island's shoreline. This information can be used to inform coastal management strategies, such as beach nourishment or erosion control measures, to preserve and enhance the island's coastal environment.

The study uses a 2D image to illustrate the spatial extents of wave patterns, as shown in Figure 5.6. Two distinct wave climate scenarios are presented: the median annual wave climate (50th percentile), representing average wave heights and directions for each year; and the 99.86th percentile wave climate, which corresponds to the wave conditions exceeded only 12 hours per year.

The model results reveal that the northern and eastern ends of Jumby Bay are subjected to the highest wave energy throughout the year. This can be attributed to the dominant wave direction and exposure of these areas to open ocean swells, which often generate more powerful waves. As a result, these sections of the island may experience increased erosion rates and require more frequent coastal management interventions, such as beach nourishment or structural protection measures.



Conversely, the southern and western ends of the island receive lower wave energy during the year. These areas are likely to benefit from natural or artificial barriers that provide shelter from prevailing wave directions. Consequently, the coastal environment in these regions may experience less erosion and sediment transport, thus requiring less intensive management efforts.

The model results for Maiden Island show that the dominant wave directions approach the island from the north northwest along the western shoreline of the island and from the east along the eastern shoreline of Maiden Island. This is due to the sheltering effects of Jumby Bay.

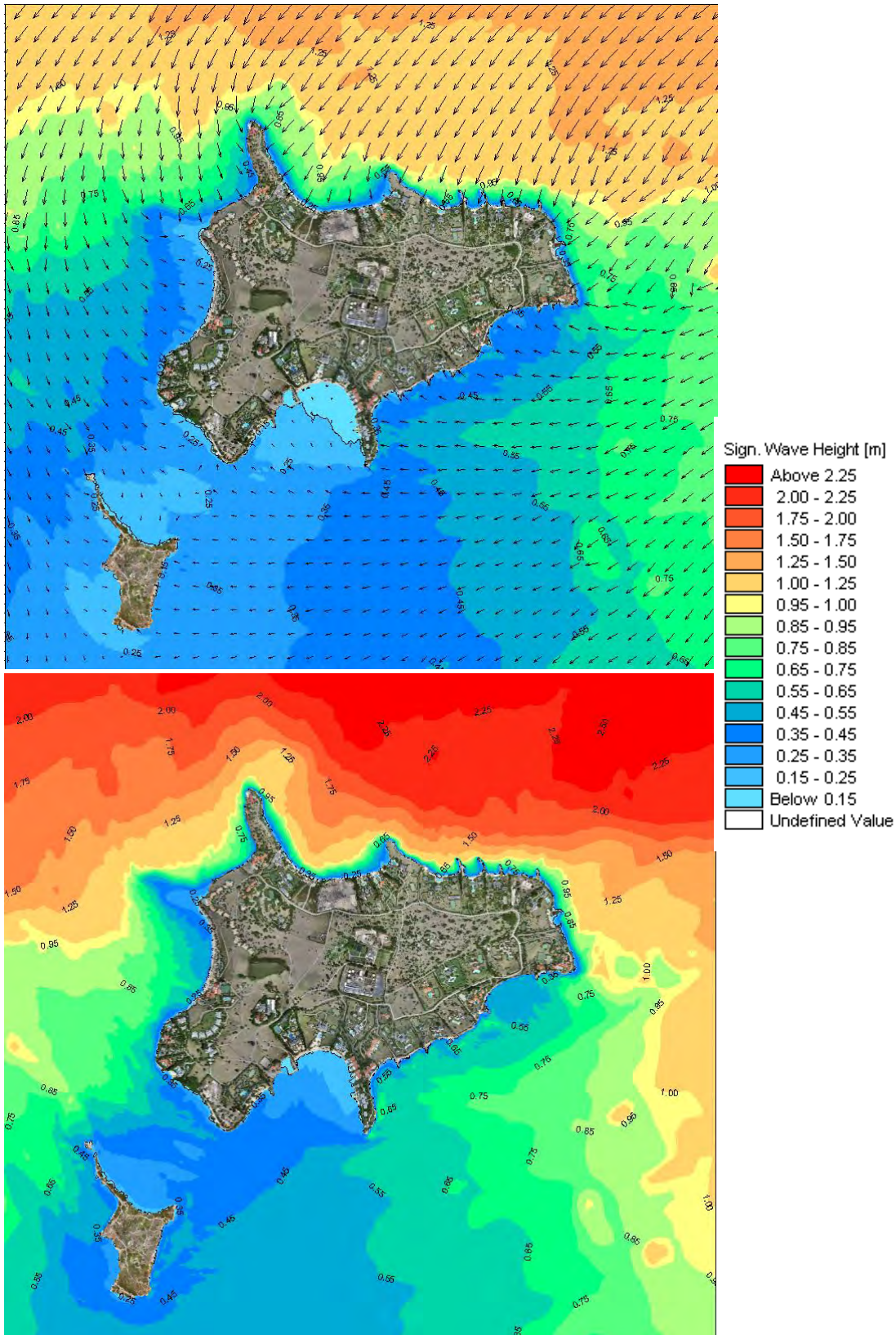


Figure 5.6 Significant wave heights along the Long and Maiden Island Shoreline. Median conditions (top) and 99.86th percentile (bottom).

5.2 Hurricane Wave Climate

The Caribbean region is highly vulnerable to tropical storms and hurricanes, which occur annually between June to November. These extreme weather events can cause dramatic and abrupt changes to the coastline, resulting in severe damage to infrastructure and communities. It is crucial to understand the potential impact of hurricanes on coastal protection structures and to design them accordingly.

Coastal protection structures should be designed to withstand wave attack from extreme storm events, which require careful consideration of factors such as the selection of an appropriate armour stone size, and determination of design wave forces. It is essential to gather decades or even centuries of data to adequately describe the statistics of extreme waves that occur infrequently.

In the case of the Atlantic Ocean, detailed information on tropical cyclones, including all hurricanes, has been collected by the US National Oceanic and Atmospheric Administration (NOAA), specifically at the National Hurricane Centre (NHC). This database of storm tracks and other parameters is a valuable source of information for understanding the individual storms and their potential impact on the Caribbean region.

Antigua & Barbuda lies directly in ‘Hurricane Alley,’ an area in the Atlantic Ocean within which hurricanes typically form due to the warmer sea surface temperatures. It is vital to understand the typical path of hurricanes in the North Atlantic basin, which tend to form between latitudes 5°N and 25°N off the west coast of Africa and then track across the Atlantic Ocean. Those formed at the lower latitudes usually move on a westerly track by the northeast trade winds, while those of the higher latitudes move more to the north and northwest.

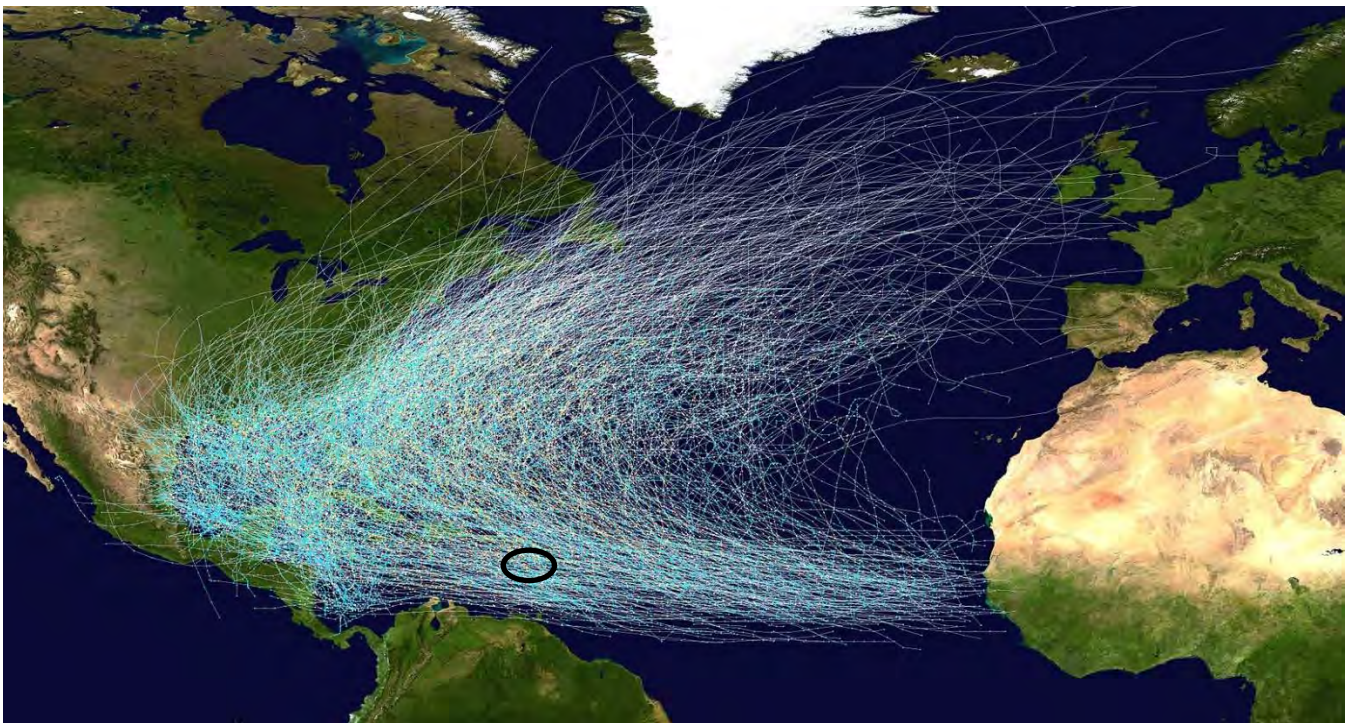


Figure 5.7 Atlantic hurricane tracks since 1851, the sweeping shape of which is commonly called ‘Hurricane Alley’. The approximate location of Antigua & Barbuda is highlighted with an oval.



5.2.1 Historical Hurricane Activity

A comprehensive analysis of historical hurricane data from NOAA's National Hurricane Centre (NHC) database has been conducted for storms occurring between 1850 and 2021. All hurricanes that passed within a 300km radius of the project site, which includes Jumby Bay and Maiden Island, were examined. The results reveal that since 1850, the study area has experienced a total of 183 tropical storms and hurricanes.

These weather events can be further categorized using the Saffir-Simpson Hurricane Wind Scale, a widely recognized classification system for hurricane intensity. Figure 5.8 illustrates the distribution of storm intensities in the study area. It is evident that tropical storms (117) were the most common occurrences, while the region was also impacted by strong hurricanes (Category 3 or higher) fairly frequently, with 29 such incidents reported.

To better understand the temporal distribution of these hurricanes and storms, Figure 5.9 provides a detailed overview of their occurrences over the years. This graph highlights the fact that there can be multiple years without any hurricanes, while also showing that in some instances, more than one storm can make landfall on the island within a single year. Additionally, it is worth noting that an upward trend in the frequency of storms is observed, which may be linked to factors such as climate change and rising sea surface temperatures.

Furthermore, it is important to consider the potential impacts of these storms on the project site, such as infrastructure damage, flooding, and coastal erosion. Proper planning and implementation of mitigation measures, such as resilient building design, storm surge barriers, and early warning systems, can help reduce the risks associated with hurricanes and tropical storms in the area.

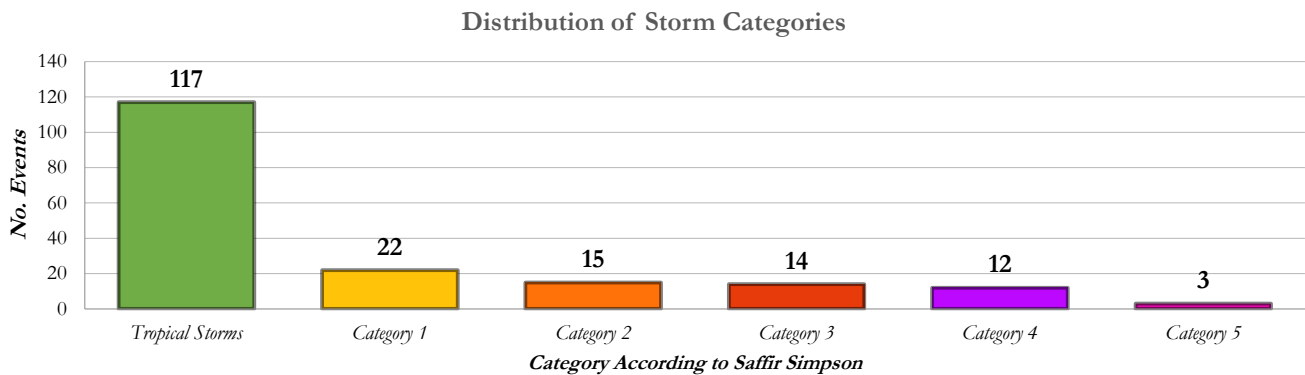


Figure 5.8 Storm distribution, according to Saffir Simpson classification, since 1850 showing storms that have passed within a 300km radius of the project site.

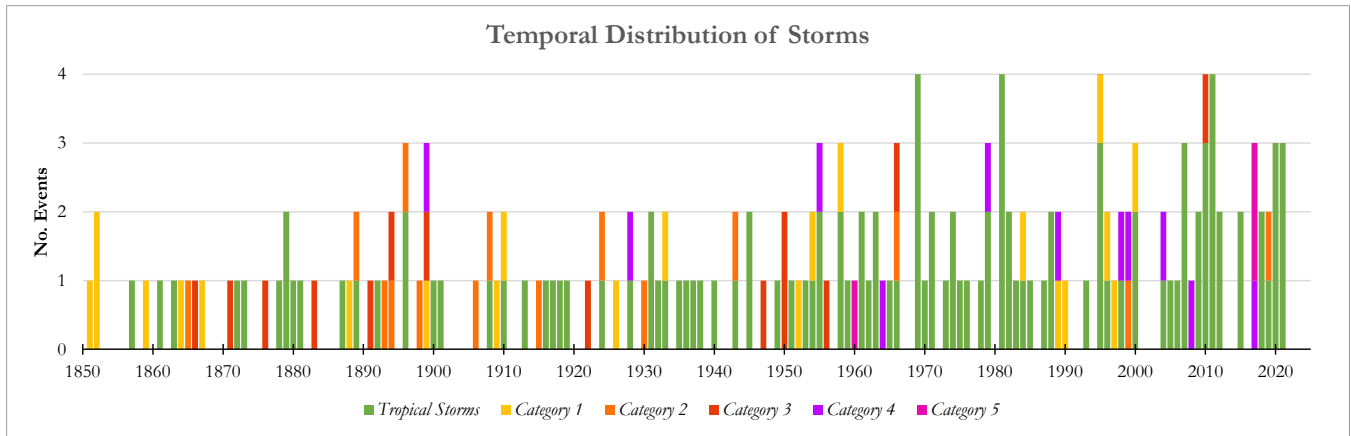


Figure 5.9 Hurricane & storm distribution by year since 1850 showing storms that have passed within a 300km radius of the area.

5.2.2 Hurricane Simulations

5.2.2.1 Hindcasting hurricane waves and surge levels

Deep water wave conditions were calculated for each selected tropical cyclone using parametric models (Cooper, 1988; Young and Burchell, 1996). The resulting wave conditions were segmented into directional sectors and fit to a statistical function describing their exceedance probability. The wave heights for two return periods (50-year and 100-year) were determined from the best-fit statistical distribution. The deep-water wave parameters corresponding to the various return periods were computed for five directional sectors of incidence. Table 5-1 shows the wave heights, wind speeds, and periods for the directional sectors investigated. The highest waves come from the eastern sector with wave heights 10m for the 25-year storm, almost 12m for the 50-year storm, and above 13m for the 100-year storm. It is interesting to note that although the hurricane waves coming from the east had the largest wave heights and longest wave periods, the highest winds came from the north-east.

Table 5-1 Wave Parameters (significant wave height and peak period) and wind conditions used for 50- and 100-year return period simulations.

| Directional Sector | Parameters | Return Period (-year) | |
|--------------------|-------------------------|-----------------------|-------|
| | | 50 | 100 |
| Southeast | Wave Height, H_s (m) | 11.7 | 12.7 |
| | Wave Period, T_p (s) | 15.5 | 16.4 |
| | Wind Speed, V_m (m/s) | 21.11 | 23.07 |
| East | Wave Height, H_s (m) | 13.9 | 15.1 |
| | Wave Period, T_p (s) | 17.3 | 18.3 |
| | Wind Speed, V_m (m/s) | 21.7 | 23.12 |
| Northeast | Wave Height, H_s (m) | 10.9 | 12.1 |
| | Wave Period, T_p (s) | 14.9 | 15.9 |
| | Wind Speed, V_m (m/s) | 24.35 | 26.45 |



| Directional Sector | Parameters | Return Period (-year) | |
|--------------------|-------------------------|-----------------------|-------|
| | | 50 | 100 |
| North | Wave Height, H_s (m) | 8.4 | 9.4 |
| | Wave Period, T_p (s) | 12.6 | 13.6 |
| | Wind Speed, V_m (m/s) | 19.33 | 21.08 |
| Northwest | Wave Height, H_s (m) | 7.9 | 8.8 |
| | Wave Period, T_p (s) | 12.2 | 13.0 |
| | Wind Speed, V_m (m/s) | 18.04 | 20.99 |

5.2.2.2 Climate Change Inclusion

Sea level rise and climate change are critical concerns for small islands, as they have the potential to cause significant social, economic, and environmental impacts. As climate change intensifies, small island nations are particularly vulnerable due to their unique characteristics, which include their small size, limited resources, and isolated locations.

1. Coastal erosion and inundation: Sea level rise can exacerbate coastal erosion, which may lead to the loss of land and infrastructure, including homes, roads, and agricultural lands. This can disrupt the livelihoods of local communities and increase the risk of displacement. Inundation, or the permanent submergence of land, is also a significant threat for low-lying islands, as it can result in the loss of entire communities or even entire islands.
2. Saltwater intrusion: As sea levels rise, saltwater can infiltrate freshwater sources, such as aquifers and surface waters, making them unsuitable for drinking, agriculture, and other uses. This poses a major challenge for small islands that already face limited freshwater resources.
3. Impact on ecosystems: Climate change and sea level rise can lead to the degradation or loss of critical ecosystems, such as coral reefs, mangroves, and seagrass beds, which provide valuable services to island communities. These ecosystems offer coastal protection, support fisheries, and contribute to tourism, among other benefits. The loss of these ecosystems can have significant consequences for the livelihoods and food security of local populations.
4. Increased vulnerability to extreme events: Climate change can lead to more frequent and intense storms, which can cause severe damage to infrastructure, housing, and ecosystems. Small islands are particularly vulnerable to these events due to their limited capacity to prepare for, respond to, and recover from disasters.

Smith Warner International’s approach to applying climate change scenarios is to assume the worst-case scenario which in the current period is the SSP5-8.5 scenario. The SSP5-8.5 climate model is a specific combination of a shared socioeconomic pathway (SSP) and a representative concentration pathway (RCP) that together depict a possible future scenario for Earth’s climate system³. Shared Socioeconomic Pathways

³ [A new scenario framework for climate change research: the concept of shared socioeconomic pathways | SpringerLink](#)



(SSPs) are narratives that describe various possible socioeconomic futures, covering aspects such as population growth, economic development, and technological progress. There are five SSPs, numbered from 1 to 5, each representing a different trajectory for global development.

Representative Concentration Pathways (RCPs) are four greenhouse gas concentration trajectories used by the Intergovernmental Panel on Climate Change (IPCC) to model future climate change⁴. RCPs are defined by their radiative forcing values, which represent the additional energy that is being absorbed by the Earth due to increased greenhouse gas concentrations. The RCPs range from RCP2.6, representing a low-emission scenario, to RCP8.5, representing a high-emission scenario.

SSP5-8.5 combines SSP5, which represents a future characterized by rapid and unconstrained economic growth and relatively high levels of fossil fuel use, with RCP8.5, the highest emission scenario. In this scenario, greenhouse gas emissions continue to increase throughout the 21st century, leading to high levels of global warming and associated climate impacts⁵. SSP5-8.5 is often referred to as a "business-as-usual" or "worst-case" scenario, as it depicts a world with limited climate mitigation efforts, resulting in significant negative consequences for ecosystems, human health, and global stability.

To compute the total static storm surge level in deep water, global sea level rise (GSLR) for the projected year and the highest astronomical tide were added to the Inverse Barometric Rise (IBR) values, which were also calculated from the NHC database using extreme value statistical analyses. The results for the 50-year and 100-year surface level values are listed in Table 5-2.

⁴ [The Shared Socioeconomic Pathways and their energy, land use, and greenhouse gas emissions implications: An overview - ScienceDirect](#)

⁵ [AR6 Synthesis Report: Climate Change 2023 — IPCC](#)



Table 5-2 IBR and design deep water surface level (m) for return periods of 50 and 100 years.

| Parameter | Return Period (-years) | | Notes |
|--|---------------------------|-------------|---|
| | 50 | 100 | |
| IBR (m) | 0.40 | 0.47 | Determined through statistical hind-casting analysis |
| Highest Astronomical Tide (m) | 0.25 | | Determined through historical analysis |
| Rate of Sea Level Rise (mm/year) | 8.6 | | Average of SSP5-8.5's ('2040 to 2060' and '2080 to 2100') |
| Time Horizon (years) | 50 | | How long structure is to last (not related to design storm) |
| Design Deep Water Surface Level (m) | 1.08 | 1.15 | Sum of IBR, Highest Astronomical Tide, and Sea Level for 50years. |

5.2.2.3 Nearsore wave transformation of hurricane waves

In the analysis of deep-water conditions and their transformation to nearshore regions and the project site, MIKE21 was used. The extreme wave climate conditions presented in Table 5-1, as well as the deep-water surface levels from Table 5-2, were applied to the model boundary and transformed to the nearshore across five main directional sectors: south-east, east, north-east, north, and north-west. The wind fields (magnitude and direction) were treated as constants throughout the entire model domain. The worst-case scenario incorporated a combination of all directions, with a statistical maximum from each direction extracted and plotted.

The coupling of hydrodynamics and waves in the numerical model is crucial for storm surge computations, particularly in regions like the Caribbean where wave set-up contributes significantly to the overall storm surge. As large waves approach shallow water or a reef and break, water levels rise, generating localized currents. These currents and fluctuating water levels influence waves, allowing them to travel farther inland. The coupling of waves and currents in MIKE21 facilitates accurate simulation of these factors. Utilizing the extreme wave climate conditions mentioned earlier, the model was executed and maximum conditions near the shoreline were extracted.

Results from the 50-year return period storm are illustrated in Figure 5.10, depicting hurricane waves impacting the project shoreline (top plot) and the anticipated static storm surge under this specific return period scenario (bottom plot). Like the operational wave scenario, the highest energy wave conditions are found along the north and eastern sections of the shoreline, with lower wave energy observed along the southern sections of Jumby Bay and Maiden Island. Wave heights range from 1.25 to 1.5m along the north and eastern sections of Jumby Bay, and from 0.75 to 1.25m along the southern section of Jumby Bay and Maiden Island.

Static storm surge results under the design storm range from 1.0 to 1.3m along the entire shoreline of Jumby Bay and Maiden Island. The storm surge plot (Figure 5.10 – bottom plot) indicates potential inundation at the Jumby Bay hotel property and a low-lying pond along the northern shoreline. At Maiden Island, the northern section of the island is entirely inundated by the static storm surge.

Under the 100-year return period storm (Figure 5.11), the model reveals wave heights ranging between 1.75 to 2m along the north and east sections of the island. Along the southern and western sections of Jumby Bay and the Maiden Island shoreline, wave heights range from 0.75m to 1.50m. Static storm surge indicates



inundation at the Jumby Bay Hotel Resort and a private property along the northern section of Jumby Bay (low lying pond). The northern section of Maiden Island is entirely inundated.

It is important to note that wave run-up has not been included in these calculations, which could lead to even higher inundation levels further inland. Wave run-up is further discussed Section 5.2.3 of this report.

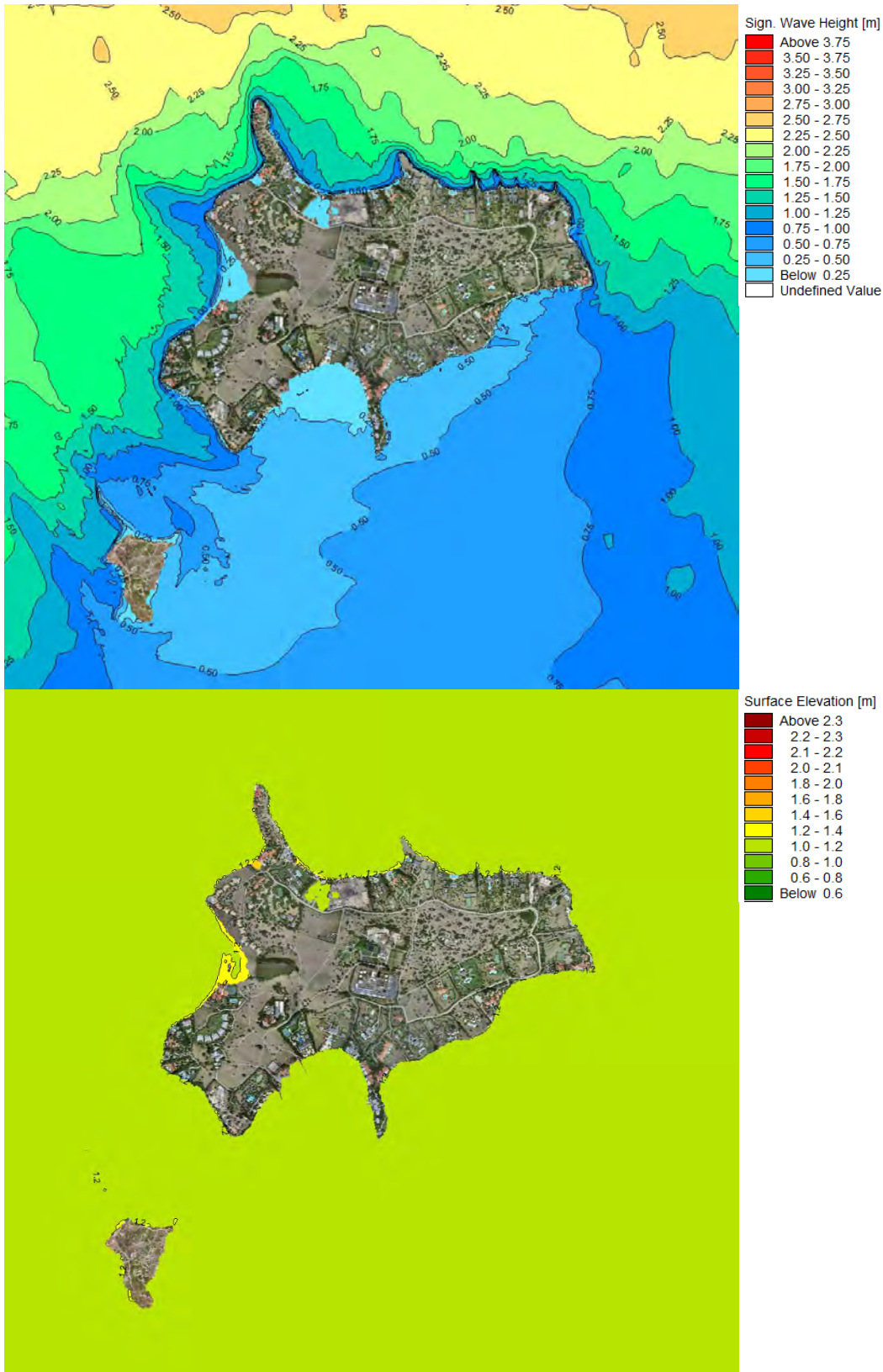


Figure 5.10 Hurricane wave heights at project shoreline (top plot) and storm surge inundation (bottom plot) during the 50-year storm event.

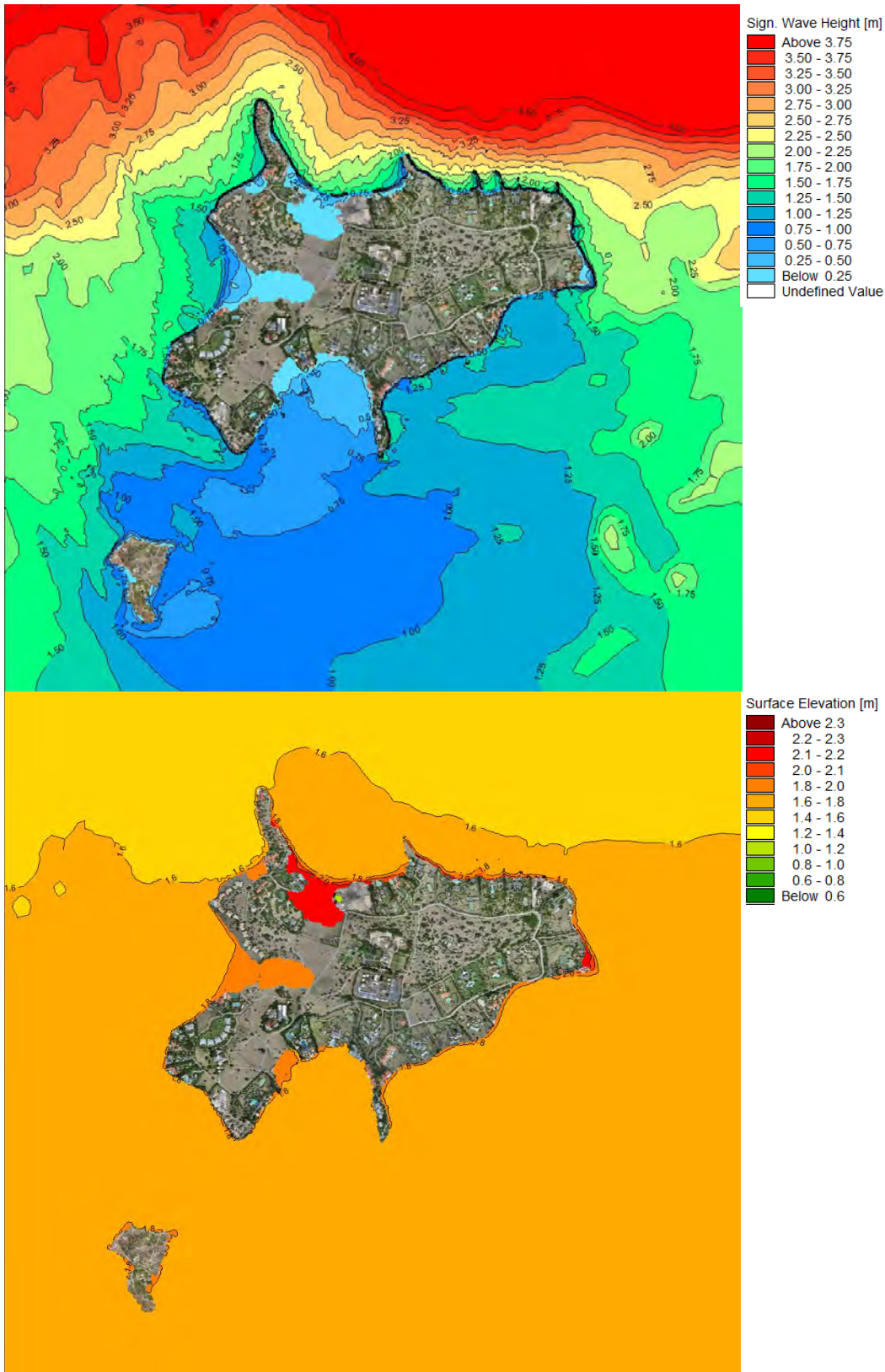


Figure 5.11 Hurricane wave heights at project shoreline (top plot) and storm surge inundation (bottom plot) during the 100-year storm event.

5.2.3 Total Inundation related to Hurricanes

The water levels associated with the hurricane wave climate analysis, as demonstrated in Figure 5.10 and Figure 5.11, represent the static water levels occurring near the shoreline during a storm event. Nevertheless, waves often run up onto the beach at the shoreline, causing an additional increase in surge and flooding levels. This dynamic component of storm surge, known as wave run-up, combined with the static surge, results in the total inundation level.

Wave run-up transpires when a wave breaks, allowing a portion of its remaining energy to travel up the face of the beach. The elevation reached by the run-up depends on the characteristics of the "swash zone" – the area where the wave interacts with the beach. If this zone consists of a smooth, impermeable surface, a higher run-up is likely. In contrast, the presence of a rough, armoured stone slope or a vegetated surface can reduce the run-up.

Due to the localized variability of wave run-up and its dynamic nature, storm surge computations in numerical models typically do not incorporate wave run-up. However, it is calculated and employed in the design of coastal structures. Both the static and dynamic components of storm surge are combined to determine the final inundation levels, ensuring a comprehensive assessment of potential flooding risks.

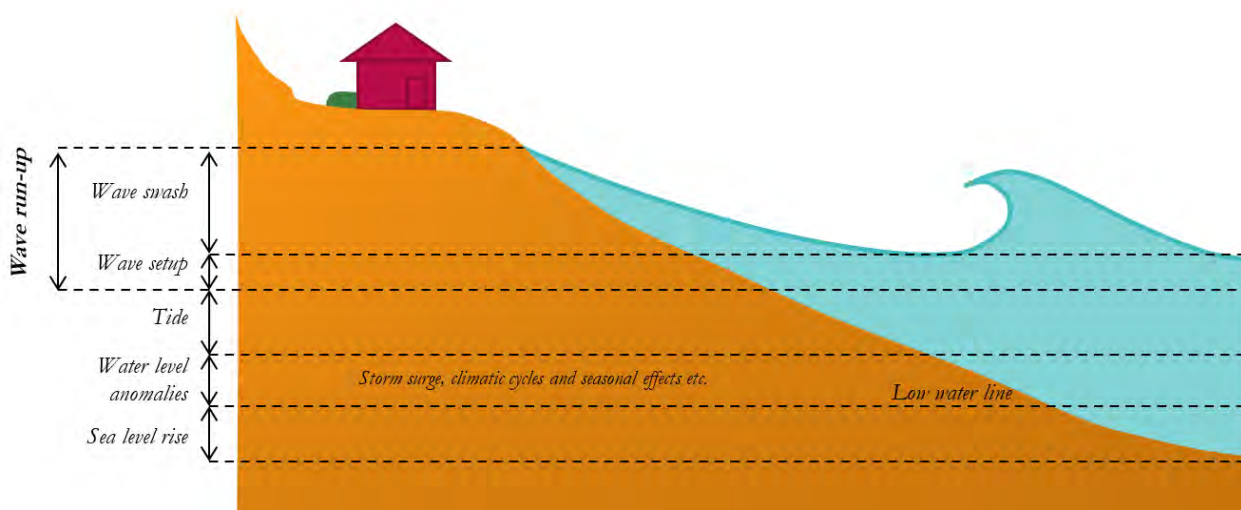


Figure 5.12 The water level components that contribute to coastal flooding.

Storm surge modeling is an essential component of coastal engineering design as it allows for the estimation of the potential impact of coastal storms on infrastructure and coastal communities. While MIKE 21 models can provide a static water level near the shoreline, it is important to investigate wave run-up to define the total surge levels accurately.

In this study, SWI applied XBeach (Roelvink, 2009) in a one-dimensional format to simulate the storm-induced water level changes for the design events outlined in the prior sections. To capture the water surface dynamics, the XBeach model was run in a non-hydrostatic mode, and sediment properties were described based on sediment samples as detailed in Section 2.3.

The study used eight (8) profiles (Figure 5.13) extracted along the project site using a simple routine in GIS software that merged lidar topographic data and EOMAP satellite-derived bathymetry. The data was

interpolated to provide one-dimensional profiles that extended perpendicularly from the shoreline to about the 12m depth contour for exposed coasts. Profiles taken from sheltered locations such as the western beach were shortened to account for wave refraction. All profiles were then formatted and used as input files for the model. Some profiles were taken where there are existing structures. Profiles P2, P3 and P4 had revetments which were added in the model setup as areas that were non-erodible.

To properly capture the storm-induced water level changes, wave heights, wave periods, wind speeds, and water level set-up from the 50-year and 100-year storm events were extracted at the seaward end of the profiles in the domain of the MIKE 21 results. This data was then input into the XBeach model with a direction perpendicular to the shore, representative of the worst-case scenario.

Overall, this approach provides a comprehensive methodology for storm surge modelling that considers wave run-up to define the total surge levels. The use of one-dimensional profiles derived from dense elevation data provides a detailed representation of the local topography, allowing for the accurate simulation of storm-induced water level changes. The combination of data from MIKE 21 models and XBeach allows for a more comprehensive understanding of the potential impact of coastal storms on the islands.

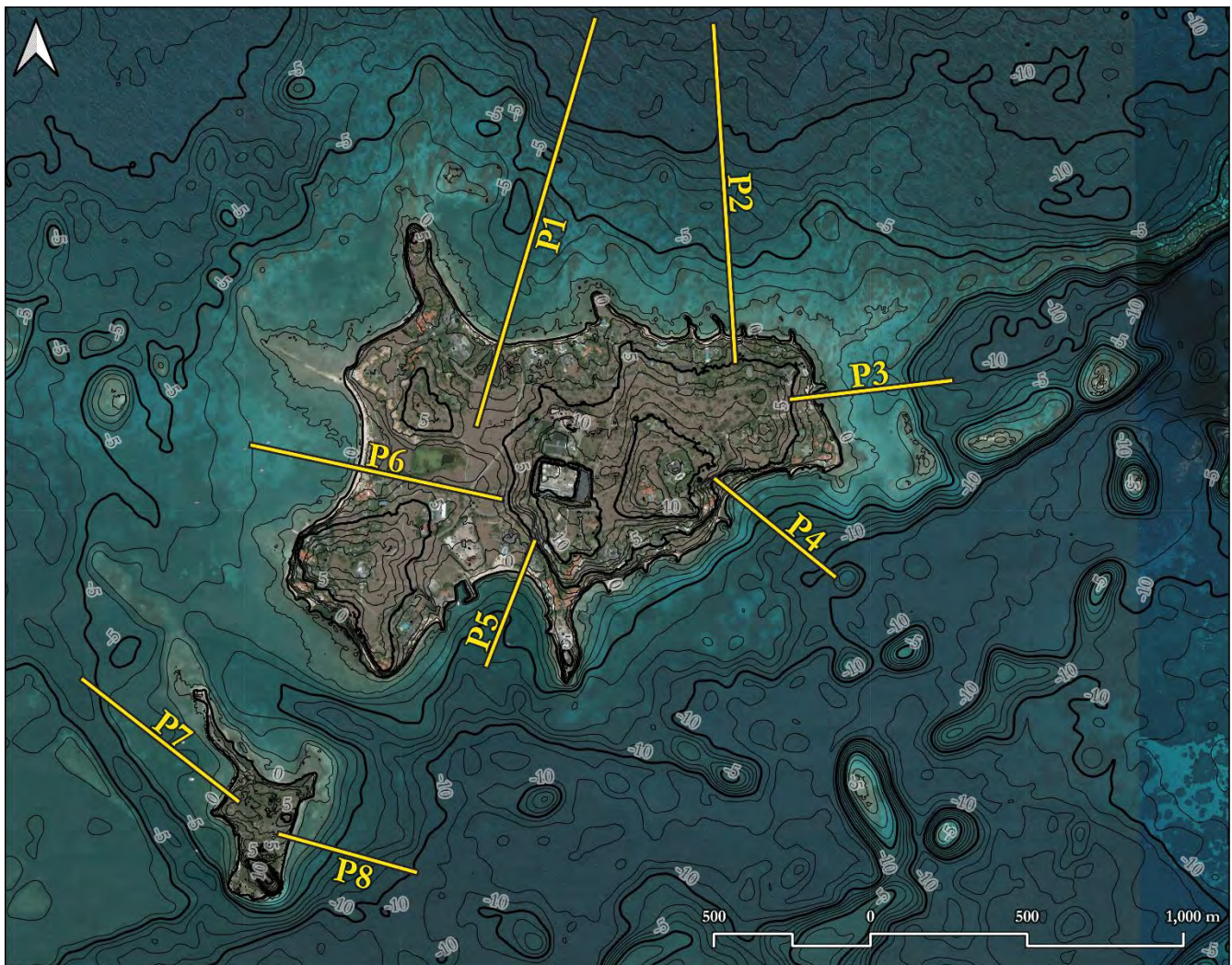


Figure 5.13 Location of XBeach Profiles.



The static storm surge modeling results indicate that profiles P1 and P4 experienced the worst inundation extents based on both the MIKE 21 and XBeach models. However, the dynamic component of wave run-up revealed an increase in vertical elevations of surge, indicating that the surge may have been higher than what was estimated by the MIKE 21 models alone. The XBeach modeling results are presented in Appendix A.3.

The results of the 100-year storm event for vulnerable areas around profiles P1 and P4 are presented in Figure 5.14. The figures show that both profiles experienced significant inundation, likely due to their low-lying nature, which allowed water to run up and overtop the main dune areas. Once the dunes were overtopped, the surge went another 150m further inland, causing more flooding.

Additionally, both dunes experienced scouring of the dune face, with the northern profile (P1) experiencing 0.6m of scour and the western profile (P2) experiencing 0.2m of scour. These results highlight the potential for significant damage to coastal infrastructure and property in the event of a major storm event.

XBeach was also run for two profiles on Maiden Island. The results on the island showed significant scour on both sides of the island. Figure 5.16 shows the results for the 100-year storm conditions on Profile 8 (P8). Although the wave height was low in that area, the vertical scarp was undercut by wave action and thus eroded by up to 1.1m during the simulation.

Overall, the storm surge modeling results provide valuable information for coastal engineering design and planning. The incorporation of XBeach modeling, which considers wave run-up, helps to provide a more accurate representation of the potential impact of storm surges on coastal communities and infrastructure. The results highlight the importance of considering not just the static water level near the shoreline, but also the dynamic component of wave run-up and its potential impact on vulnerable areas.

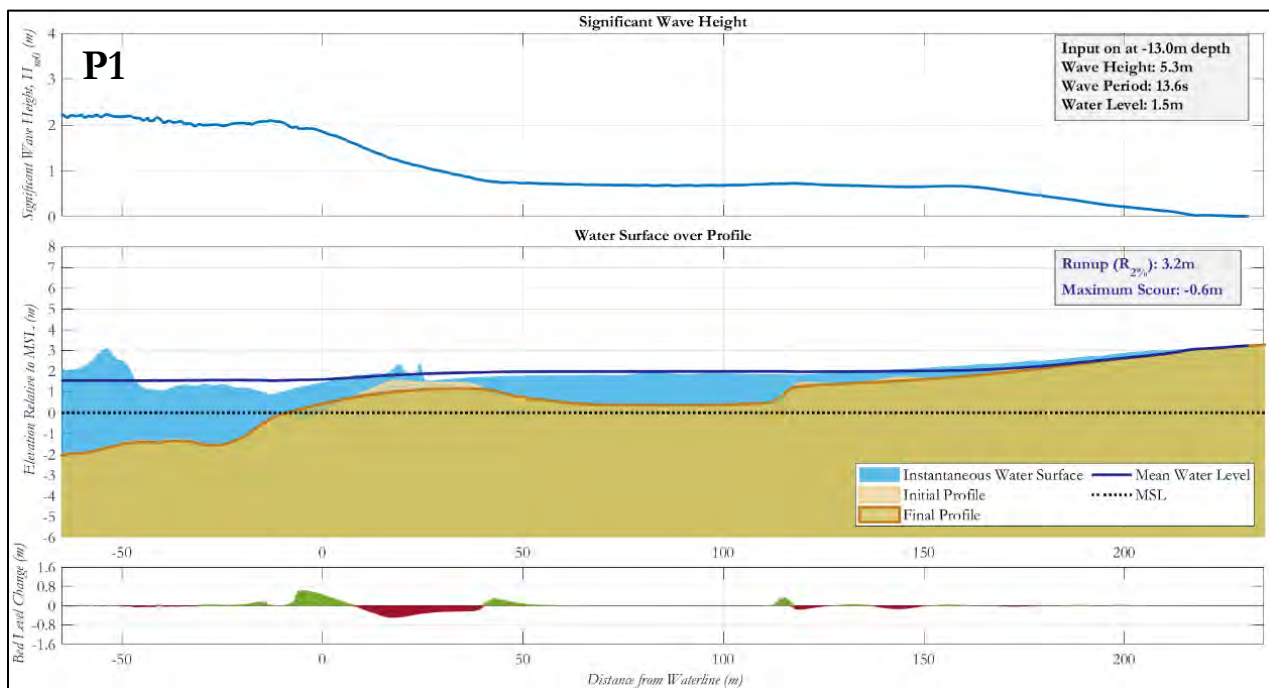


Figure 5.14 Key wave runup result for Profile 1 on the island of Jumby Bay.

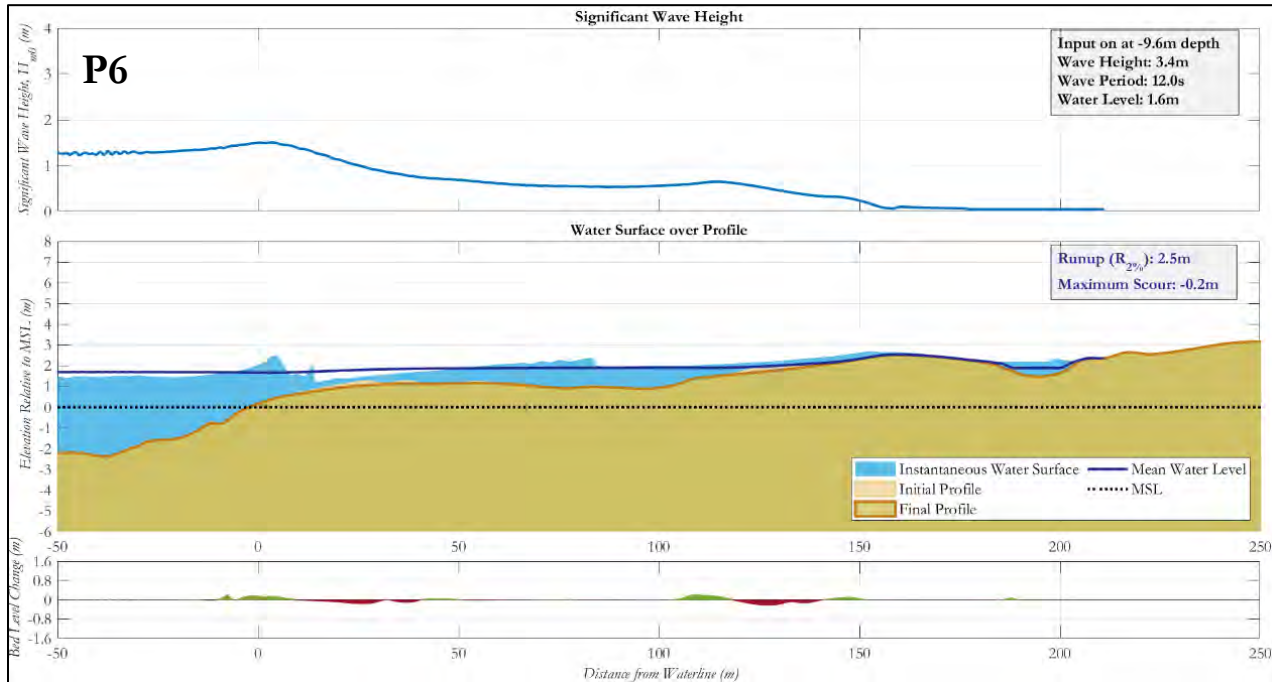


Figure 5.15 Key wave runup result for Profile 6 on the island of Jumby Bay.

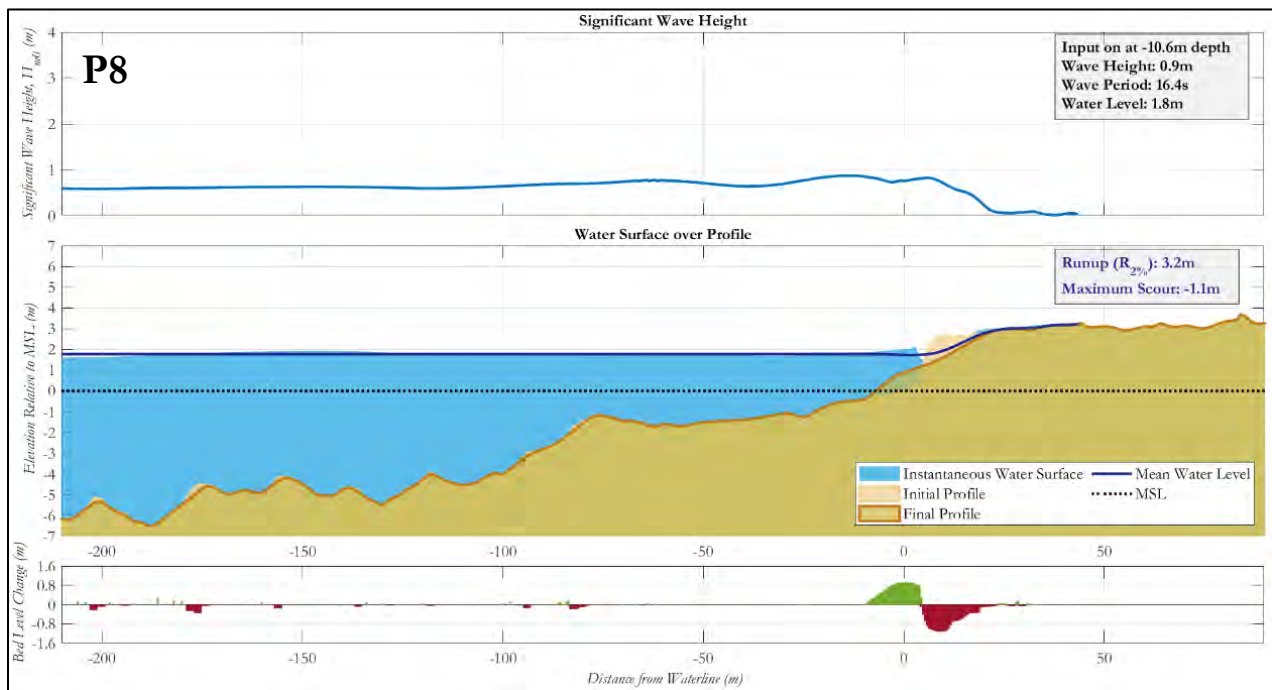


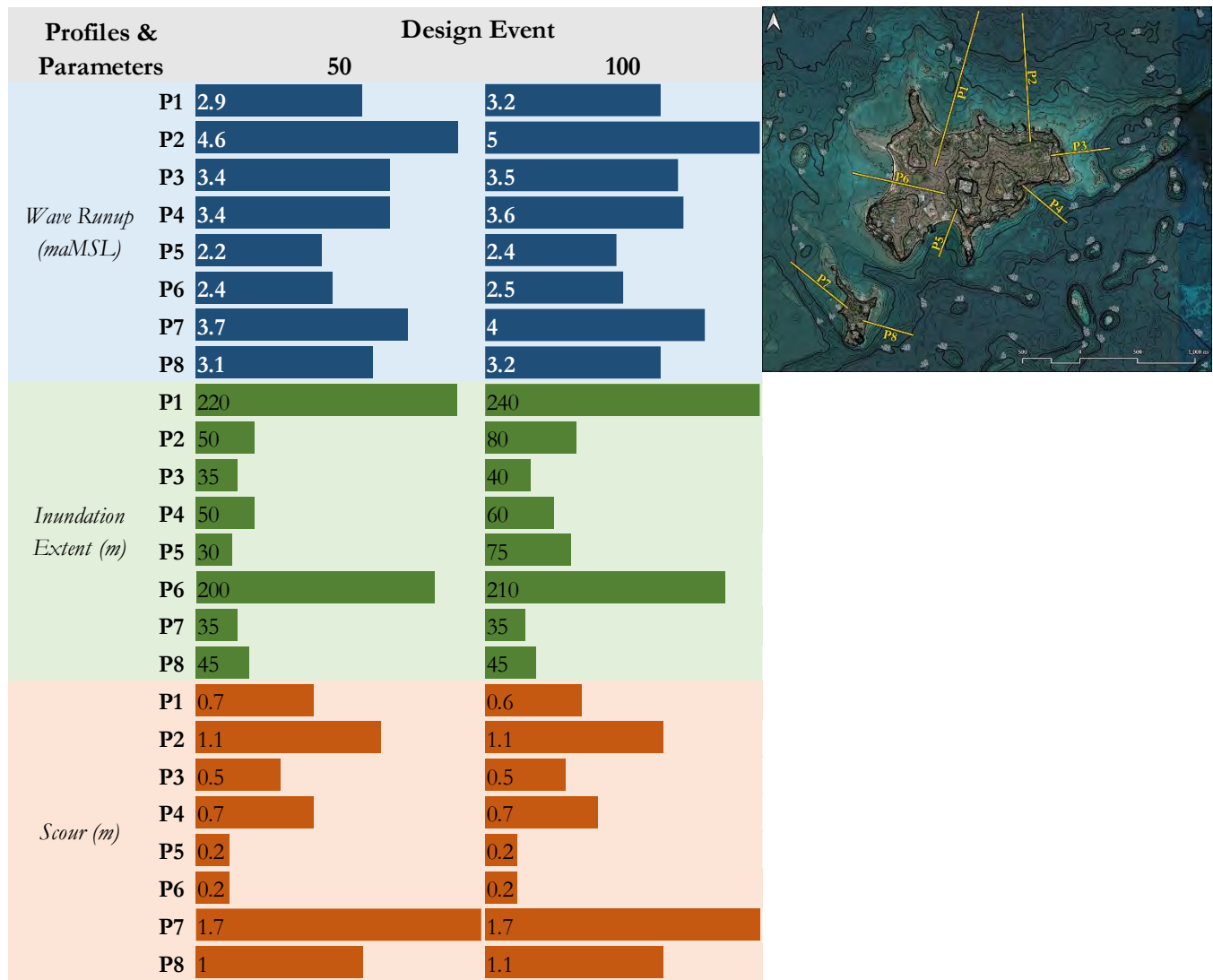
Figure 5.16 Key wave runup result for Profile 8 on the island of Maiden Island.

The XBeach modelling results are summarized in Table 5-3, providing a comprehensive overview of the storm-induced water level changes for each profile. Profiles P1 and P4 had the furthest inundation extent, but the wave runup levels were not very high. Profile P2 had the highest inundation level of up to 5m in the 100-

year storm event. This elevation was due to the steep topography in the area and the high storm waves on the north coast. Profile P2 also experienced high wave runup levels of 4.6m in the 50-year storm event.

Profile P3 was taken in the sheltered southern bay, which experienced much calmer conditions than the other areas. P3 had wave runup levels of up to 2.3m in the 100-year storm event and inundation of around 30m. Profiles P5 and P6 were taken on Maiden Island, and the profiles' steep topography caused some cliff erosion in both storm cases. Profile P5 experienced higher wave runup and scour due to high northern waves in that area.

Table 5-3 All XBeach profile results for the 50-year and 100-year storm.



5.2.4 Flooding Estimate

Flooding extents are useful in the early stages of a project as they help to delineate vulnerable areas and assets. The flood zones may guide new projects, the relocation of coastal assets and the refurbishing of existing structures like a dock or seawall. The horizontal flooding extents, shown in Figure 5.17, were delineated from the final elevations of wave run-up over the topography of the site for the 50-year and 100-year storm.

On Jumby Bay, 30% of the island was inundated in the 50-year storm event. During the 100-year storm, 33% of the island was inundated. Maiden Island had similar extents for both events with the 100-year storm showing 70% of the island being inundated. The public beach areas had the furthest inundation extents as has been shown in the model results up to this point. These results are intended to be interpreted as guides for future works and to help the client group make decisions on how much flooding they are prepared to tolerate.

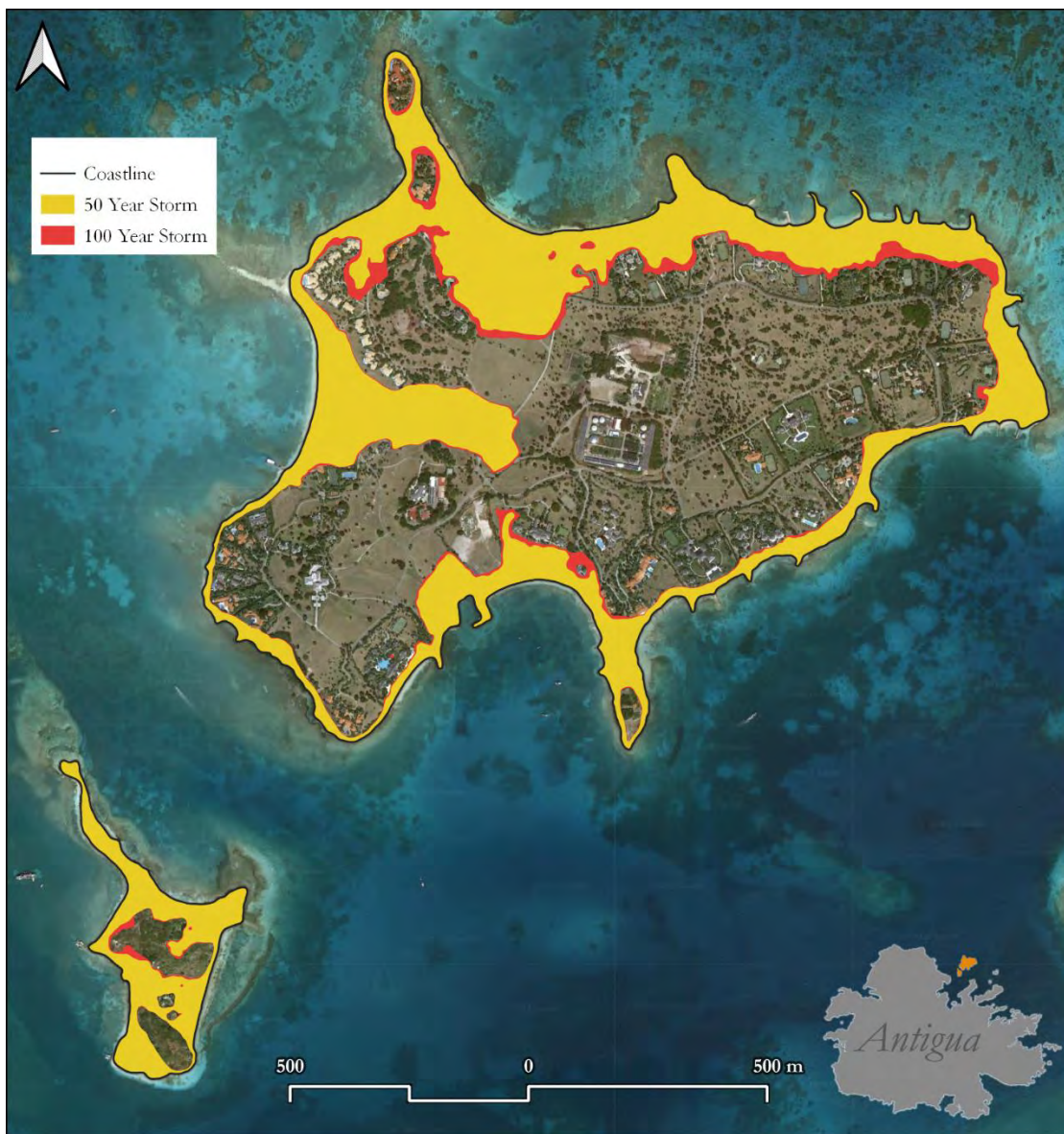


Figure 5.17 Flooding extents with wave runup for the 50-year event and 100-year event.

6 Currents and Tides

A review of the literature indicates that the main current stream around Antigua and Barbuda is the North Equatorial Current. The North Equatorial Current (NEC) is a significant westward-flowing ocean current that plays a critical role in the circulation of water in the tropical and subtropical regions of the North Atlantic Ocean. Originating around the Canary Islands at approximately 10-20°N latitude, the NEC is driven primarily by the trade winds and moves westward across the Atlantic. As it approaches the Caribbean Sea, it splits into two branches - the Antilles Current and the Caribbean Current (Figure 6.1).

Antigua and Barbuda, located in the northeastern Caribbean region, experience the direct influence of the Antilles Current. This current flows northwestward along the island chain, passing through the Lesser Antilles and into the Caribbean Sea. The Antilles Current not only affects ocean circulation around the islands but also contributes to the overall water temperature, marine ecosystem, and local weather patterns. The warm waters brought by this current support diverse marine life, including coral reefs and various fish species, which are essential for the local economy and ecosystem health.

The Caribbean Current, the other branch of the NEC, moves westward into the Caribbean Sea, affecting the circulation patterns throughout the region. Although it is not in the direct vicinity of Antigua and Barbuda, it does influence the general ocean circulation and weather patterns in the area.



Figure 6.1 Dominant ocean currents in the Northern Atlantic Ocean.

6.1 Global Tide Model

The DTU 10 Global Tide Model is a high-resolution ocean tide model developed by the Technical University of Denmark (DTU) Space division. It provides detailed information on global ocean tides, including both amplitude and phase, at a spatial resolution of 0.125 degrees. The model is based on a combination of satellite altimetry data and in-situ measurements, which have been assimilated using a least-squares technique to optimize the model's accuracy.

Key features of the DTU 10 Global Tide Model include:

1. High-resolution coverage: The model offers a spatial resolution of 0.125 degrees, which enables the study of local tidal phenomena and coastal areas with improved detail.
2. Comprehensive tidal constituents: The model includes a total of 69 tidal constituents, allowing for a more accurate representation of the ocean tide dynamics.
3. Data assimilation: The model incorporates both satellite altimetry data and in-situ tide gauge measurements, which enhances its overall accuracy and reliability.
4. Versatile applications: The DTU 10 Global Tide Model is useful for various applications such as oceanographic research, coastal engineering, sea level studies, and satellite orbit determination.

In general, the tidal signal near Antigua consists of a combination of diurnal (one high and one low tide per day) and semidiurnal (two high and two low tides per day) tidal components. The most prominent tidal constituents in this region are the lunar semidiurnal constituent (M2), with a period of approximately 12.42 hours, and the solar semidiurnal constituent (S2), with a period of about 12 hours.

Using the DTU global tide model, the tidal range within the project area varies from 0.1m range during the neap tidal cycle up to 0.33m during the spring tidal cycle.

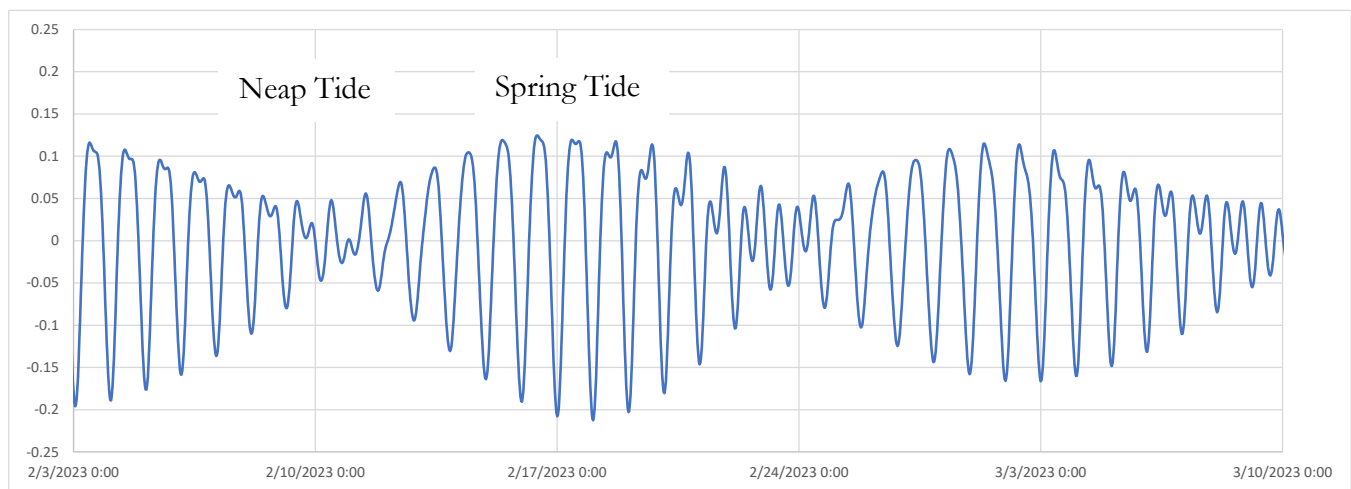


Figure 6.2 Predicted tide levels near to Long and Maiden Island February to March 2023.

Water levels from the DTU global tide model were used as inputs to force the numerical model and derive daily currents around the project area.

6.2 Nearshore Tidal Currents

Tidally-induced currents, or tidal currents, play a critical role in shaping coastal areas, as they are responsible for the redistribution of sediments along the shoreline, which helps form and maintain various coastal features such as beaches and sandbars⁶. They are also crucial for the mixing of nutrients and oxygen in coastal waters, promoting biological productivity and facilitating the transport of nutrients between coastal ecosystems, including estuaries, wetlands, and coral reefs⁷. Tidal currents can contribute to coastal erosion, particularly during storm events, and influence navigation in coastal areas, making knowledge of tidal currents essential for safe navigation and planning of maritime activities⁸. Therefore, understanding and predicting the behaviour of tidally-induced currents is vital for coastal management, conservation, and sustainable development in coastal areas.

Day-to-day or operational hydrodynamics were run over a period of 43 days to capture a spring and neap tidal cycle for both Long and Maiden Islands to determine the influence of tidally-induced currents in the nearshore area.

The hydrodynamic modelling results show similar current speeds during the neap and spring tidal cycles, which indicates that there isn't a big difference between the neap and spring tides. The higher currents occur along the eastern end of Jumby Bay and between Jumby Bay and Maiden Island where the deep shipping channel is located along with the constrained space between the two islands. Along the southern and northern coastlines of Jumby Bay the currents are very low in both spring and neap tidal cycles.

The current speeds for the tidally driven currents seem to indicate that the coastal processes will be dominated by wave-induced currents rather than tidally driven currents for both Long and Maiden Island shorelines.

A study done by Davis and Gibeaut⁹ proposed a classification system for tidal inlets (Figure 6.3) that takes into account the hydrodynamic processes that govern their formation and evolution. This classification is based on parameters such as the tidal range and wave energy, as well as the sediment supply.

The classification system includes three primary categories of tidal inlets:

1. Wave-dominated inlets: These inlets are characterized by high wave energy and low tidal range. The morphology of these inlets is primarily controlled by wave action, and they often exhibit well-developed ebb and flood tidal deltas.
2. Tide-dominated inlets: These inlets have a high tidal range and low wave energy. Tidal currents are the main controlling factor in the inlet's morphology, resulting in asymmetric, elongated shapes and the presence of extensive tidal flats.

⁶ Komar, P.D. (1998) *Beach Processes and Sedimentation*. 2nd Edition, Prentice-Hall, Englewood-Cliffs. - [References - Scientific Research Publishing \(scirp.org\)](#)

⁷ [Turbidity as a control on phytoplankton biomass and productivity in estuaries - ScienceDirect](#)

⁸ Pugh, D. (1987) *Tides, Surges and Mean Sea Level A Handbook for Engineers and Scientists*. John Wiley & Sons, Chichester, 472 p. - [References - Scientific Research Publishing \(scirp.org\)](#)

⁹ [Historical morphodynamics of inlets in Florida: models for coastal zone planning \(noaa.gov\)](#)

3. Mixed energy inlets: These inlets experience a combination of significant wave and tidal energy, leading to a complex morphological response. The inlets in this category can exhibit characteristics of both wave- and tide-dominated inlets, depending on the balance between wave energy and tidal range.

The classification system presented here is a valuable tool for understanding how hydrodynamic processes shape the morphology of tidal inlets. By providing a framework to interpret the complex interactions between waves and tides, this system can aid coastal managers and researchers in analysing and predicting the behavior of these dynamic environments.

Furthermore, this system can also be applied to the study of tidally influenced and wave influenced currents along coastal shorelines. By using the graph below, and assuming a spring tidal range of 0.4m and a mean annual wave climate range of 0.25 to 0.5m (or 25 to 50cm), it is apparent that the dominant processes shaping Long and Maiden Island are wave-dominated.

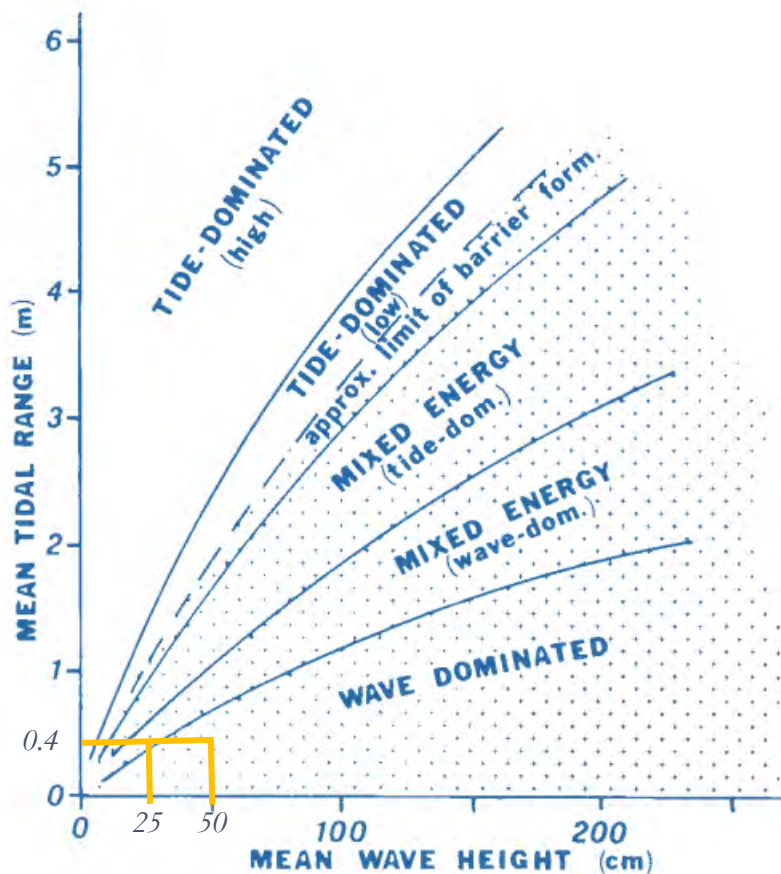


Figure 6.3 Plot of tide range versus mean annual wave height showing dominant coastal processes.

Figure 6.4 and Figure 6.5 show current speeds for neap and spring tides during both rising and falling tides.

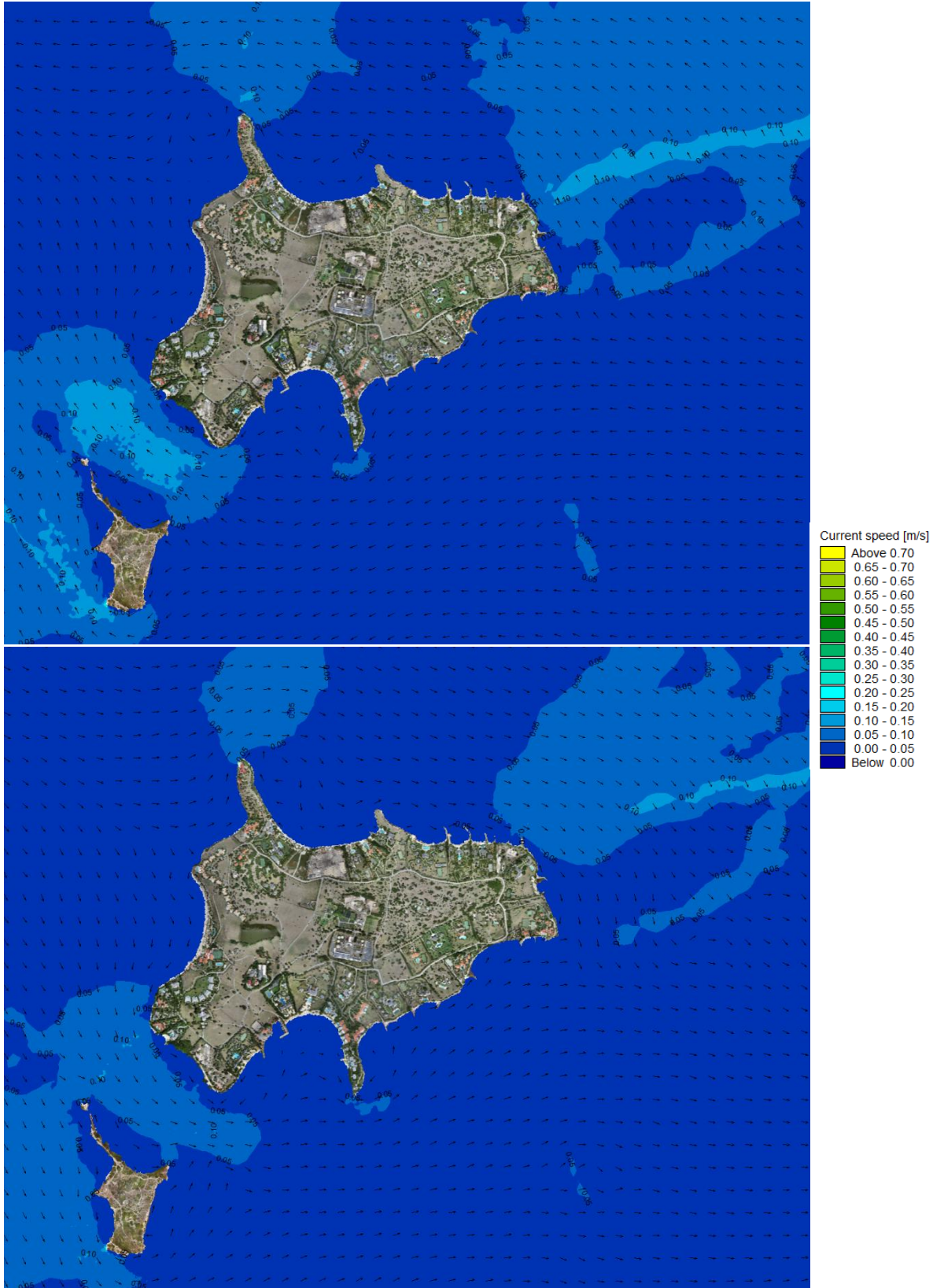


Figure 6.4 Falling (left) and rising (right) neap tidal cycle around Long and Maiden Island.

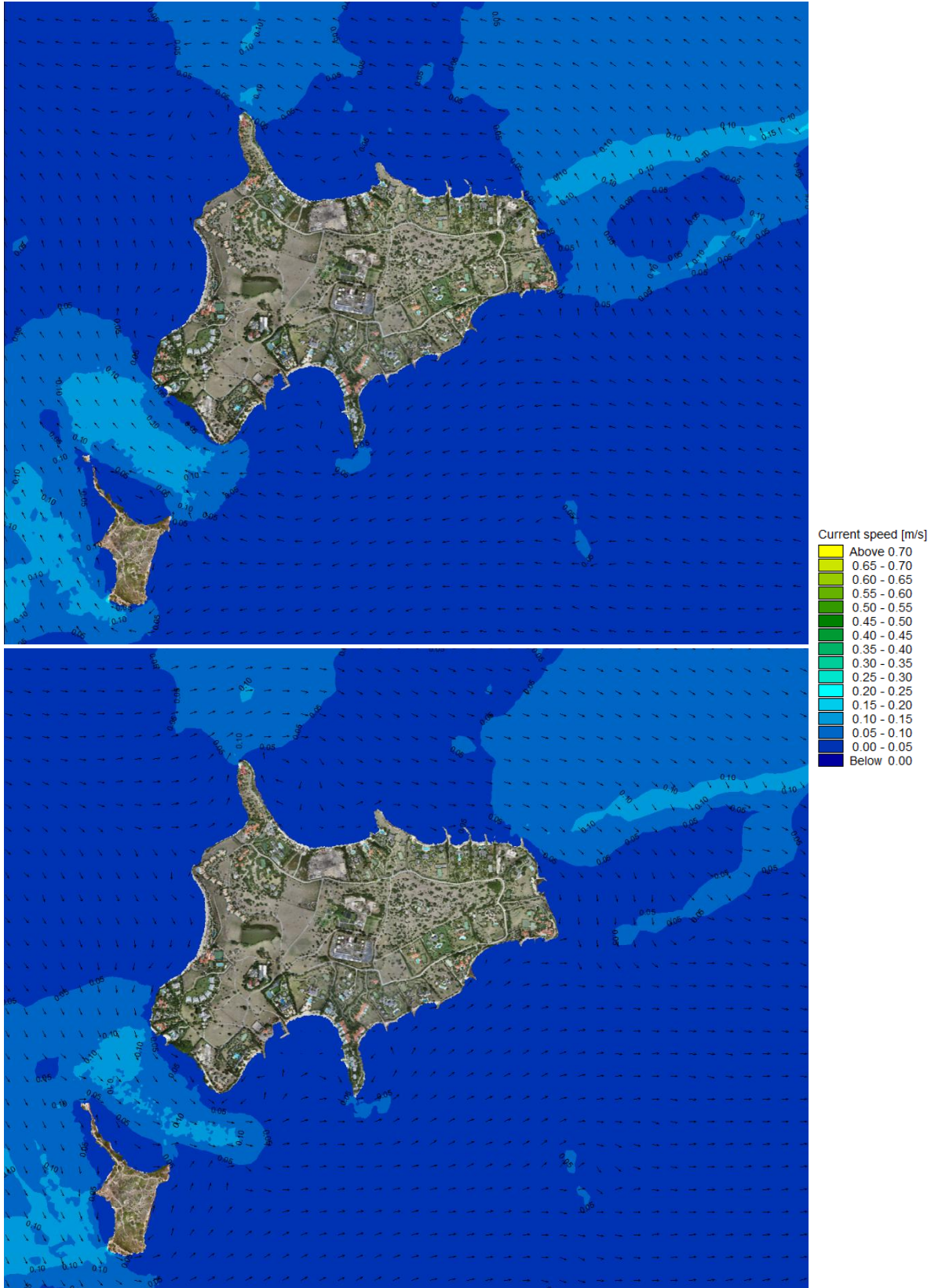


Figure 6.5 Falling (left) and rising (right) spring tidal cycle around Long and Maiden Island.

6.2.1.1 *Wave-Induced Currents*

Figure 6.6 presents rose plots of the wave-induced currents along the Jumby Bay shoreline. In the northern section of Jumby Bay, the predominant direction of wave-induced currents is towards the west, primarily due to the wave approach from the north-northeast. The eastern end of the island experiences the strongest wave-induced currents moving in a southerly direction, which is also influenced by the wave approach from the northeast and east directions. Both the northern and eastern shorelines exhibit the strongest wave-induced currents, as these areas are exposed to high-energy wave conditions.

The southern and western ends of the island, on the other hand, experience slower wave-induced currents. This can be attributed to the lower wave energy climate in these regions, which is a result of natural barriers that provide shelter from the prevailing wave directions.

The varying wave-induced currents along the island's shoreline have significant implications for sediment transport. In areas with strong wave-induced currents, such as the northern and eastern sections of the island, the sediment is more likely to be mobilized and transported in the direction of the currents. This can lead to increased erosion rates, beach migration, and changes in the shoreline configuration. Consequently, coastal management efforts in these high-energy areas may require frequent interventions, such as beach nourishment, dune restoration, or the implementation of coastal structures to mitigate the impacts of sediment transport and maintain shoreline stability.

In contrast, the slower wave-induced currents observed along the southern and western ends of the island including Maiden Island (Figure 6.7) suggest less sediment mobilization and transport, resulting in more stable beach profiles and potentially slower rates of erosion.

Figure 6.8 shows a 2D image that illustrates the spatial extents of wave-induced patterns for Jumby Bay and Maiden Island.

The model results demonstrate that the northern and eastern ends of Jumby Bay experience the strongest wave-induced currents throughout the year, which can be attributed to the prevailing wave direction, as discussed previously. Consequently, when sediment from the shoreline becomes mobilized during high-energy wave events, these wave-induced currents provide insights into the potential sediment transport pathways along the shoreline.



Figure 6.6 Rose plots showing the mean annual wave-induced currents around Jumby Bay.



Figure 6.7 Rose plots showing the mean annual wave-induced currents around Maiden Island.

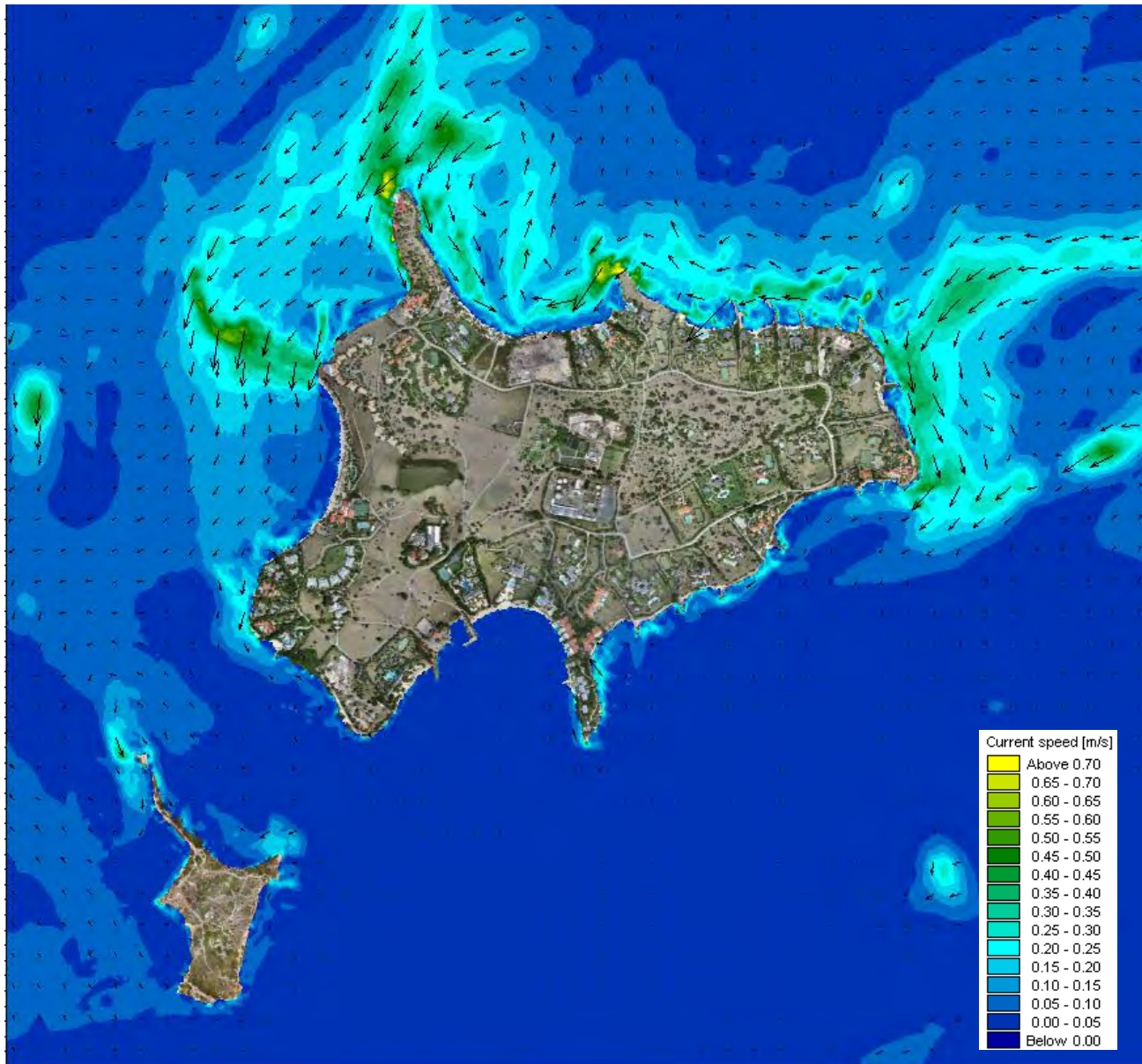


Figure 6.8 Mean annual wave-driven currents along the Maiden and Jumby Bay shoreline.

7 Floodplain Modelling

Rainfall events in Antigua typically have a short duration and low intensity. This led to peak rainfall intensities being quite low when compared to other Caribbean countries. Simulations were run to determine how the rainfall events described in Section 2.5 would flood the islands being studied.

The rainfall depths from the 50-year and 100-year rainfall events were input over the entire model domain and allowed to flow. The simulations were run with an input water level that included sea level rise and high tide. Full saturation of the ground was assumed to provide a conservative estimate of the flooding. Two key parameters of flooding depth and flow speeds were extracted from the simulation result to show flooded areas and indicate where there is the potential for beach scour.

7.1 Flooding Depth

Flooding/inundation is represented by the total water depth at the final timestep in the simulation. The results are shown in Figure 7.1 with the 50-year results on the left and 100-year results on the right. The palette shows different shades of blue to represent water depth in ponding areas. Areas without a value experienced runoff to ponding areas.

On Jumby Bay in the 50-year event multiple areas had shallow ponds up to 0.2m in depth. The existing pond areas acted as storage areas during the event and had water depths of up to 0.5m in the western pond and 0.7m in the northern pond. Some ponding was seen on the construction site; however, it is assumed that the property will be built up to provide better runoff. The maintenance offices have a berm around them which allowed for ponding to occur within the berm. This ponding had a depth of up to 0.4m. Finally, there was shallow ponding near to the service dock.

The 50-year event on Maiden Island flooded the northern spit and all the beach areas. Some ponding was also noted by the abandoned facilities close to the centre of the island. This ponding was shallow with a depth of around 0.2m. The high mound to the south of the island had runoff to low areas which aided in the ponding at its base.

In the 100-year event Jumby Bay had similar ponding locations as the 50-year with wider extents. The existing ponds which were to the north and west collected the most water. The pond to the west still had a maximum depth of 0.5m however the pond surface area increased. The western pond had a stream that connected it to the west public beach. The existing north pond increased in depth up to 1.1m and had a larger surface area which went as far as the neighbouring construction site. Small ponds were shown on most properties however the depths were shallow (about 0.1m to 0.2m). Maximum ponding depths at the maintenance offices and service dock areas were like those in the 50-year simulation.

On Maiden Island, the 100-year event created about double the flooding of the 50-year event. The northern spit was flooded with a maximum depth of 0.9m at the coastline and 0.1m at the centre of the spit. Other beach areas had a flood depth of about 1.4m at the coastline which then covered all the sandy/pebbly beach areas. Two large shallow ponds (up to 0.2m) formed in the island's interior.



Figure 7.1 Flooding (ponding) simulation results from the 50-year rainfall event (left) and from 100-year rainfall event (right).

7.2 Overland Flow Speeds

Another concern in the floodplain modelling is the current speeds that may be generated on the islands as water flows over slopes. Currents speed results are shown in Figure 7.2 for the 50-year rainfall event to the left and 100-year rainfall event to the right. Generally, the current speeds are low in ponding areas however, the locations of flow to the beach areas were higher.

In the 50-year simulation on Jumby Bay current speeds were mainly below 0.02m/s. The western beach area had two flow inlets with speeds between 0.1 and 0.12m/s. The northern existing pond connected to the sea in this simulation, however, the current speeds were quite low which may be related to this connection to the sea being wider than on the west beach. Some ponds on the land had currents speeds up to 0.3m/s, these locations would be near to the inlets for the ponds. On Maiden Island, all current speeds were below 0.02m/s with no strong inlets to the sea.

In the 100-year simulation on Jumby Bay currents were still mainly below 0.02m/s. However, the current speeds at the beach inlets increased. On the western beach, the stormwater flowed from the western pond and connected with the sea. The current speed increased to 0.2m/s along the stream and 0.3m/s at the beach. At the northern pond, the current speeds were about 0.1m/s. As before, most current speeds on Maiden Island were below 0.02m/s in the 100-year rainfall simulation.

Floodplain modelling results show that the islands have adequate grading to prevent significant ponding in heavy rainfall events. The existing ponds provided storage in both simulations; however, the 100-year event showed the ponds overflowing. The flow speeds on the public beaches may be of concern as they could scour away beach sand.



Figure 7.2 Current speed simulation results from the 50-year rainfall event (left) and from 100-year rainfall event (right).

8 Shoreline Stability and Sediment Transport Potential

Beaches serve as the first line of defence against coastal hazards such as storm surges, tsunamis, and erosion. They also provide valuable ecosystem services, recreational opportunities, and economic benefits to local communities. Hence, maintaining the stability of a beach is of paramount importance.

During operational wave conditions, which are the day-to-day wave and tide conditions, a stable beach helps dissipate wave energy, reducing the risk of coastal erosion and flooding. This is achieved through the natural processes of sediment transport and deposition, which help maintain the shape and size of the beach. A stable beach also provides habitat for various species, supports the coastal food chain, and contributes to the aesthetic value of the coastline.

During annual extreme wave conditions, such as those caused by storms, hurricanes, or other intense weather events, a stable beach is even more crucial. In such conditions, the beach's ability to absorb and dissipate wave energy can help prevent or mitigate potentially catastrophic impacts on coastal infrastructure, natural habitats, and human lives. Moreover, a stable beach can recover more quickly from the effects of extreme events, ensuring the continued provision of its benefits to the coastal zone.

8.1 Sediment Transport Potential Zones

Another analysis carried out on both islands is the use of the Hallermeier equation¹⁰. The Hallermeier equation is a tool used in coastal engineering to help us understand how sand and other sediments move along the shore due to the action of waves and currents. It considers variables like wave height and direction, water depth, and the characteristics of the sediment itself.

Houston¹¹ simplified the equation by using a particular type of wave spectrum and a modified distribution of significant wave height over time. This allowed him to express the equation in terms of mean annual significant wave height.

$$h_{in} = 8.9\bar{H}_s$$

Where \bar{H}_s is the mean annual significant wave height.

The Hallermeier equation was used to calculate the inactive (clear) and active (yellow) sediment transport zones for Long and Maiden Islands based on mean annual wave conditions. As shown in Figure 8.1, the north offshore area of Jumby Bay is an active zone of sediment transport up to a depth of 8m, indicating high wave energy in this region as previously noted. In contrast, the southern section of the island exhibits a less active sediment transport zone that extends only to a depth of 4m, suggesting a relatively calm environment. Notably, the dredged channels exhibit no sediment transport potential and can thus serve as sediment sinks if any sediment falls into them. Overall, there is a potential for active sediment zones around both islands based on mean annual wave conditions, with the lowest potential occurring in the southwest of Jumby Bay where wave energy is lowest.

¹⁰ [Closure depth - Coastal Wiki](#)

¹¹ Houston, J. R. 1995. Beach-fill volume required to produce specified dry beach width. Coastal Engineering Technical Note 11-32, U.S. Army Engineer Waterways Experiment Station, Vicksburg, MS.

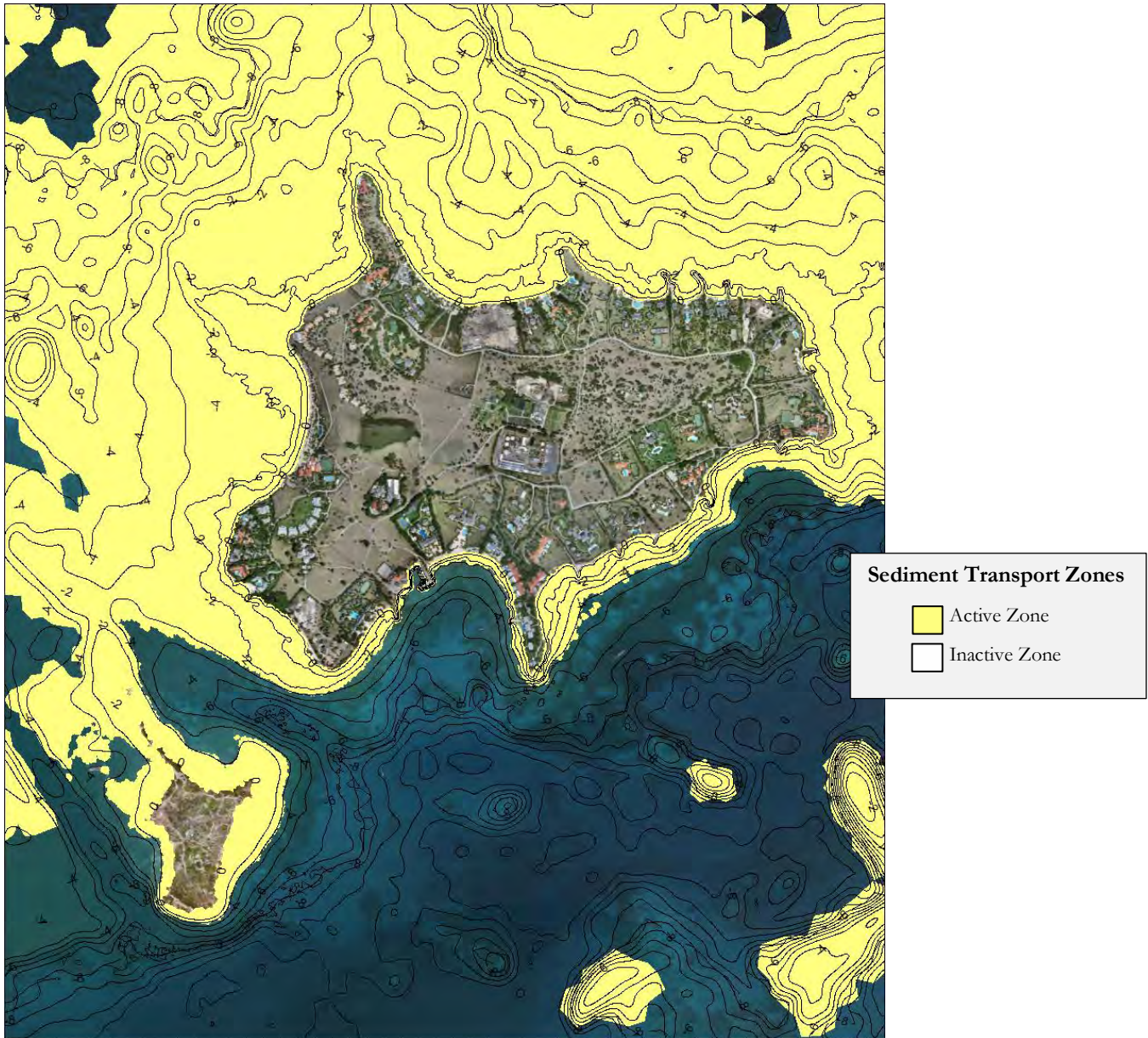


Figure 8.1 Sediment transport zones under the mean annual wave climate.



8.2 Shoreline Retreat

Bruun Rule is a model that relates shoreline retreat on a sandy beach to an increase in local sea level, which estimates the response of the shoreline profile to sea-level rise based on a concave-upward beach profile. Bruun (1962) proposed that under rising sea levels a beach’s equilibrium profile, i.e., its average form, would be maintained while rising with sea level. It can be used to correlate sea-level rise with eroding beaches and estimate the surface of land loss due to erosion.

The active slope of sand transport is required for the model, which starts from the depth of closure to the shoreline and can be estimated using data on the movement of sediment offshore or the effect of waves on sand movement. Figure 8.2 shows calculations of representative shoreline retreat for nine sub-zones on the islands. The retreat would be seen along sandy beach areas within the sub-zone. Calculations were done for three time horizons (20, 50, and 100 years) under two climate change scenarios (SSP2 - 4.5 and SSP5 - 8.5).

Unfortunately, the Bruun Rule has limitations, especially in complex systems such as Jumby Bay and Maiden Island. Some of these limitations are noted in the assumptions inherent in its formulation, such as straight and parallel nearshore bottom contours, consistency in a sandy erodible beach throughout, no longshore transport, no cliff or hardened shoreline. As such, the erosion profiles, which were applied only to beach areas as much as possible, should be considered with caution.

The three horizons were calculated to provide the reader with a more comprehensive view of how the areas could retreat in 20, 50 and 100 years. However, the 50-year time horizon was used for the calculation of storm surges and waves. It is typically used to provide designs that balance future risk with current costs. Also, the SSP5 – 8.5 projection was used when incorporating climate change in the modelling works done. This projection assumes that the world will continue the emission trends of the past decades. The results for the 50-year time horizon for SSP5 – 8.5 are tabulated below.

Table 8-1 Highlighted shoreline retreat results of the SSP5-8.5 scenario in 50 years for the nine zones across the islands.

| Shoreline Zone | Shoreline Retreat under the SSP5 – 8.5 scenario in 50 years |
|----------------|---|
| Zone 1 | -29 |
| Zone 2 | -32 |
| Zone 3 | -19 |
| Zone 4 | -13 |
| Zone 5 | -3.3 |
| Zone 6 | -2.7 |
| Zone 7 | -7.4 |
| Zone 8 | -7.2 |
| Zone 9 | -5.7 |

The highlighted results correspond to the fourth bar in the bar charts shown in Figure 8.2.

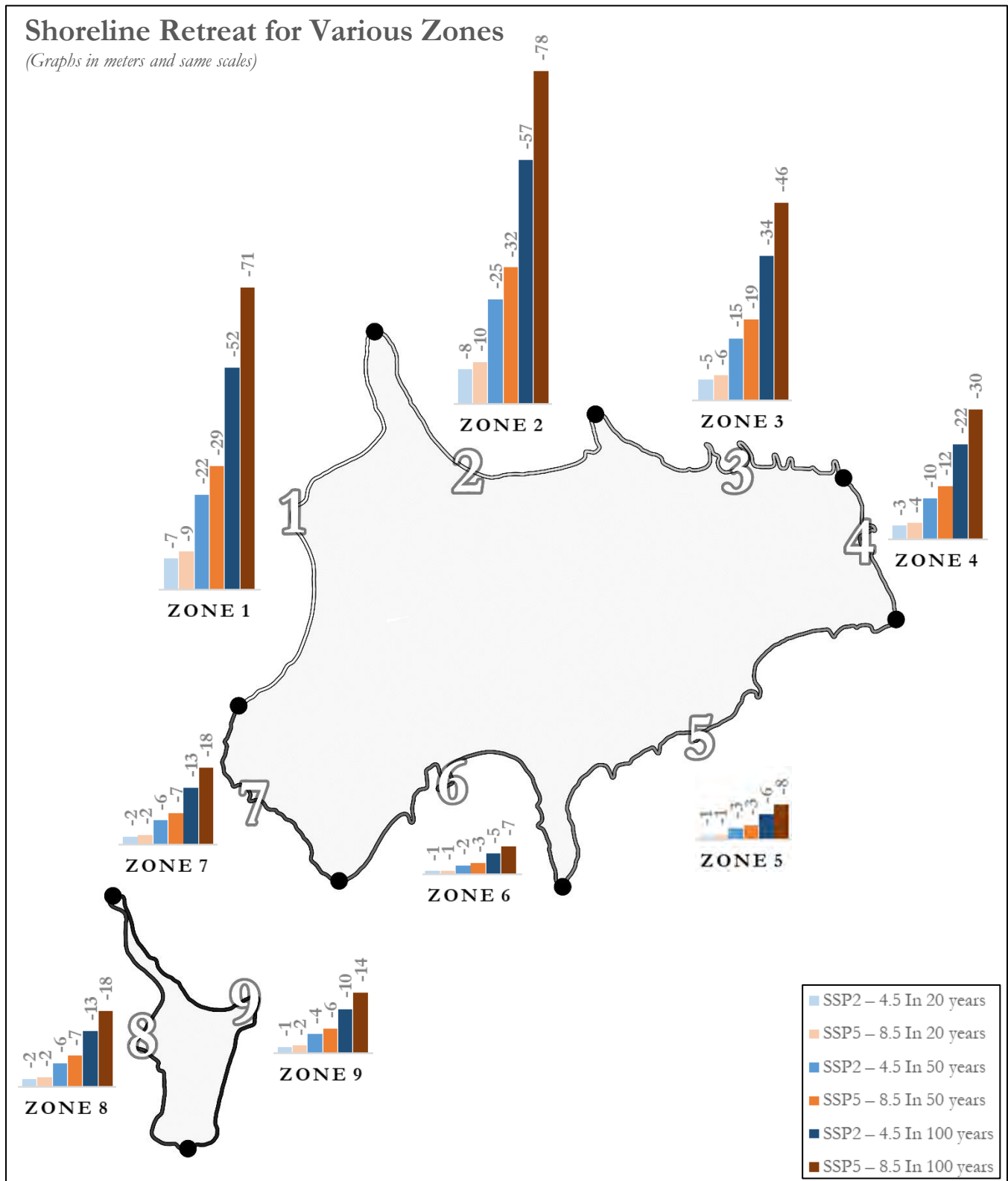


Figure 8.2 Shoreline retreat comparison between Bruun Rule estimates for various zones on both islands.

Shoreline retreat describes the future changes in the waterline position around the islands. Another consideration is how active the coastal zones are at present. The following section will detail the current wave climate around the islands and if sand will tend to erode or accrete within an average year.

The stability of the beach sediment is a separate consideration for the beach cells and may seem counterintuitive to shoreline retreat. The main difference is that while shoreline retreat speaks to erosion of the waterline in the future, sediment stability speaks to whether the current wave climate will erode beach sand or not.

8.3 Sediment Stability Zones

Coastal engineers use the Ahrens formula to estimate sediment stability in various situations, such as beach nourishment projects, the design of breakwaters, or the assessment of coastal erosion and sedimentation patterns.

The Ahrens beach stability formula is a valuable tool for coastal engineers and scientists to assess the stability of a beach. Developed by J. Ahrens in 1981, the formula takes into account various factors that influence beach stability, including the beach slope, sediment size, and wave climate. The formula is as follows:

$$U_t = [(\rho_s - \rho_w) - 1] \cdot \frac{(g D^3)}{(18 \mu)}$$

Where U_t is the threshold flow velocity, ρ_s and ρ_w are particle and water densities, g is the acceleration due to gravity, D is the particle diameter, and μ is the water viscosity.

Smith Warner International conducted a comprehensive sediment sampling campaign around Jumby Bay and Maiden Island focusing on the variations in sediment size and their relationship with the local wave energy. The samples were subsequently sent to a laboratory for dry sieve analysis to ascertain the average sediment size.

On Jumby Bay, the sediment sizes along the northern section of the island varied from 0.33 to 0.75mm, while on the southern end, the sediment sizes ranged from 0.24 to 0.35mm. One of the observations in the sediment sampling is that there were no samples taken along the eastern section, as this section of the island was mainly platform, which is a hard seafloor surface. It is important to note that most of the beaches are artificially nourished with sand, which means the sand is not native to the area. Nonetheless, the data reveals a trend in which the northern shoreline, characterized by higher wave energy, exhibits larger sediment sizes compared to the southern shoreline where the sediments are, on average, smaller. To evaluate the beach stability across Jumby Bay and Maiden Island (Figure 2.9), the Ahren's formula was used to determine what the recommended sediment size would be within each zone (East, North, West, South and Maiden Island). This data is presented the following Sections 8.3.1 to 8.3.5.

Jumby Bay was broken up into zones based on the extreme annual wave conditions that occur on average within each zone. The zones were the (i) eastern, (ii) northern, (iii) western and (iv) southern. Maiden Island was then looked at as a whole, given the limited number of beaches on that island.

8.3.1 Eastern Zone

In Figure 8.3 below which illustrates wave conditions, a distinct pattern emerges that highlights the eastern shoreline's exposure to a high-energy wave environment, especially during peak tourist seasons. Our comprehensive analysis reveals that under typical circumstances, wave heights along the 1m contour line vary between 0.55 and 0.65m, rendering the area unsuitable for recreational swimming activities.

During extreme annual wave events, such as the swell season, wave heights along the eastern shoreline can escalate to as much as 0.75m. Based on these findings, confirmed by field observations, it becomes clear that the implementation of beach nourishment in this section of the island necessitates the installation of meticulously designed coastal protection structures. These structures will serve the dual purpose of retaining nourished sediment and ensuring a safe swimming area for beachgoers.

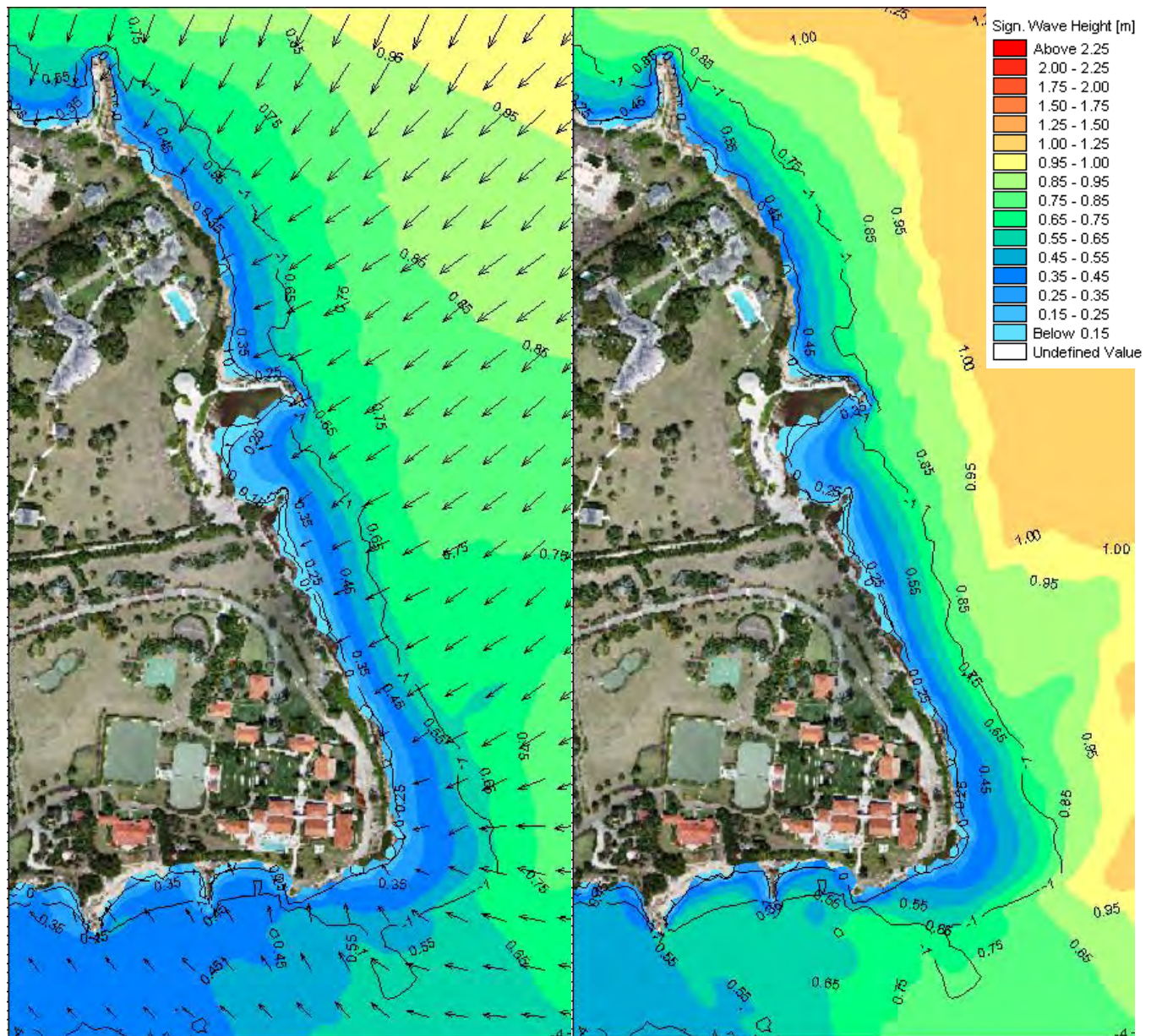


Figure 8.3 Mean (left) and extreme (right) annual wave climate along the eastern end of Jumby Bay.



8.3.2 Northern Zone

The northern section of Jumby Bay is similarly characterized by a high wave energy environment, as substantiated by our model results. Average mean wave heights fluctuate between 0.55 and 0.65m, while extreme annual wave events can yield wave heights reaching 0.75m. These wave conditions bear a striking resemblance to those observed along the eastern shoreline.

Field observations along the northern shoreline reveal that coastal protection structures have been constructed to establish sheltered areas, with the aim of maintaining stable beaches on several properties within this zone. Our model indicates that high-energy waves continue to approach the shoreline in this area. Employing the Ahren's beach stability formula, the recommended sediment size for this shoreline, in the absence of substantial coastal protection, would be 0.5mm. This relatively large sediment grain size may pose challenges in terms of sourcing.

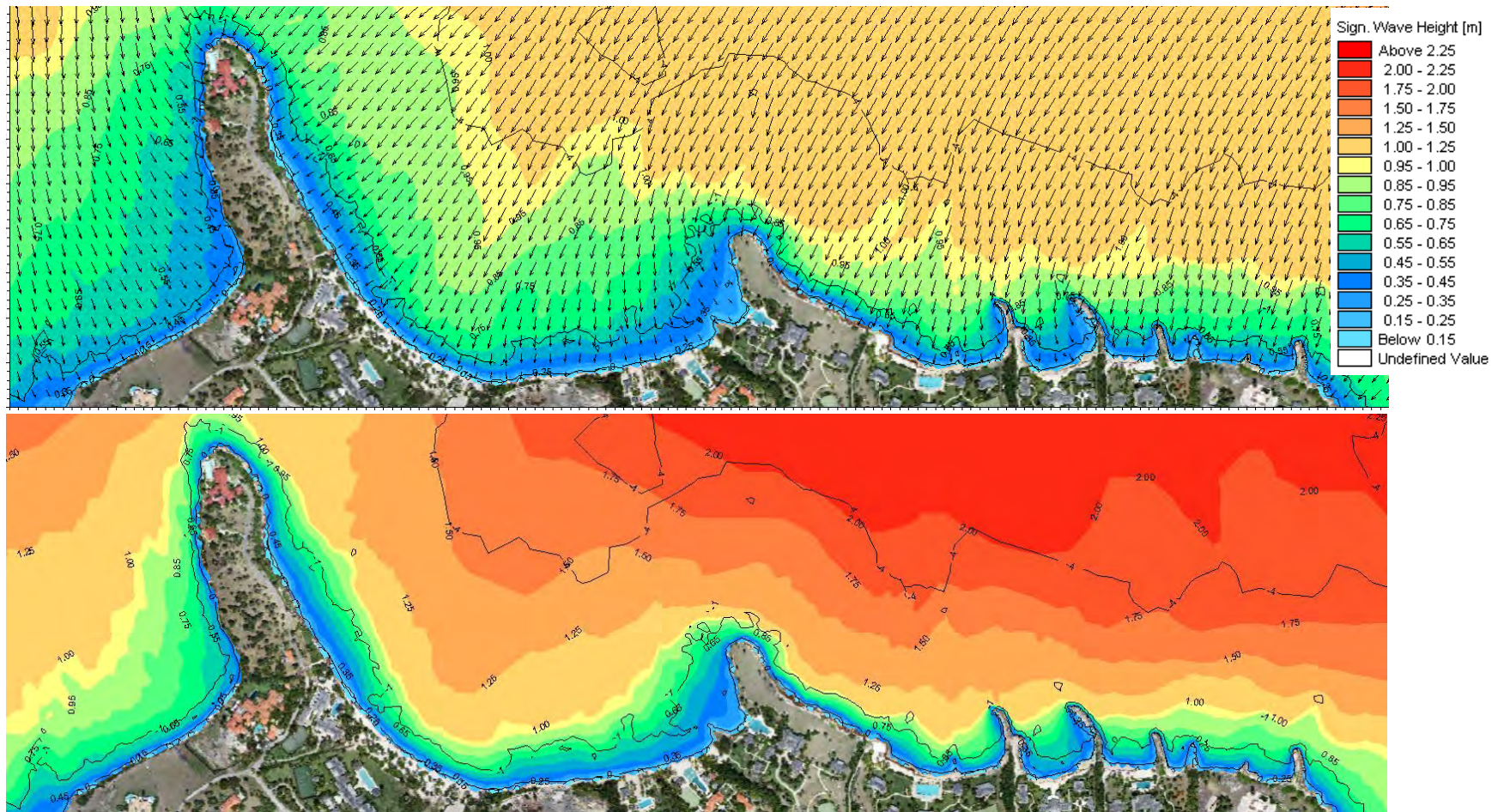


Figure 8.4 Mean (top) and extreme (bottom) annual wave climate along the northern end of Jumby Bay.

8.3.3 Western Zone

Figure 8.5 illustrates the mean annual wave climate and the extreme annual wave climate for the western end of the island, revealing wave heights ranging from 0.35 to 0.55m along the western shoreline. This wave climate is comparatively lower than that of the eastern and northern sections of the shoreline due to the sheltering effect provided by the reef at the northern end of Jumby Bay. Consequently, the lower wave energy environment along this shoreline can accommodate a broader range of sediment sizes, including smaller diameters.

Smith Warner International has previously made a recommended sediment size that would be stable along this section of the island; this recommended sediment size of 0.45mm would not need coastal structure interventions.

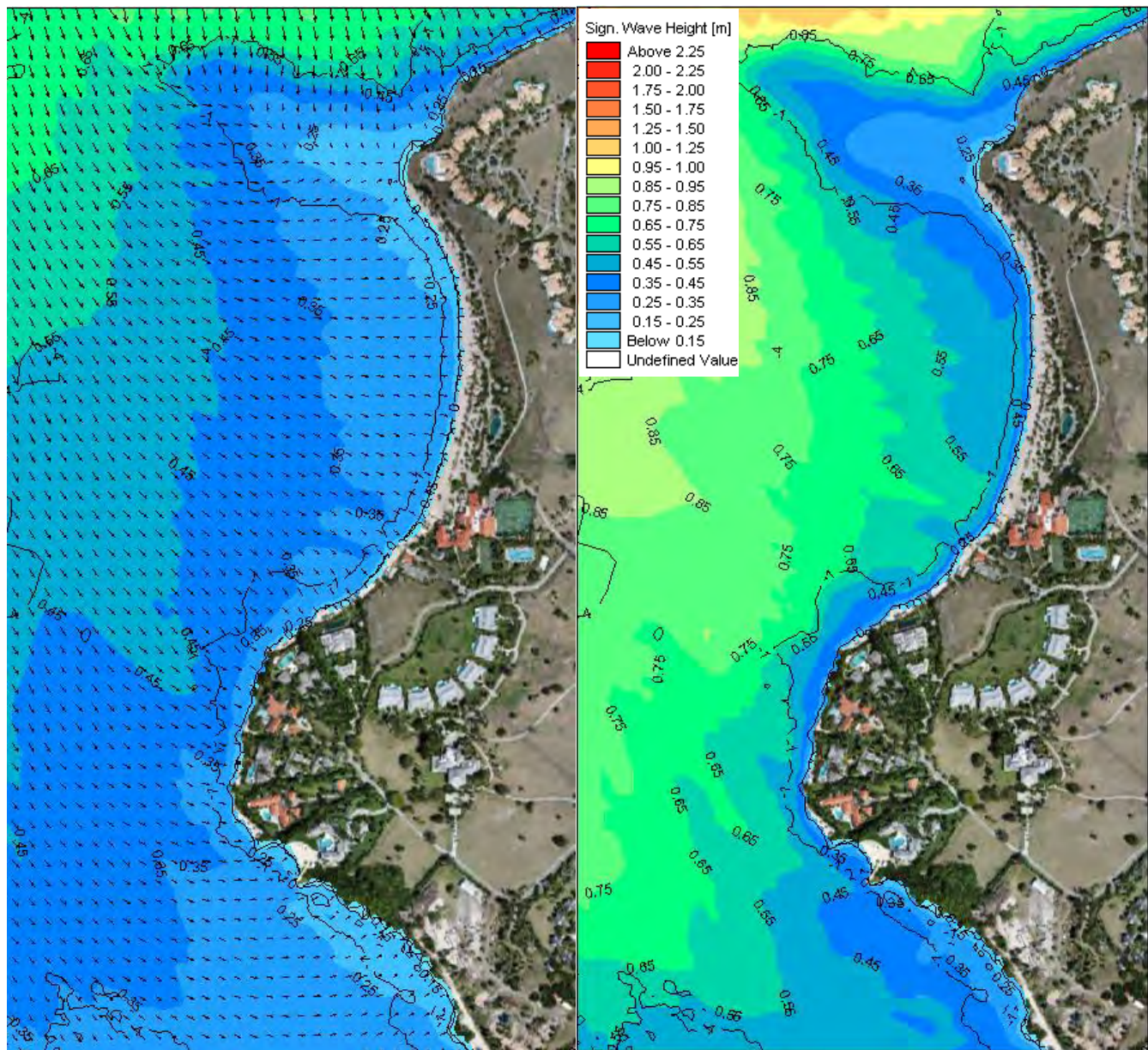


Figure 8.5 Mean (left) and extreme (right) annual wave climate along the western end of Jumby Bay.



8.3.4 Southern Zone

The southern zone is the most sheltered area on the island, as it is protected from the high wave energy associated with northerly swells (Figure 8.6). Wave heights along the southern coastline range from 0.15m at the southwestern end of the island to 0.55m at the south-eastern section. In the south-eastern section of Jumby Bay, the Ahren's beach stability formula suggests a minimum sediment size of 0.4mm for optimal stability. In contrast, the southwestern section experiences calm conditions throughout the year, allowing sediment sizes as small as 0.30mm to remain stable along this stretch.

Nonetheless, it is crucial to continuously monitor the shoreline and adapt management strategies as necessary to ensure the long-term stability and ecological health of these coastal areas.

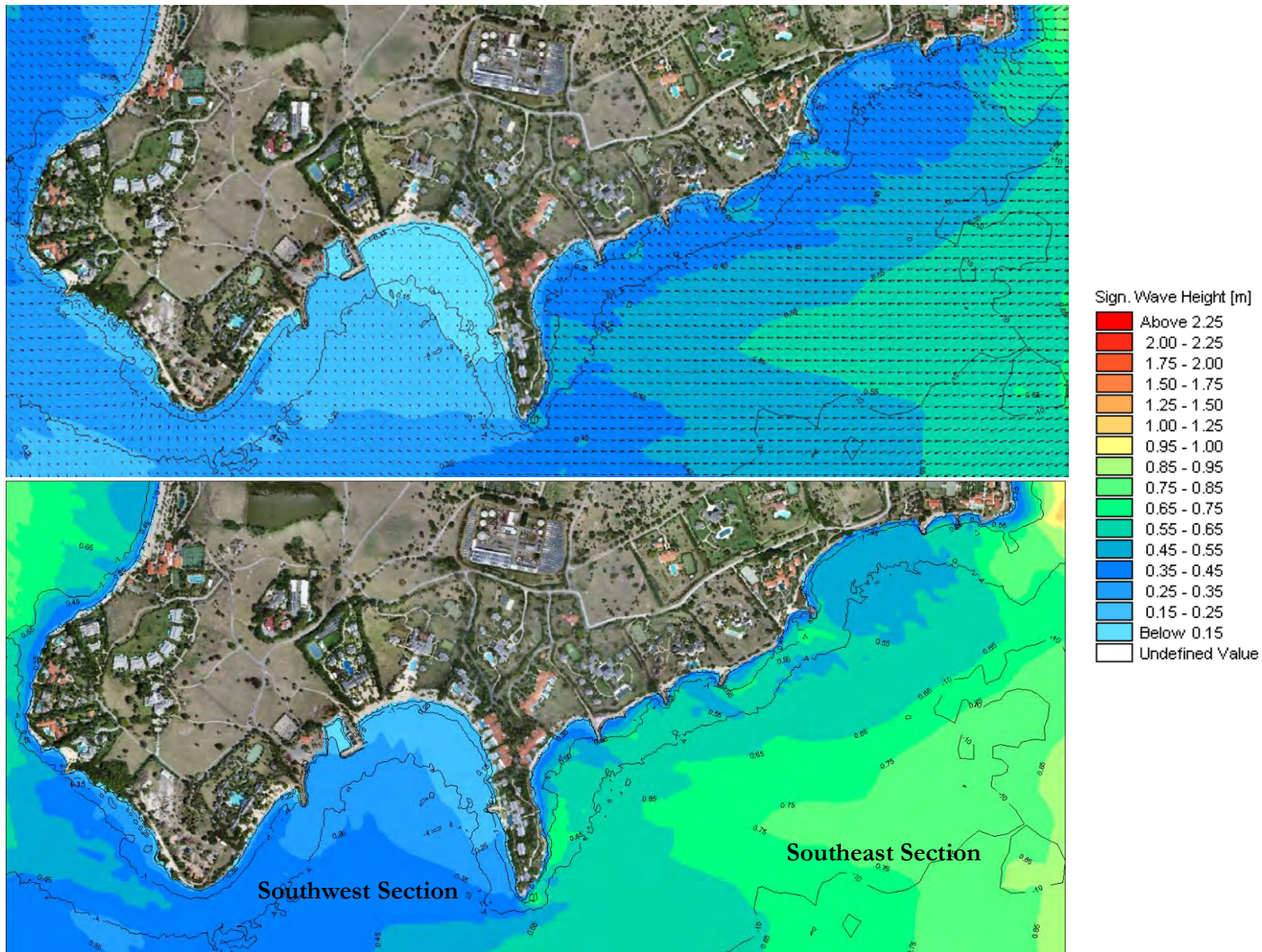


Figure 8.6 Mean (top) and extreme (bottom) annual wave climate along the southern end of Jumby Bay.



8.3.5 Maiden Island

Maiden Island, benefiting from the sheltering effects of Jumby Bay, exhibits the lowest wave energy among all the zones, with annual mean wave heights ranging from 0.25m to 0.45m during the extreme annual conditions of the swell season. Given the consistently low wave energy environment throughout the year, the Ahren's beach stability formula results, and the sediment size (0.42mm) on the main beach on Maiden Island, it appears this beach would likely maintain stability on a yearly basis. Consequently, no coastal modifications would be necessary to ensure the long-term stability of the beach.

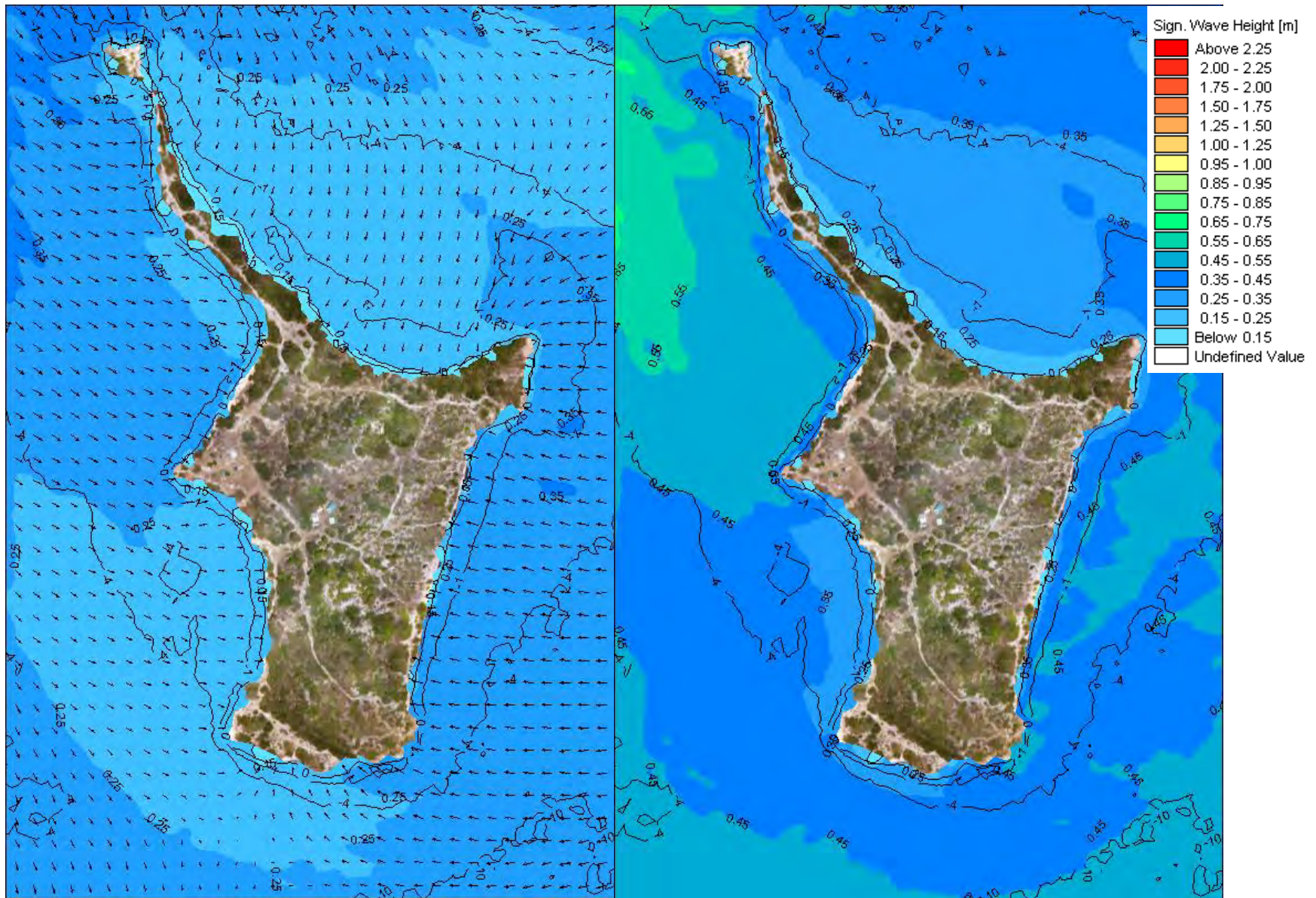


Figure 8.7 Mean (left) and extreme (right) annual wave climate for Maiden Island.

9 Key Results Summary and Recommendations

9.1 Summary of Bathymetric Changes

Satellite-derived bathymetry (SDB) data was analysed to determine bathymetric changes between 2003 and 2022. A two-dimensional difference plot illustrated depth variations over the period, revealing changes within a range of $\pm 4\text{m}$. The latest period (between 2017 and 2022) had shallower waters in the northern area of the study zone, with an average decrease in water depth of about 0.75m. In contrast, the eastern and south-eastern offshore regions experienced an increase in water depth up to 1.5m. Nearshore areas also showed deeper waters in 2022 compared to 2017, but with a smaller magnitude of approximately 0.75m. This comprehensive analysis offers crucial insights into the evolving coastal environment and informs coastal management, infrastructure planning, and ecological conservation efforts.

9.2 Summary of Seafloor Classification Changes

Six years of seafloor classification (SFC) data was evaluated to study benthic resource distribution trends between 2003 and 2022. The analysis showed that coral habitats remained relatively stable, while seagrass cover increased significantly, nearly doubling during the period. The sediment-dominated seafloor decreased substantially, as seagrass cover expanded, positively impacting the coastal ecosystem's health. Notably, a large sargassum bloom in 2015 coincided with a tipping point for seagrass growth, warranting further investigation into potential influencing factors. The dynamic nature of coastal environments emphasizes the importance of ongoing monitoring and assessment for sustainable coastal management strategies and ecosystem preservation.

9.3 Summary of Operational Wave Conditions

The operational wave climate at the project site on Jumby Bay and Maiden Island reveals distinct wave patterns and intensities, which can be primarily divided into two components: day-to-day calm conditions and seasonal winter swells from December to May. While winter swells are infrequent, they have a more significant impact on the shoreline due to their higher energy. The ERA5 dataset was used to analyse the deep-water operational wave climate, and MIKE 21 SW was used to develop the nearshore wave climate.

Jumby Bay's northern and eastern sections face higher wave energy and wave-induced currents, primarily due to their exposure to open ocean swells and dominant wave directions. Consequently, these areas are more susceptible to erosion and may require frequent coastal management interventions, such as beach nourishment, dune restoration, or structural protection measures. In contrast, Jumby Bay's southern and western sections, as well as Maiden Island, experience lower wave energy and wave-induced currents. This is attributed to the natural barriers that provide shelter from prevailing wave directions, resulting in more stable beach profiles, slower erosion rates, and less sediment mobilization and transport.

To properly manage these coastal zones, it is essential to implement targeted strategies based on the wave conditions and potential impacts on each shoreline section. For high-energy areas, frequent interventions like beach nourishment, dune restoration, or coastal structures can help mitigate sediment transport and maintain shoreline stability. In contrast, lower-energy areas require fewer intensive efforts, focusing on maintaining

existing barriers and monitoring erosion rates. This information is crucial for effective coastal engineering design and management strategies to preserve and enhance the islands' coastal environments.

9.3.1 Recommendations for the Eastern section of Jumby Bay

Given the wave conditions and shoreline orientation, the recommendations for this area would be a combination of coastal protection measures to facilitate beach nourishment and create a safe swimming environment along the coastline. Possible coastal solutions are as follows:

1. Offshore breakwaters: Construct offshore breakwaters parallel to the shoreline to dissipate wave energy before it reaches the shore. These structures can reduce wave heights in their lee and create calmer water zones, promoting sediment deposition and providing a safer swimming environment.
2. Groynes: Install a series of groynes along the coastline to interrupt the southerly movement of the wave-induced currents and trap sediment. This can help maintain the beach width and provide a more stable beach for swimming. *It is crucial to carefully design the groyne layout and spacing to avoid unintended impacts, such as downdrift erosion.*
3. Beach nourishment: Replenish the beach with compatible sediment to maintain a wide and gently sloping profile, which can enhance the beach's resilience to erosion and provide a larger recreational area for swimming. Regular monitoring and maintenance may be required to ensure the beach remains stable.

By implementing a combination of these coastal measures, it will be possible to promote beach accretion, provide a safe swimming environment, and protect the shoreline from erosion. It is essential to consider the specific conditions of the coastline and engage in thorough planning and design processes to optimize the effectiveness of these measures.

9.3.2 Recommendations for the Northern section of Jumby Bay

Considering the potential challenges associated with sourcing the recommended 0.5mm sediment size, an alternative approach may involve the implementation of coastal structures designed to mitigate wave energy as waves approach the shoreline. By employing these strategies, the need for larger sediment grains can be reduced, and more readily available materials may suffice for beach nourishment.

Given that this shoreline is oriented east to west and waves approach from the north to northeast, the subsequent wave-induced current predominantly moves in a westerly direction. To address these specific conditions, several coastal solutions can be considered:

1. Submerged breakwaters: These offshore structures can be constructed to dissipate incoming wave energy and reduce wave heights along the shoreline. By attenuating wave energy, they help create a more favorable environment for beach nourishment.
2. Groynes: By building groynes perpendicular to the shoreline, the westward movement of sediment can be intercepted, aiding in the retention of nourish sediment and slowing down the erosion process.
3. Artificial reefs: Constructing artificial reefs can serve as an effective means to dissipate wave energy and encourage sediment deposition, while simultaneously providing ecological benefits, such as enhanced marine habitats.

By adopting one or more of these coastal solutions, the wave energy along the northern shoreline of Jumby Bay can be reduced, rendering the area more conducive to beach nourishment, and promoting long-term stability.

9.3.3 Recommendations for the South-eastern section of Jumby Bay

Considering the wave-induced currents affecting the south-eastern portion of the island, which flow from east to west, implementing groynes perpendicular to the shoreline can effectively mitigate east-to-west sediment transport by capturing sand on their updrift side. *Careful design and strategic placement of groynes are essential to minimize any negative consequences for adjacent coastal areas.*

9.4 Summary of Hurricane Conditions

The Caribbean region, particularly Antigua and Barbuda, is highly vulnerable to tropical storms and hurricanes, with annual occurrences from June to November. Coastal protection structures must be designed to withstand extreme storm events, taking factors such as armour stone size and wave forces into account. NOAA's National Hurricane Centre (NHC) database provides valuable data on tropical cyclones for understanding their impact on the region. The study area has experienced a total of 183 tropical storms and hurricanes since 1850, with tropical storms being the most common and strong hurricanes (Category 3 or higher) occurring fairly frequently.

Hurricane simulations were conducted using historical data and parametric models to calculate deep water wave conditions, while MIKE21 was used for nearshore wave transformation. Climate change concerns were addressed by assuming the worst-case scenario (SSP5-8.5) for sea level rise calculations. The results indicated that the northern and eastern sections of Jumby Bay and Maiden Island are more prone to wave impacts and storm surge inundation, with the potential for significant damage to infrastructure and communities.

Mitigation measures such as resilient building design and properly designed coastal structures can help reduce the risks associated with hurricanes and tropical storms in the area.

9.5 Summary of Currents and Tides

The North Equatorial Current (NEC) is the primary ocean current affecting Antigua and Barbuda. It splits into the Antilles Current and the Caribbean Current, with the former directly influencing Antigua and Barbuda by impacting ocean circulation, water temperature, marine ecosystems, and local weather patterns. The Caribbean Current, on the other hand, affects the region's overall ocean circulation and weather patterns.

Daily currents around the project area were derived using water levels from the DTU model. Nearshore tidal currents significantly shape coastal areas by redistributing sediments and facilitating nutrient transport. Hydrodynamic modelling results reveal weak current speeds during both neap and spring tidal cycles, indicating that wave-induced currents are more dominant than tidally driven currents along the shorelines of Long and Maiden Island.

A classification system for tidal inlets, proposed by Davis and Gibeaut, is based on tidal range, wave energy, and sediment supply. Long and Maiden Islands are classified as wave-dominated, given a spring tidal range of 0.4m and a mean annual wave climate range of 0.25 to 0.5m.

Wave-induced currents along Jumby Bay's shoreline have substantial implications for sediment transport. In areas with high wave-induced currents, sediment is more likely to be mobilized and transported in the direction of the currents. This leads to increased erosion rates, beach migration, and changes in shoreline configuration. In contrast, the lower wave-induced currents observed along the southern and western ends of the island suggest less sediment mobilization and transport, resulting in more stable beach profiles and potentially slower rates of erosion. Model results demonstrate that the highest wave-induced currents are experienced at the northern and eastern ends of Jumby Bay throughout the year.

9.6 Summary of Beach Stability

Historical shorelines at an irregular frequency were assessed to determine whether there were trends of erosion or accretion on the islands. The presence of multiple structures and nourishment activities highlighted the need for a profile-by-profile analysis to determine localised trends. Thirty-three profiles were analysed on Jumby Bay; twelve areas were considered as accreting, thirteen eroding and the remainder stable. On Maiden Island, the western side was found to be accreting while the eastern side was eroding.

Shoreline retreat was assessed for three design horizons under two different climate change scenarios. The results show that the western and northern sections of Jumby Bay are most at risk for shoreline retreat resulting from sea level rise. The average retreat value in 100 years for Jumby Bay was 27m and for Maiden Island was 12m.

Jumby Bay was divided into four zones based on the extreme annual wave conditions: eastern, northern, western, and southern. Maiden Island is analysed separately due to its limited beaches. The eastern and northern zones experience high wave energy environments, with average wave heights of 0.55 to 0.65m and up to 0.75m during extreme annual events. Coastal protection structures and beach nourishment are recommended to ensure shoreline stability and safe swimming areas.

The western and southern zones have lower wave energy due to natural sheltering effects. The western zone can accommodate a broader range of sediment sizes, including smaller diameters, with a recommended sediment size of 0.45mm. The southern zone experiences calm conditions, allowing sediment sizes as small as 0.30mm to remain stable in the southwestern section, while a minimum sediment size of 0.4mm is recommended for the south-eastern section.

Maiden Island exhibits the lowest wave energy, with annual mean wave heights ranging from 0.25 to 0.45m. Given the consistently low wave energy environment and the main beach's sediment size (0.42mm), the beach is expected to maintain stability without the need for coastal modifications.

The Hallermeier equation was used to calculate the inactive and active sediment transport zones for Jumby Bay and Maiden Islands based on mean annual wave conditions. The north offshore area of Jumby Bay is an active zone of sediment transport up to 950m from the shoreline (8m water depth contour), while the southern section exhibits a less active zone. The dredged channels exhibit no sediment transport potential and can serve as sediment sinks if any sediment falls into them. Overall, there is a potential for active sediment zones around both islands based on mean annual wave conditions.

Appendix A – Numerical Modelling

A.1 MIKE 21 Description and Additional Data

Coastal processes along the Jumby Bay and Maiden Island coastline were investigated using a combination of hydrodynamic and spectral wave modules integrated within the MIKE 21 software. Developed by the Danish Hydraulic Institute, MIKE 21 is a sophisticated engineering software package designed for simulating tides, waves, sediment transport, and ecological processes in various water bodies, including rivers, lakes, estuaries, bays, coastal regions, and seas.

The MIKE 21 model employs several modules to simulate hydrodynamic variations in surface elevation and currents (HD) as well as spectral waves (SW). By coupling these modules, the mutual interaction between waves and currents is accurately represented, with results from one module iteratively exchanged with the other to enhance the efficiency and precision of the simulations.

The Spectral Wave (SW) module calculates wave conditions throughout the model domain, while the Hydrodynamic (HD) module computes water levels, current velocities, and directions. The HD module is integrated with the SW module to account for wave-induced currents. Furthermore, water levels and currents that impact waves are reciprocally incorporated into the SW module, refining the accuracy of the simulated wave conditions.

This comprehensive approach to modeling coastal processes offers a more precise representation of the complex interactions between hydrodynamics and spectral waves, ultimately leading to better-informed decision-making for coastal management and engineering projects.

Flexible Mesh Development

The fundamental foundation of the model lies in the development of a computational mesh, which allows for the determination of spatial variations at each simulation time step. MIKE 21 utilizes a flexible mesh, composed of linear triangular elements that depict the seabed and land elevations (bathymetry and topography of the region). The adaptable element mesh is particularly advantageous for modeling extensive and intricate areas that simultaneously demand a detailed resolution of specific features or zones.

As previously mentioned, all pertinent bathymetric and topographic data for the area were consolidated and implemented as input to the model to establish land and seabed elevations. Within the model, interpolation techniques are employed to bridge data gaps and generate a smooth surface. This information was then incorporated into the MIKE Zero mesh generator, which crafted the flexible mesh to represent the existing conditions, as illustrated in Figure A.0 1.

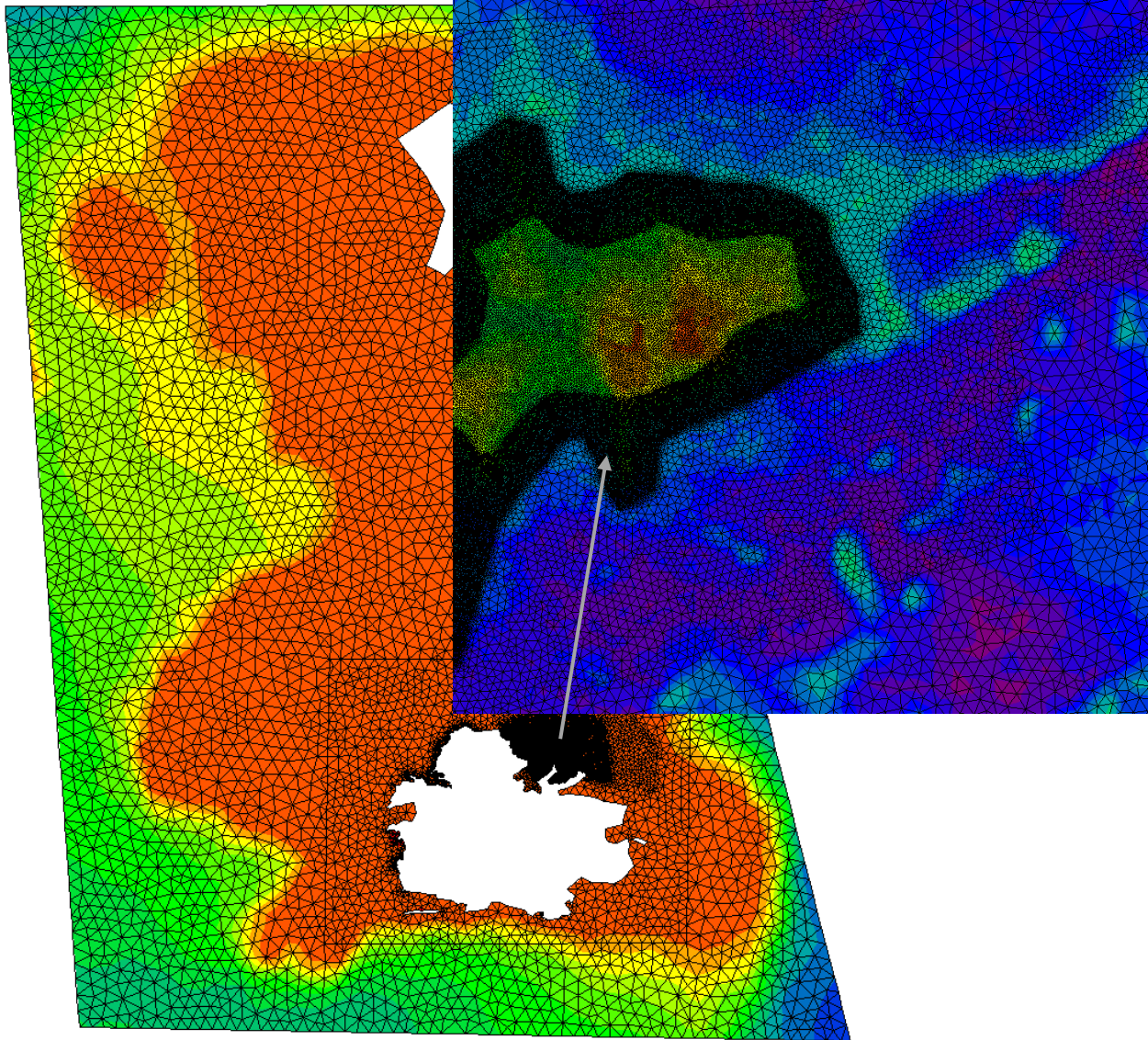
As demonstrated, smaller mesh elements were strategically utilized in areas near the project site. Moreover, smaller elements were deployed around regions with significant contour variations to effectively capture wave movements and accurately represent the bathymetry at a higher resolution in these specific areas. This approach ensures a more accurate and detailed representation of the coastal environment, which is essential for the success of the model and the project as a whole.

The spatial domain of the numerical model has been extended to encompass Barbuda, considering its significant sheltering effects on incoming waves from the north. Furthermore, the shallow shelf between

Antigua and Barbuda necessitates the inclusion of deep water within the mesh to accurately simulate hurricane-induced wave conditions.

Advantages of extending the mesh and including deep water in the model are:

1. **Enhanced accuracy:** By accounting for the sheltering effects of Barbuda and the shallow shelf between the two islands, the model can better capture wave interactions and transformations, resulting in more accurate predictions of wave conditions during hurricanes.
2. **Improved spatial resolution:** An extended mesh ensures that relevant physical processes occurring across the spatial domain, including wave refraction, shoaling, and diffraction, are well-represented within the model, leading to higher-quality wave simulations.
3. **Informed coastal management:** Incorporating these key factors into the model allows for a more comprehensive understanding of the wave dynamics in the region. This can inform the development of effective coastal protection measures, early warning systems, and emergency response plans.
4. **Versatility:** The updated mesh configuration can be used to analyze a range of scenarios and environmental conditions, such as varying storm intensities, wave directions, and sea level rise projections, providing valuable insights for both short-term and long-term planning.
5. **Robust validation:** Including deep water in the mesh allows for the validation of the numerical model against a broader range of observational data, improving confidence in the model's performance and overall credibility.

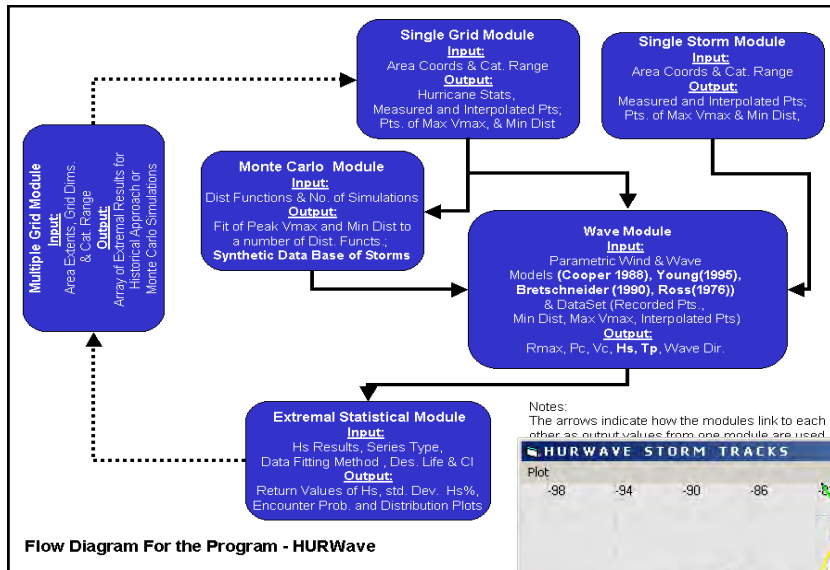


Appendix Figure A Computational mesh used in MIKE 21 simulations.

A.2 HURWave Description

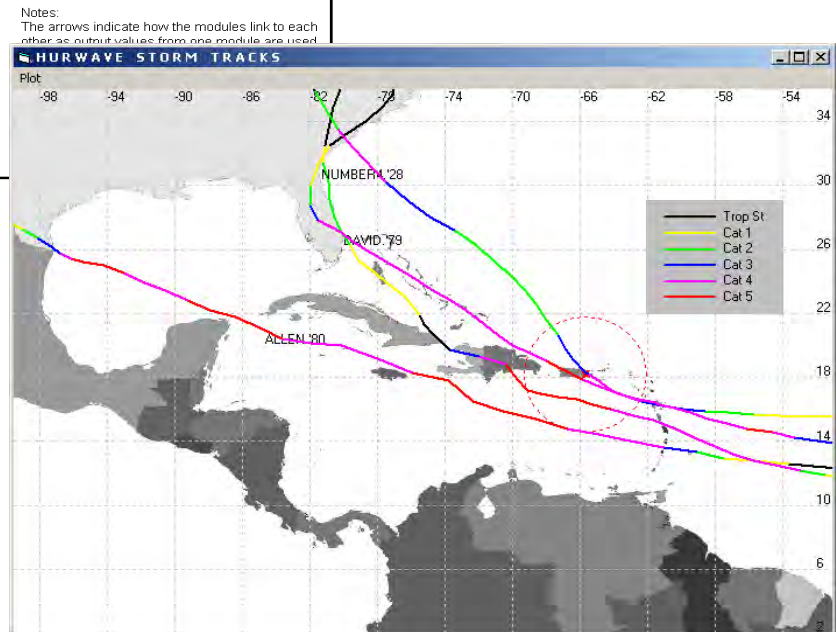
A package of Hurricane Parametric Wave Models and Extremal Statistical Analyses by Jamel D. Banton.

HURWave combines the database of the National Oceanic and Atmospheric Administration (NOAA), of hurricane tracks, with wind and wave distribution algorithms to statistically determine deep-water design wave conditions at any location within the Caribbean and the Gulf of Mexico.



The program consists of 6 main modules, namely: The Single Grid Module; The Single Storm Module; The Wave Module; The Extremal Statistical Module; The Monte Carlo Module; and The Multiple Grid Module. These are shown in the flow chart following.

The NOAA database consists of Atlantic hurricane track positions along with wind and pressure conditions at 6-hour intervals since the late 19th century. For any specified location within the North Atlantic Basin, HURWave searches this database for Tropical storms and hurricanes that have passed within a specified distance from the point of interest. The program produces several statistical descriptions for this result.



A number of widely used wind and wave models are applied to produce a hindcast dataset of hurricane wave conditions at the point in question. These models include Cooper (1988) and Young (1995).

The Cooper model was developed by statistically analysing the output from numerical wind and wave models for 6 Gulf of Mexico hurricanes. The storms used covered a wide cross-section of hurricane conditions.

In the case of Young, he first developed an extensive synthetic database by running a numerical wave prediction model for a wide range of hurricane parameters. The data from these numerical experiments were then used to clarify the wave generation process within hurricanes and further to develop the parametric



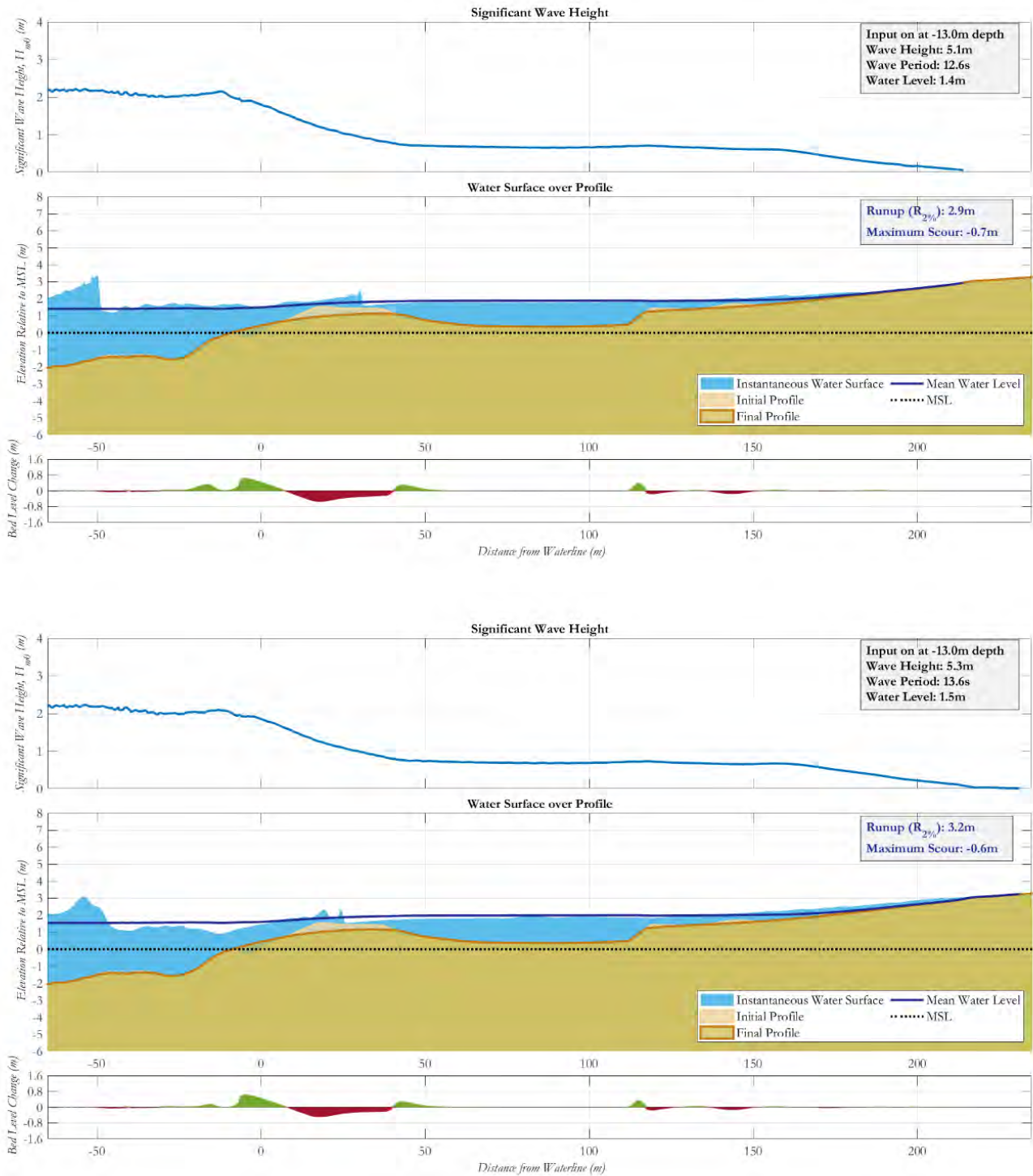
model suitable for wave prediction in deep water. This model was further calibrated with over 100 measurements made by the GEOSAT satellite.

With the results of these models, a range of extremal statistical analyses may be carried out in HURWave. The extremal methods applied are based on work published by Yoshima Goda in 1988 for statistically analysing extreme events such as hurricane waves. Distribution functions such as Weibull and Fischer Tippet (Type I) are fitted to the model results and the best fit chosen. The results include the values for wind, wave and water level conditions for various return periods.

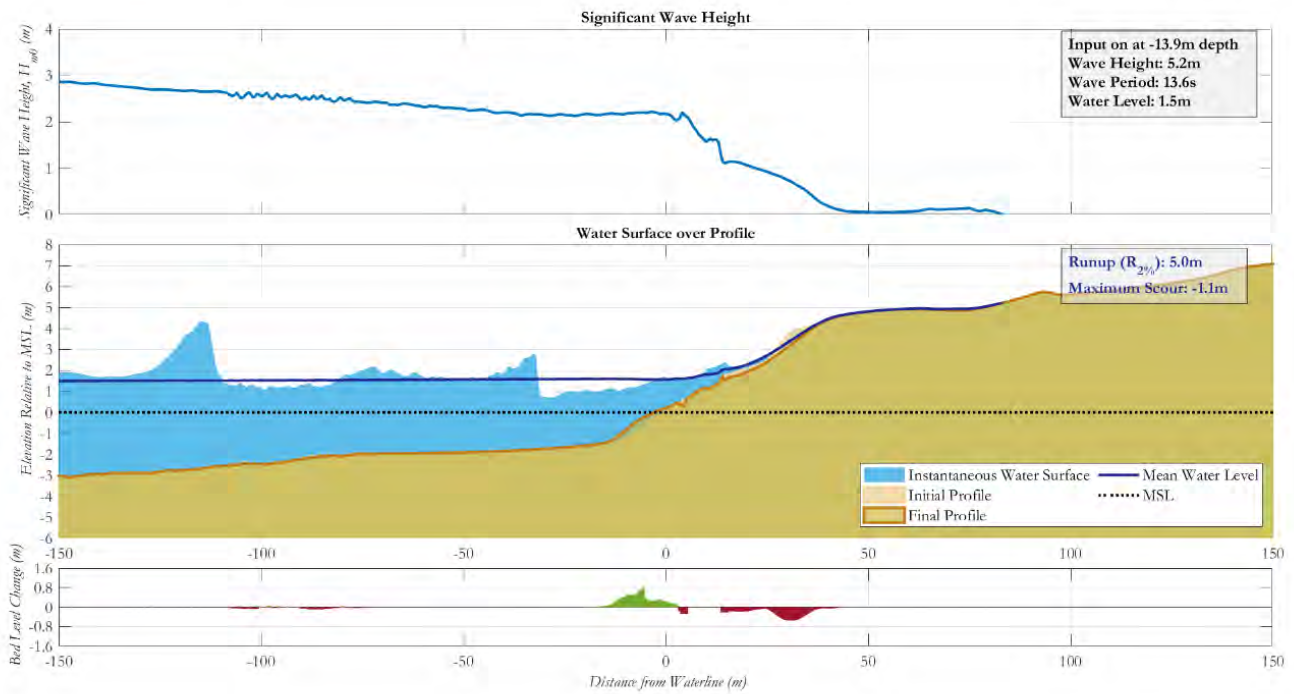
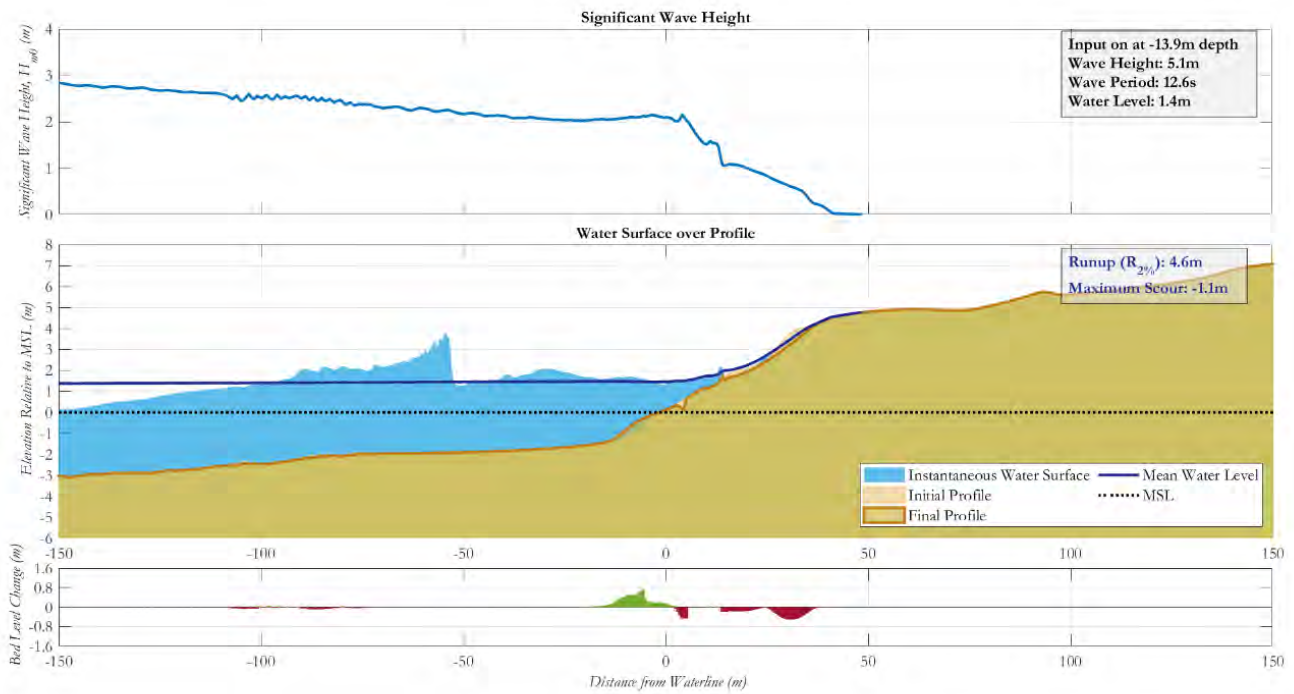
| Return Wave Heights and Variations | | | | | | | | | | | | | | | | | | | | | |
|---|--------|----------|------|-------|----------|----------|------|-------|----------|----------|------|-------|----------|----------|------|-------|----------|----------|------|-------|--|
| Refresh | | | | | | | | | | | | | | | | | | | | | |
| Return Values For The Peak Value Series | | | | | | | | | | | | | | | | | | | | | |
| Rp | FT - I | | | | k = 0.75 | | | | k = 1.00 | | | | k = 1.40 | | | | k = 2.00 | | | | |
| | Hs | σ | Hs% | EP | Hs | σ | Hs% | EP | Hs | σ | Hs% | EP | Hs | σ | Hs% | EP | Hs | σ | Hs% | EP | |
| 2 | 4.15 | 0.2 | 4.4 | 100.0 | 3.54 | 0.2 | 3.8 | 100.0 | 3.81 | 0.2 | 4.1 | 100.0 | 4.09 | 0.2 | 4.4 | 100.0 | 4.32 | 0.2 | 4.6 | 100.0 | |
| 5 | 5.92 | 0.3 | 6.2 | 100.0 | 5.52 | 0.4 | 5.8 | 100.0 | 5.82 | 0.4 | 6.1 | 100.0 | 6.02 | 0.4 | 6.3 | 100.0 | 6.11 | 0.3 | 6.4 | 100.0 | |
| 10 | 7.14 | 0.4 | 7.4 | 99.5 | 7.25 | 0.5 | 7.5 | 99.5 | 7.34 | 0.6 | 7.6 | 99.5 | 7.29 | 0.4 | 7.6 | 99.5 | 7.18 | 0.3 | 7.5 | 99.5 | |
| 20 | 8.33 | 0.5 | 8.6 | 92.3 | 9.16 | 0.7 | 9.5 | 92.3 | 8.87 | 0.8 | 9.2 | 92.3 | 8.47 | 0.5 | 8.8 | 92.3 | 8.11 | 0.4 | 8.4 | 92.3 | |
| 25 | 8.70 | 0.5 | 9.0 | 87.0 | 9.80 | 0.8 | 10.1 | 87.0 | 9.36 | 0.8 | 9.6 | 87.0 | 8.84 | 0.6 | 9.1 | 87.0 | 8.39 | 0.4 | 8.7 | 87.0 | |
| 50 | 9.87 | 0.6 | 10.2 | 63.6 | 11.89 | 1.0 | 12.2 | 63.6 | 10.88 | 1.0 | 11.2 | 63.6 | 9.93 | 0.6 | 10.2 | 63.6 | 9.20 | 0.5 | 9.5 | 63.6 | |
| 100 | 11.03 | 0.7 | 11.3 | 39.5 | 14.09 | 1.2 | 14.4 | 39.5 | 12.40 | 1.2 | 12.7 | 39.5 | 10.97 | 0.7 | 11.3 | 39.5 | 9.95 | 0.5 | 10.2 | 39.5 | |
| CI = | 95 % | | | | | | | | | | | | | | | | | | | | |
| | Cor= | 0.996 | | | Cor= | 0.867 | | | Cor= | 0.951 | | | Cor= | 0.991 | | | Cor= | 0.998 | | | |



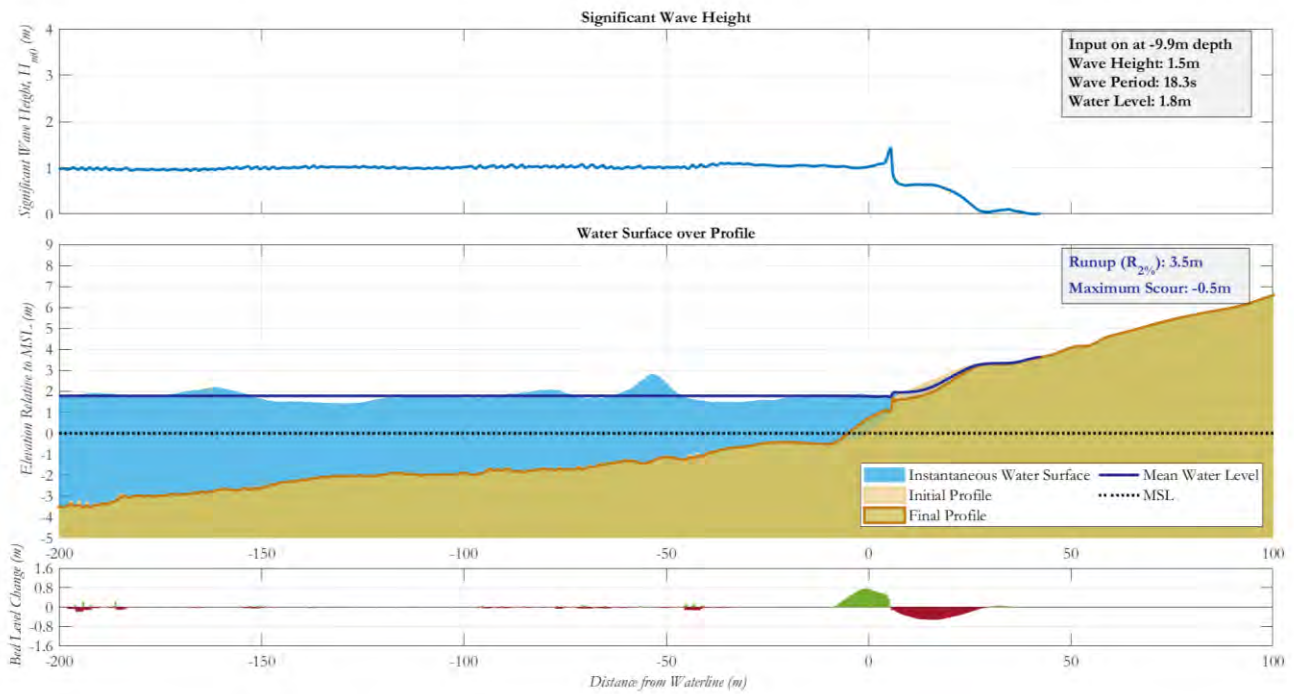
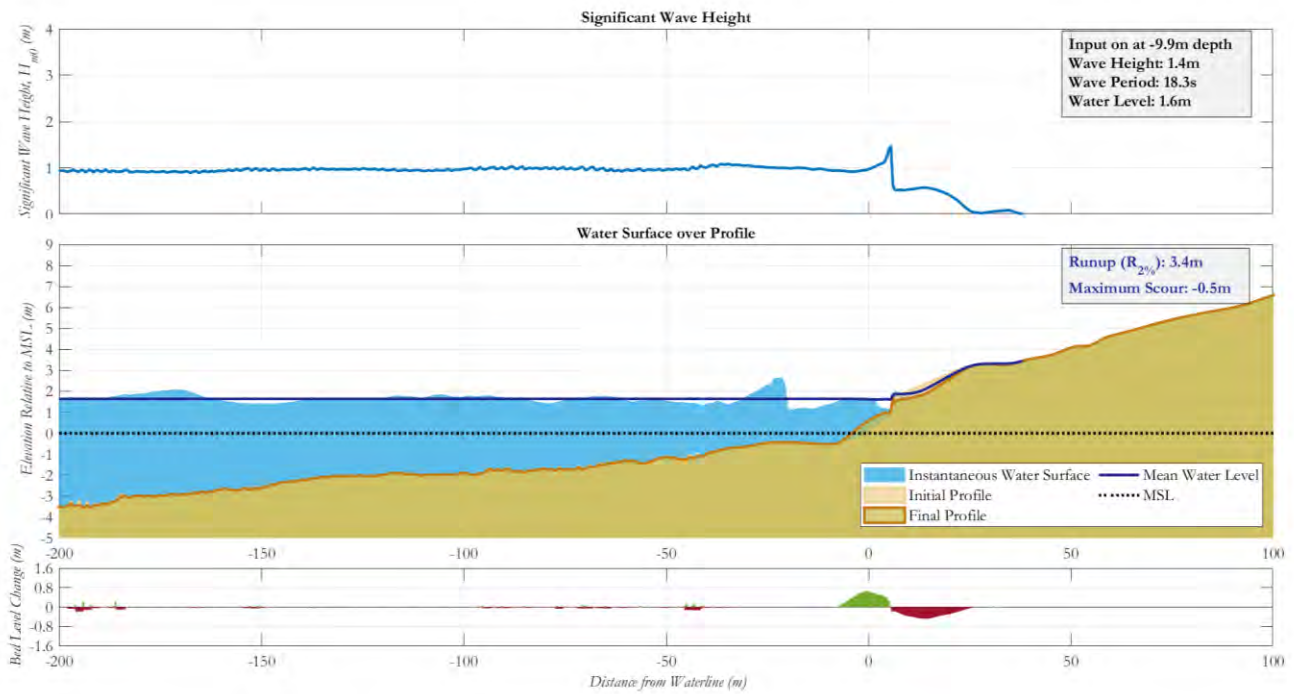
A.3 XBEACH Plots



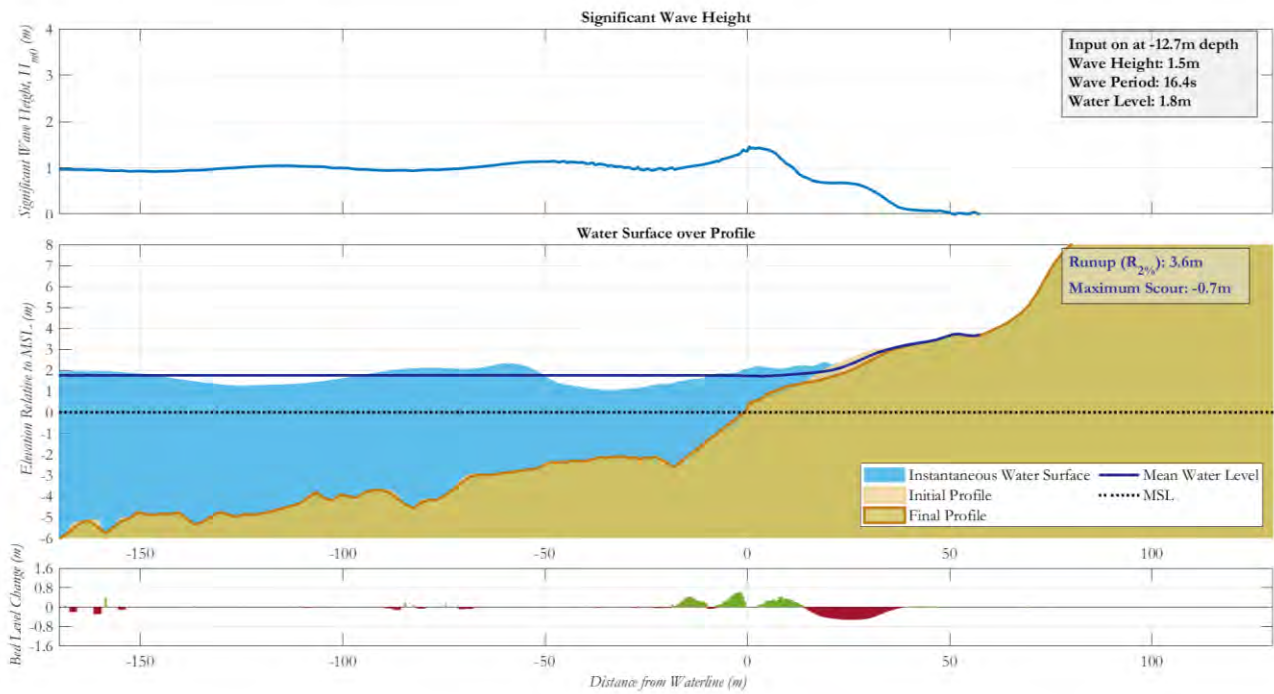
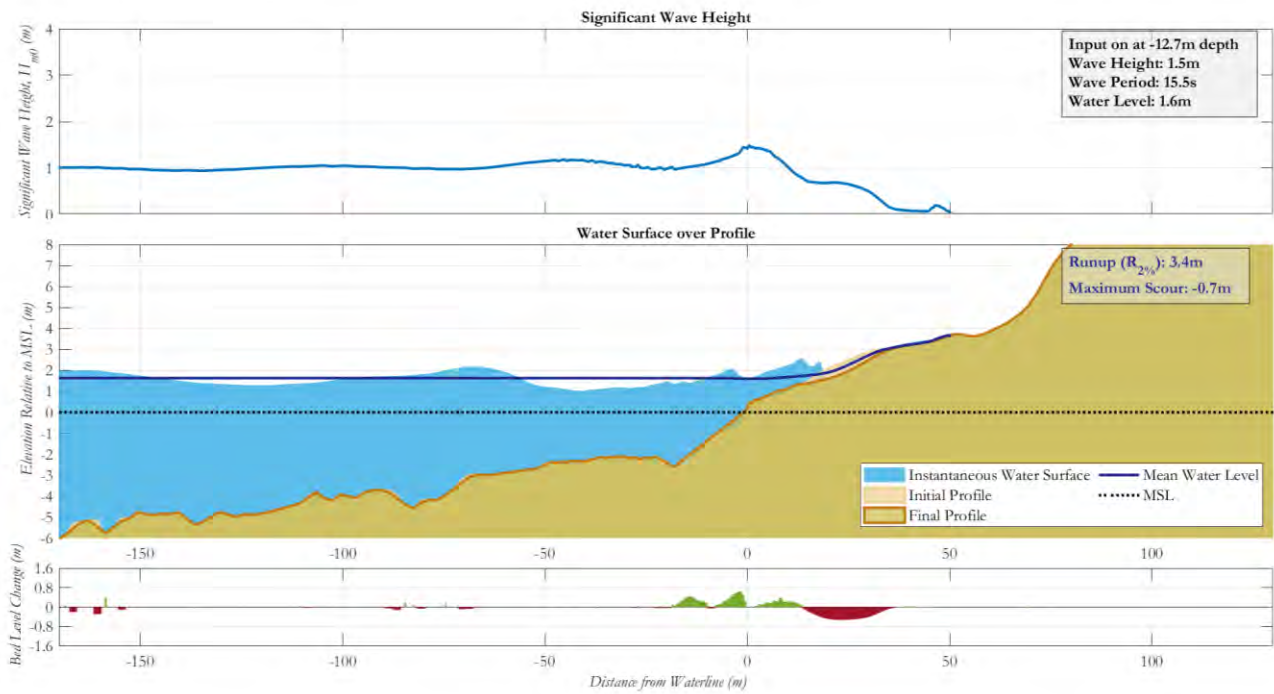
Appendix Figure B Significant wave heights, wave runup and inundation levels along Profile 1 for the 50yr and 100yr events.



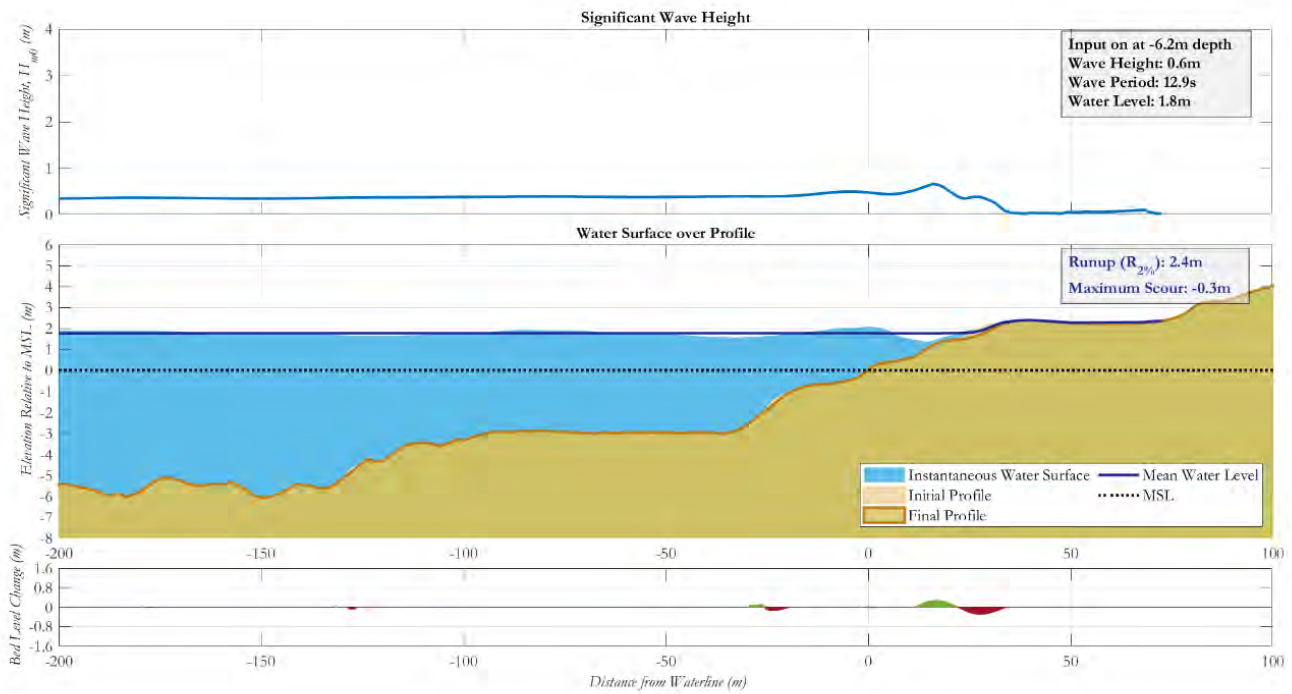
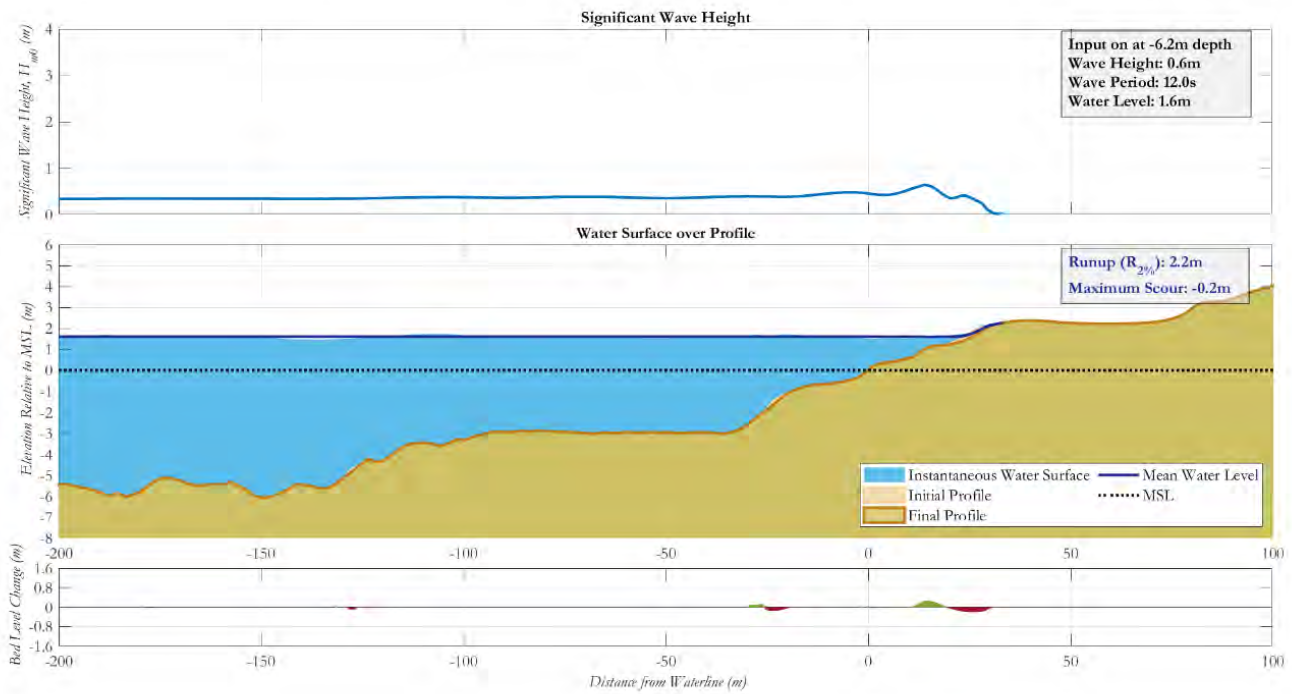
Appendix Figure C Significant wave heights, wave runup and inundation levels along Profile 2 for the 50yr and 100yr events.



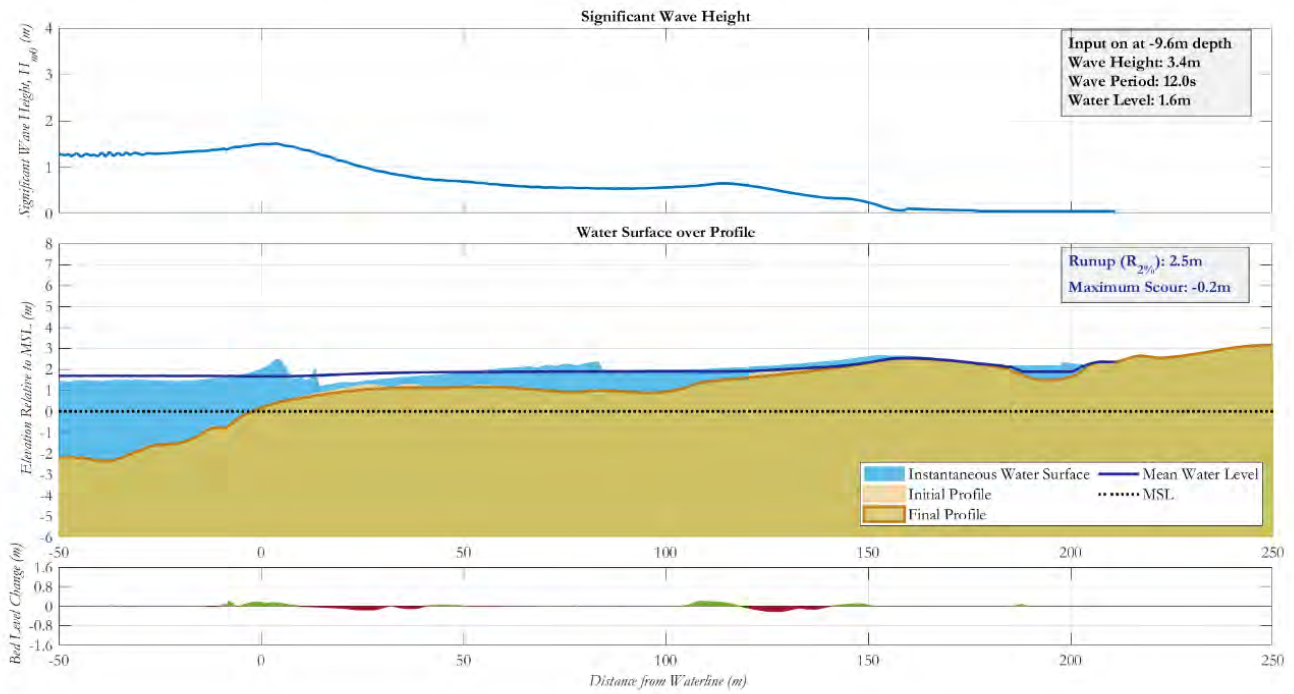
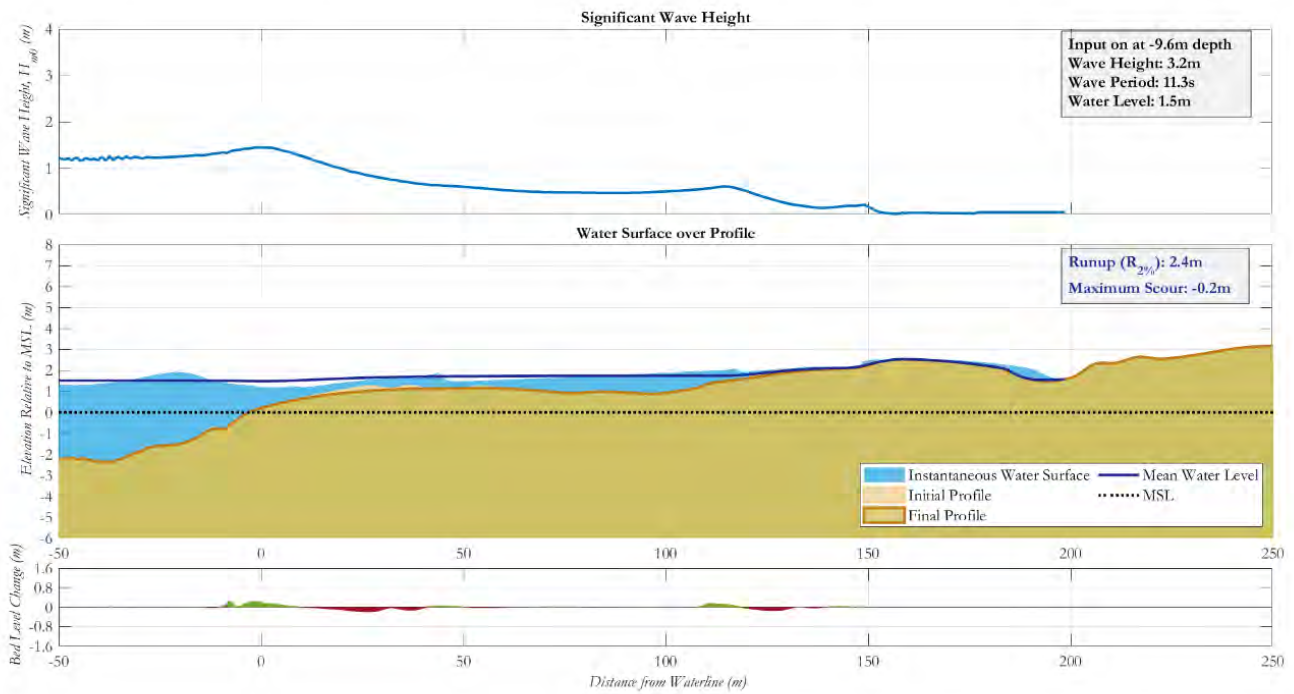
Appendix Figure D Significant wave heights, wave runup and inundation levels along Profile 3 for the 50yr and 100yr events.



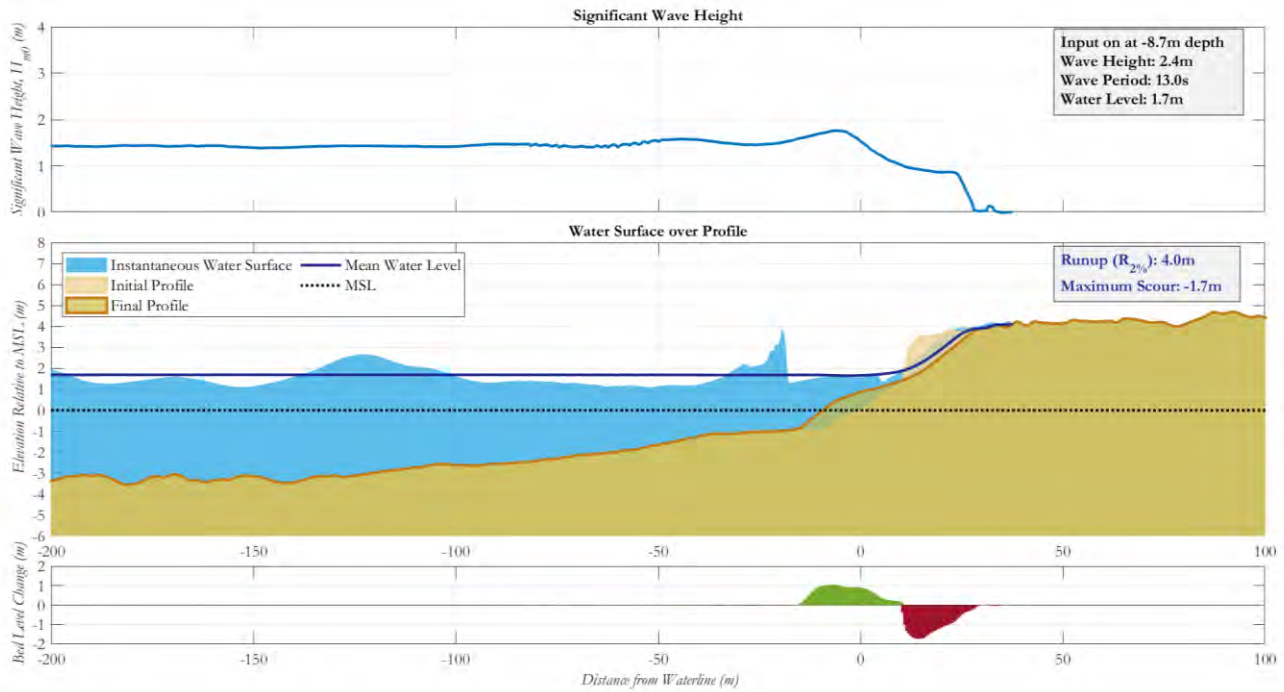
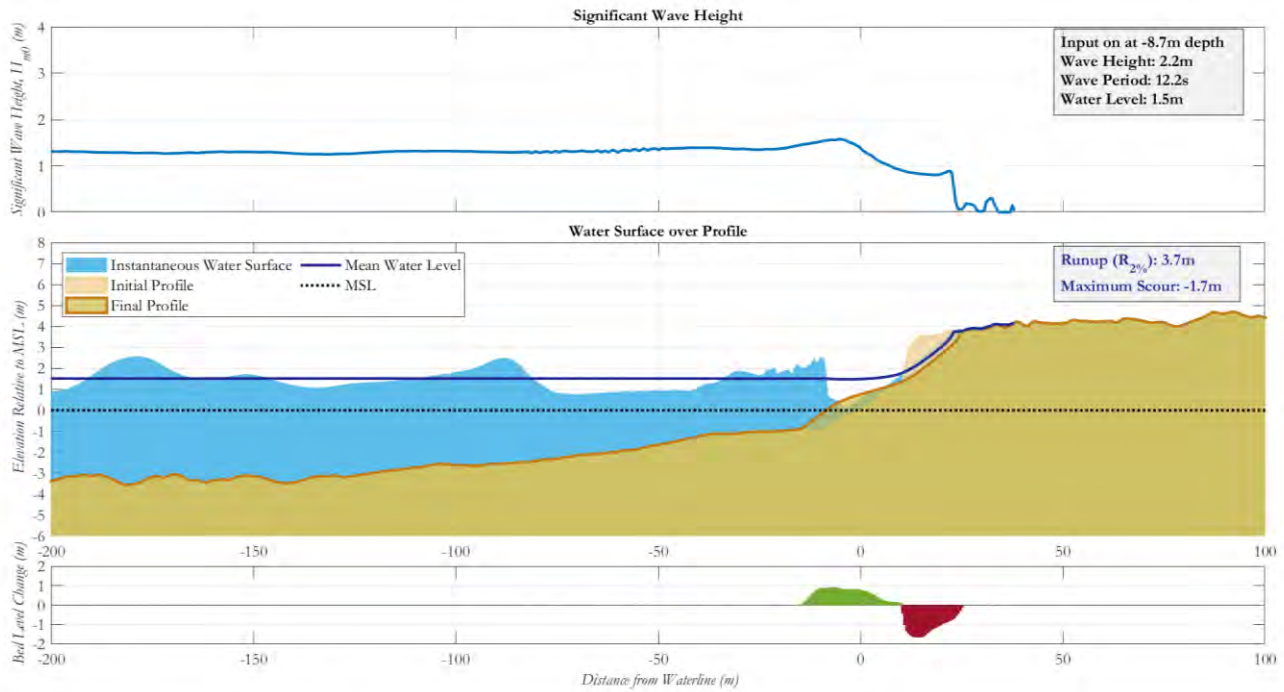
Appendix Figure E Significant wave heights, wave runup and inundation levels along Profile 4 for the 50yr and 100yr events.



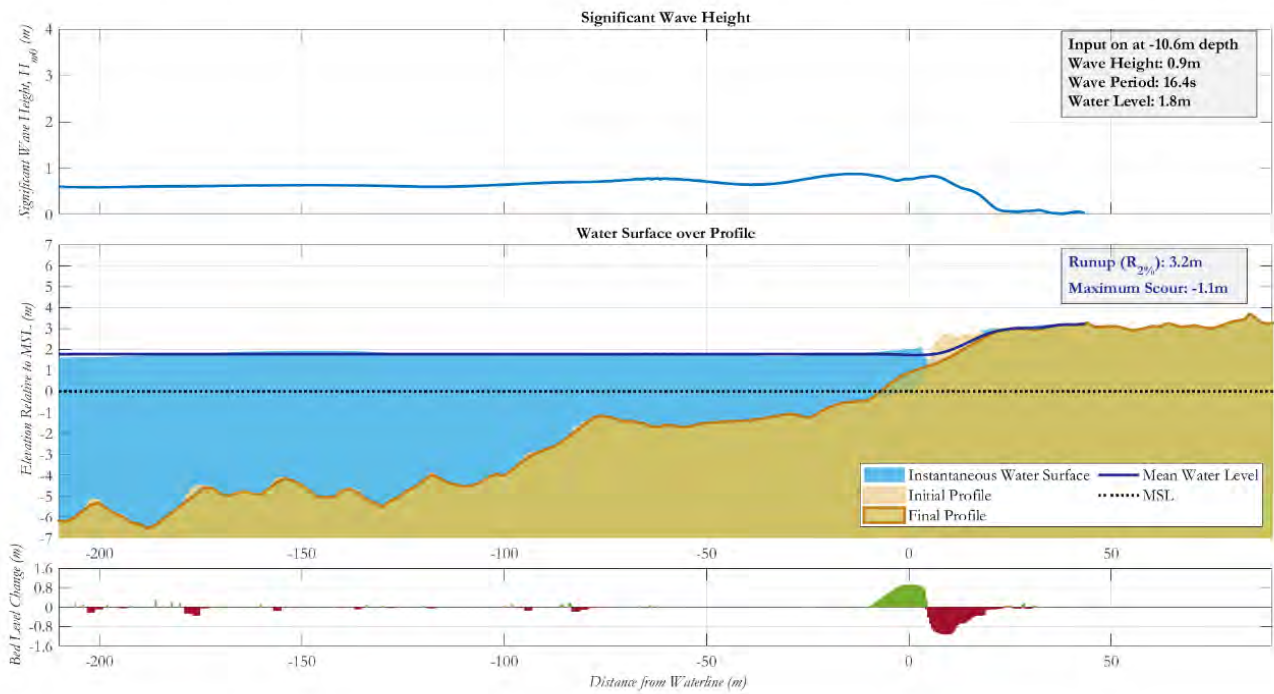
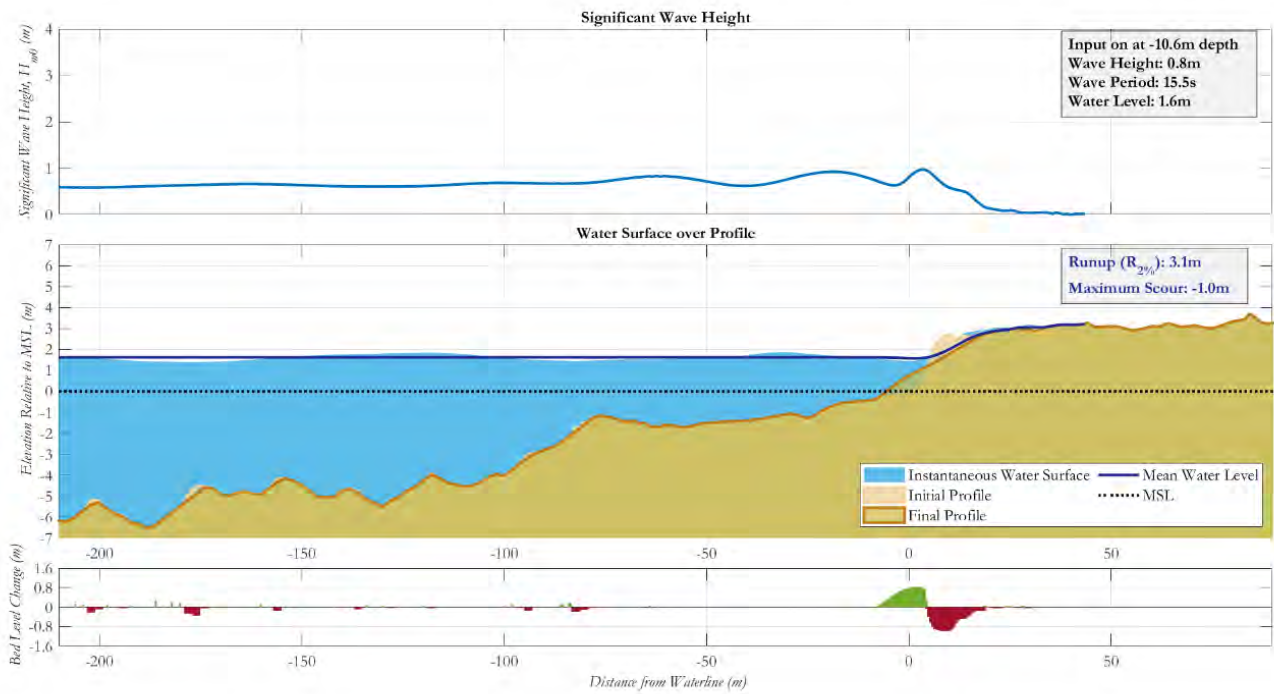
Appendix Figure F Significant wave heights, wave runup and inundation levels along Profile 5 for the 50yr and 100yr events.



Appendix Figure G Significant wave heights, wave runup and inundation levels along Profile 6 for the 50yr and 100yr events.



Appendix Figure H Significant wave heights, wave runup and inundation levels along Profile 7 for the 50yr and 100yr events.



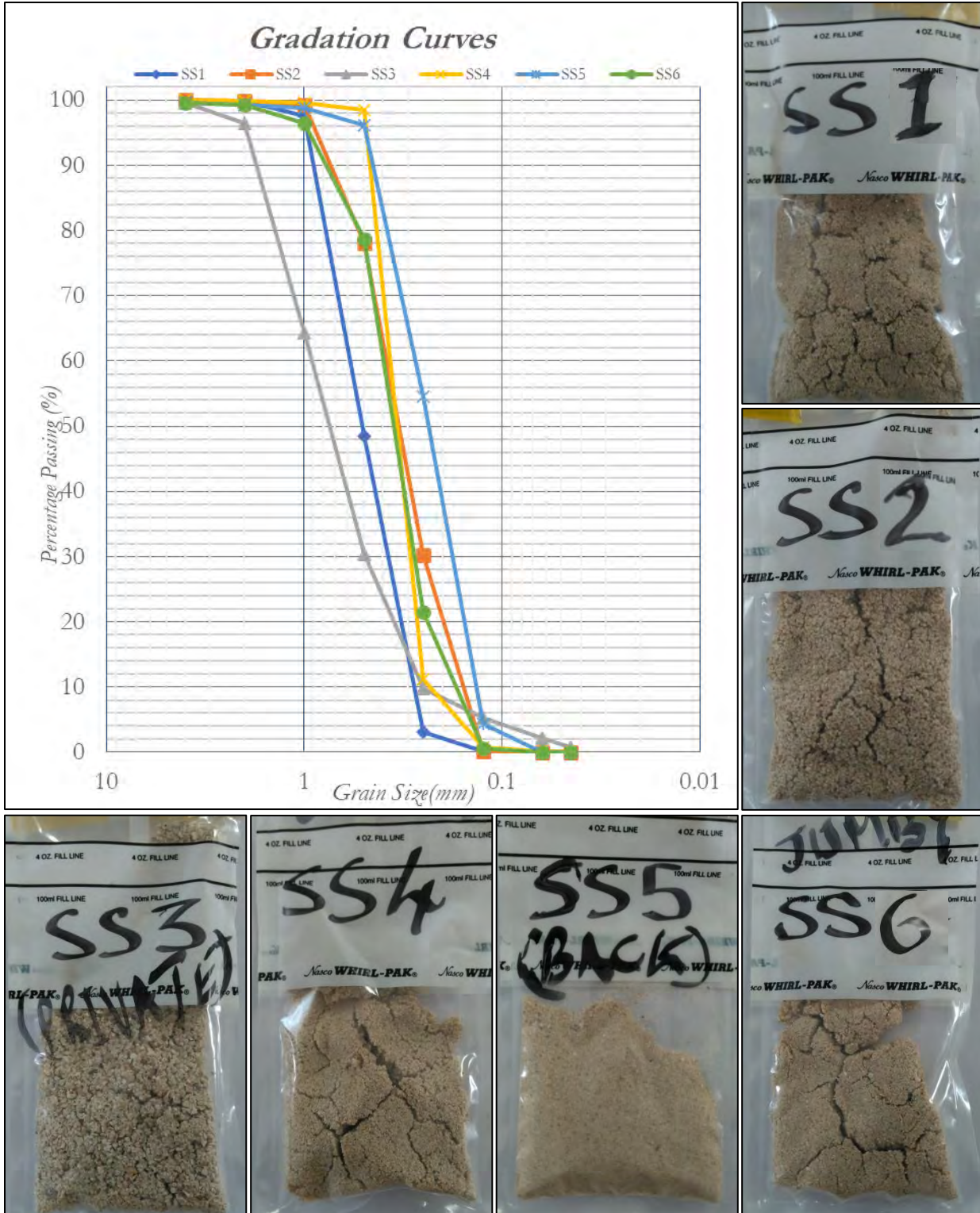
Appendix Figure I Significant wave heights, wave runup and inundation levels along Profile 8 for the 50yr and 100yr events.



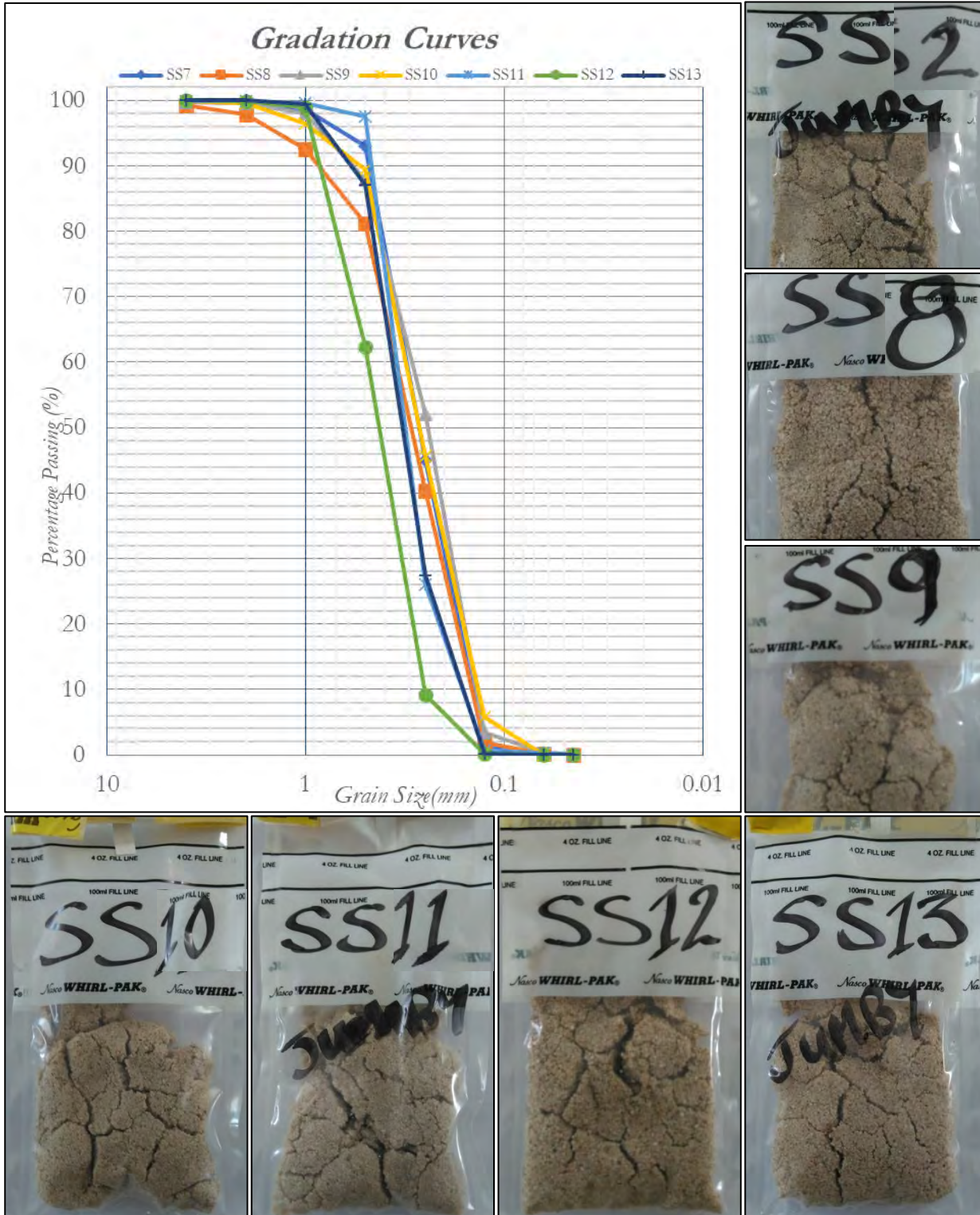
Appendix B – Additional Data Collection Reporting

Figures J through L following show the sediment samples and their respective grain size distributions. As seen in Figure J, SS3 is noticeably coarser than the other samples, with the curve shifted to the left (larger grain sizes). Figure K highlights the steep curves for samples SS7 to SS11, which occur when most grains tested belong to the same group (sand, in this instance).

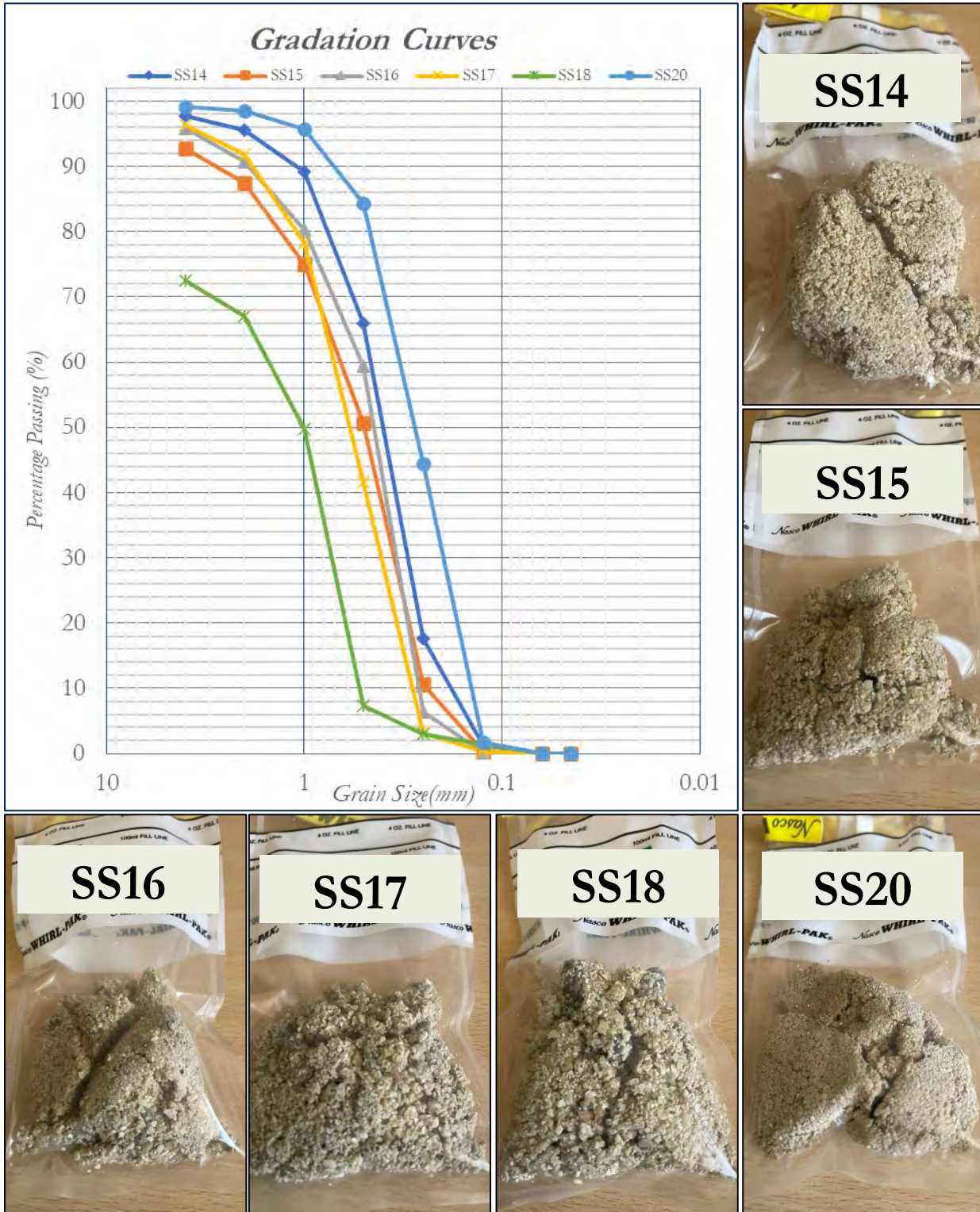
Grain size distributions reveal that Samples 15 (SS15) and 16 (SS16) exhibit similar patterns. However, Samples 17 (SS17) and 18 (SS18), collected from neighboring beach cells, show significant differences in sediment distribution, indicating rapid changes in sediment characteristics across short distances. Sample 20 (SS20), featuring the smallest grain size, was collected from a small beach cell, where a reef may provide shelter that traps finer sediment. This hypothesis will be further investigated in the wave climate analysis.



Appendix Figure J Grain size distribution and sediment sample photos for SS1 to SS6.



Appendix Figure K Grain size distribution and sediment sample photos for SS7 to SS13.



Appendix Figure L Grain size distribution and sediment sample photos for SS14 to SS18 and SS20.